Analysis of regulatory mechanisms governing aromatic compound degradation in *Acinetobacter baylyi*

Dissertation

Submitted for the fulfillment of the requirements for the doctoral degree Dr. rer. nat
at the Faculty of Natural Sciences, University of Ulm

ulm university universität ulm

By Fenja Sabine Bleichrodt from Berlin

2011

The current study was prepared at the Institute of Microbiology and Biotechnology, University of Ulm.

Dekan: Prof. Dr. Thomas Wirth

1. Reviewer: apl. Prof. Dr. Ulrike Gerischer
2. Reviewer: Prof. Dr. Peter Dürre

Tag der Promotion: 31.05.2011

Contents

Abbreviations

A	
A	Adenine
α	Alpha
A. baylyi	*Acinetobacter baylyi*
aa	Amino acids
Ala	Alanine
Ap	Ampicillin
APS	Ammonium persulfate
Arg	Arginine
Asn	Asparagine
Asp	Aspartic acid
ATP	Adenosine triphosphate
B	
β	Beta
B. subtilis	*Bacillus subtilis*
BSA	Bovine serum albumin
Bps	Base pairs
C	
C	Cytosine
°C	Degree Celcius
CCM	*cis, cis*-muconate
cDNA	copy DNA
Co	Company
CoA	Coenzyme A
Conc.	Concentration
Cys	Cysteine
D	
Δ	Delta
dATP	Deoxyadenosine triphosphate
ddATP	Dideoxyadenosine triphosphate
Da	Dalton
ddCTP	Dideoxycytidine triphosphate
ddGTP	Dideoxyguanosine triphosphate
ddTTP	Dideoxythymidine triphosphate
dNTP	Deoxyribonucleotide triphosphate
ds	double stranded
DTT	Dithiothreitol
E	
E. coli	*Escherichia coli*
EDTA	Ethylenediaminetetraacetic acid
EMSA	Electro mobility shift assay
et al.	and others (*et alii*)
F	
FF	Fast flow
Fig.	Figure
G	
γ	Gamma
g	gramm
G	Guanine
Gln	Glutamine
Glu	Glutamic acid; Gluconate
Gly	Gycine
GSP	Gene specific primer
H	
h	hour
His	Histidine

HPLC	High performance liquid chromatography
H_2O	Water
I	
Ile	Isoleucine
Inc.	Incorporation
IPTG	Isopropyl β-D-1-thiogalactopyranoside
J	
K	
Kn	Kanamycin
k	kilo
L	
λ	Bacteriophage Lambda
l	Liter
Lac	Lactate
LB	Luria Bertani
Leu	Leucine
Ltd.	Limited company
Lys	Lysine
M	
µ	micro, 10^{-6}
M	molar
mAU	milli absorption units
MCS	Multiple cloning site
Met	Methionine
Min	minute
mRNA	messenger RNA
N	
n	nano, 10^{-9}
O	
OD	Optical density
P	
P. putida	*Pseudomonas putida*
PAGE	Polyacrylamide gel electrophoresis
PCA	Protocatechuate
PCR	Polymerase chain reaction
pH	negative decimal logarithm of the hydrogen ion activity
Phe	Phenylalanine
PIPES	1,4-Piperazinediethanesulfonic acid
POB	*p*-hydroxybenzoate
PQQ	Pyrrolquinoline quinone
Pro	Proline
Pyr	Pyruvate
R	
®	Registered
RACE	Rapid amplification of cDNA ends
RBS	Ribosome binding site
RLU	Relative light units
RNA	Ribonucleic acid
RNase	Ribonuclease
RNAP	RNA polymerase
Rpm	Rounds per minute
rRNA	ribosomal RNA
RT	Room temperature

S

SDS	Sodium dodecyl sulfate
Sec	seconds
Ser	Serine
Spc	Spectinomycin
Sm	Streptomycin
ss	single stranded

T

T	Thymine
TAE	Tris acetate EDTA
TB	Terrific broth
TBE	Tris borate EDTA
TE	Tris EDTA
TEMED	Tetramethylethylenediamine
Thr	Threonine
Tm	Melting temperature
™	Trade mark
Tris	tris (hydroxymethyl) aminomethane
Trp	Tryptophan
TSS	Transcriptional start site
Tyr	Tyrosine

U

UV	Ultra violet
U	units

V

V	Volt
Val	Valine
Vol	Volume
v/v	Volume per volume

W

w/v	Weight per volume

X

X-Gal	5-bromo-4-chloro-3-indolyl-β-D-galactopyranoside

1 Introduction

Acinetobacter baylyi strain ADP1 (Vaneechoutte *et al.*, 2006) is a Gram-negative, strictly aerobic soil organism, that is highly competent for natural transformation (Juni, 1972). The bacterium was originally isolated from soil on a mineral salts medium with butane 2,3-diol and designated as BD-4 (BD: butane diol; (Taylor & Juni, 1961)) and later classified as *Acinetobacter calcoaceticus*. An uncapsulated mutant was obtained by ultra violet irradiation and called BD413 (Juni & Janik, 1969). The strain was renamed in *Acinetobacter* sp. ADP1 in 1975, and was then called *Acinetobacter baylyi* ADP1 (Vaneechoutte *et al.*, 2006). This strain was fully sequenced by Genoscope in 2004 (Barbe *et al.*, 2004); a complete knock-out collection (de Berardinis *et al.*, 2008) is available.

A. baylyi is able to degrade a number of aromatic compounds (Williams, 2008) and is thus participating in the natural circulation of carbon. The degradation of aromatic compounds is accomplished by the enzymes of the β-ketoadipate pathway ((Harwood & Parales, 1996); Fig. 1.1), leading to the formation of succinyl-CoA and acetyl-CoA, which are directly fed into the citric acid cycle. The pathway is composed of two main branches with its central intermediates protocatechuate (PCA) and catechol (Canovas & Stanier, 1967). Several short funneling pathways lead to the formation of PCA and catechol from complex aromatic precursors (Fig. 1.1). A crucial step within the catabolic pathway is the ortho-cleavage of the aromatic rings of PCA and catechol and the incorporation of molecular oxygen by dioxygenases. In addition to the short funneling pathways leading to the central starting compounds PCA and catechol, there is another short funneling pathway, feeding dicarboxylates into the pathway at a later level. Here, the degradation of dicarboxylates appears to proceed through classic β-oxidation and converges with the β-ketoadipate pathway at the level of β-ketoadipyl-CoA (Parke *et al.*, 2001).

Genes encoding enzymes for the degradation of aromatic compounds in *A. baylyi* are localized in catabolic islands on the chromosome ((Barbe *et al.*, 2004); Fig. 1.2), and are part of two large clusters that each encodes pathways for the catabolism of plant-derived carbon sources (*sal-are-ben-cat* and *dca-pca-qui-pob-hca*; (Young *et al.*, 2005)). It is worth to note that genes encoding information of neighboring reactions are located adjacent to each other. Keeping that in mind, it is striking that the *van* and *ant* genes, encoding enzymes for the degradation of vanillate to PCA (Segura *et al.*, 1999) and anthranilate to catechol (Bundy *et al.*, 1998), are not part of the two large clusters and lie separated on the *Acinetobacter* chromosome (Fig. 1.2).

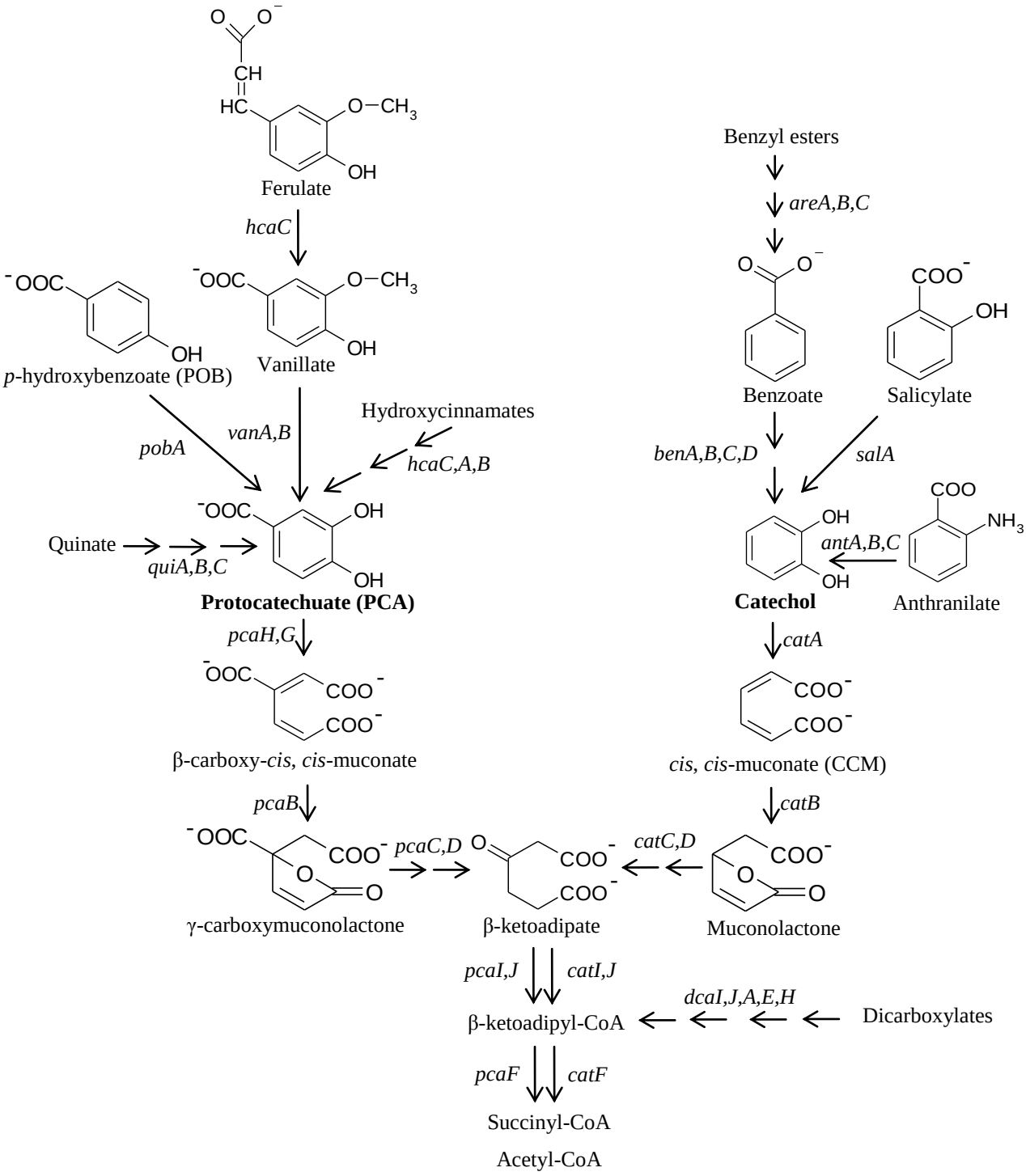

Figure 1.1: The β-ketoadipate pathway of *Acinetobacter baylyi* strain ADP1.

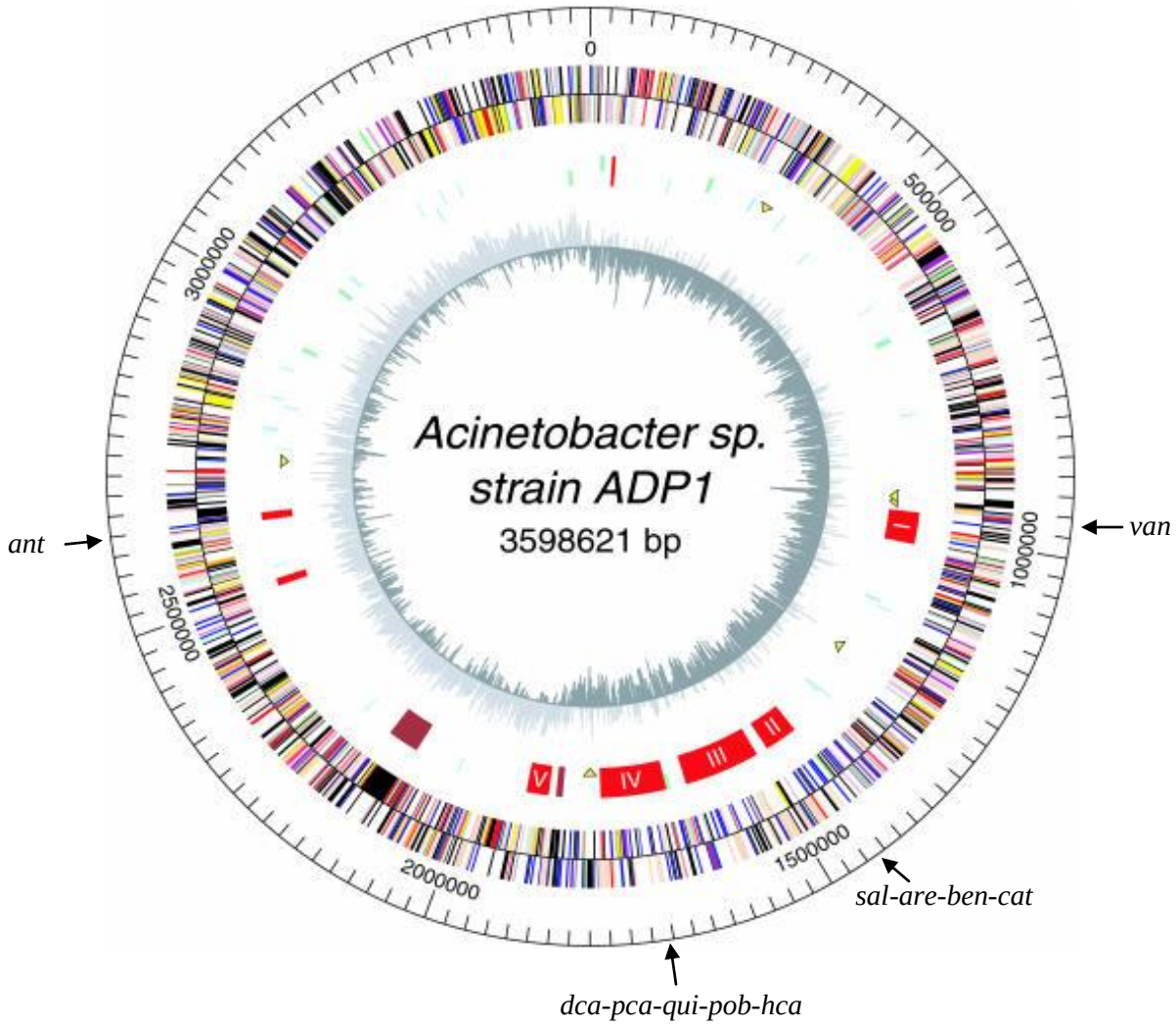

Figure 1.2 Circular representation of the *Acinetobacter* ADP1 genome (Barbe *et al.*, 2004). The positions of genes under study are indicated. Circles display (from the outside): (i) predicted coding regions transcribed in the clockwise direction. (ii) Predicted coding regions transcribed in the counterclockwise direction. Genes displayed in (i) and (ii) are color coded according to different functional categories: salmon, amino acid biosynthesis; light blue, biosynthesis of cofactors, prosthetic groups and carriers; light green, cell envelope; red, cellular processes; brown, central intermediary metabolism; yellow, DNA metabolism; green, energy metabolism; purple, fatty acid and phospholipid metabolism; pink, protein fate/synthesis; orange, purines, pyrimidines, nucleosides, nucleotides; blue, regulatory functions; grey, transcription; teal, transport and binding proteins; black, hypothetical and CHPs. (iii) Transposable elements (yellow triangles), phage regions (brown), genes involved in catabolic pathways (red); the five catabolic islands (>20 kb) are numbered from I to V. (iv) tRNAs (light blue) and rRNA (light green). (v) GC bias (G+C/G-C)

Besides its ability to use aromatic compounds as the sole carbon source, *A. baylyi* is also able to grow on organic acids such as succinate, acetate, lactate, and gluconate, as well as on the monosaccharide glucose. All substrates named here, are converted into intermediates of the citric acid cycle by divers metabolic pathways or reactions. While succinate can directly be fed into the citric acid cycle, acetate has to be converted to acetyl-CoA (an energy consuming step), which subsequently feeds into the glyoxylate cycle. Here, acetyl-CoA is added to glyoxylate by the action of malate synthase, generating malate, an intermediate of the citric acid cycle. Lactate can easily be converted into pyruvate by the enzyme lactate dehydrogenase, and pyruvate then is transformed to acetyl-CoA by the pyruvate dehydrogenase complex. Interestingly, and in striking contrast to other bacteria (e. g. *Escherichia coli*), glucose metabolism is an unusual trait among different *Acinetobacter* isolates, and they notably lack pyruvate kinase.

In any case, glucose metabolism is complex, as glucose has to be converted to gluconate by oxidation on the outer surface of the inner membrane (van Schie *et al.*, 1985). This conversion requires pyrrolquinoline quinone (PQQ), which is synthesized by a special pathway (Goosen *et al.*, 1989). Energy derived from this oxidation is then used to transfer gluconate into the cell (van Schie *et al.*, 1985), where it is likely metabolized by a modified Entner-Doudoroff pathway to pyruvate. Using this pathway, the lack of pyruvate kinase is bypassed by regenerating glucose-6-phosphate from triose phosphates (Lessie & Phibbs, 1984).

The overall topic of the current thesis is the analysis of regulatory mechanisms governing the degradation of aromatic compounds through the β-ketoadipate pathway. These regulatory mechanisms create a precise order in which carbon sources are consumed, and thus play a crucial role in the adaptation of the organism to the continuously changing composition of different carbon sources present in the environment. The β-ketoadipate pathway of *A. baylyi* undergoes a multiple level regulation (Gerischer *et al.*, 2008), creating a precise order of carbon source utilization. This hierarchy ensures minimal energy consumption and maximal energy conservation.

One part of this network is carbon catabolite repression (CCR; (Canovas & Stanier, 1967, Tresguerres *et al.*, 1970)). Although CCR is well understood in Gram-negatives as *E. coli* and in Gram-positives as *Bacillus subtilis* (Saier, 1998, Bruckner & Titgemeyer, 2002, Titgemeyer & Hillen, 2002), the mechanism leading to CCR in bacteria belonging to the genera *Pseudomonas* and *Acinetobacter* (both members of the γ-proteobacterial subdivision) is only beginning to be elucidated. While CCR in *E. coli* and *B. subtilis* depends on the presence of glucose, organic acids such as succinate and acetate play an important role in *Pseudomonas* (Collier *et al.*, 1996) and *Acinetobacter* (Dal *et al.*, 2002, Fischer *et al.*, 2008, Bleichrodt *et al.*, 2010).

In *A. baylyi*, CCR has been described for the *pca-qui* operon, the *pobA* gene (Dal *et al.*, 2002), and the *ben, ant, are, hca, dca* (Fischer *et al.*, 2008), *catA, catB,C,I,J,F,D,* and *vanA,B* operons (Bleichrodt, 2007). These operons encode enzymes required for aromatic compound degradation through the β-ketoadipate pathway (Fig. 1.1), as PCA, quinate, *p*-hydroxybenzoate (POB), benzoate, anthranilate, benzyl esters, hydroxycinnamates, dicarboxylates, catechol, *cis, cis*-muconate (CCM), and vanillate. This work was extended in the current thesis by the analysis of CCR of the *salA*, and *vanK* genes and published in 2010 (Bleichrodt *et al.*, 2010). The *salA* gene encodes an enzyme responsible for the breakdown of salicylate (Jones *et al.*, 2000) and the *vanK* gene encodes a protein probably involved in vanillate transport (Segura *et al.*, 1999).

The understanding of the molecular mechanism leading to CCR of these operons and genes is far from being understood, but there is evidence for the involvement of a protein called Crc (catabolite repression control (Wolff *et al.*, 1991, Zimmermann *et al.*, 2009, MacGregor *et al.*, 1991)). In *Pseudomonas putida*, Crc affects the expression of genes involved in aromatic compound degradation (*ben*, *cat*, *pca*, and *pobA*; (Morales *et al.*, 2004)), and a direct binding of Crc to the RNA region directing translation of the regulators BenR and AlkS was demonstrated, indicating translational repression (Moreno *et al.*, 2007, Moreno & Rojo, 2008). *A. baylyi* Crc has been shown to be involved in the degradation of the *pca-qui* transcript (Zimmermann *et al.*, 2009), acting posttranscriptional. It was further shown that *A. baylyi* Crc is involved in CCR of the *ben, catA, catB,C,I,J,F,D, dca*, *hca* and *vanA,B* operons at the transcriptional level in the presence of the substrate combination succinate and acetate in addition to an aromatic compound (Bleichrodt, 2007, Bleichrodt *et al.*, 2010). This work was extended in the current thesis for the *ant*, *are*, *vanK* and *salA* genes in the current thesis. These findings were published in 2010 (Bleichrodt *et al.*, 2010).

In addition to CCR, cross-regulation becomes effective when mixtures of substrates feeding into both branches of the pathway are present. In *A. baylyi*, cross-regulation describes a cross-talk between the two main branches of the pathway and results in a dominance of the catechol branch over the PCA branch (Brzostowicz *et al.*, 2003, Siehler *et al.*, 2007, Bleichrodt *et al.*, 2010). This mechanism was observed in the presence of benzoate, a substrate degraded through the catechol branch, in addition to substrates of the PCA branch. Expression of the *pca, pobA, hca, vanA,B,* and *dca* genes is repressed in the presence of benzoate in comparison to the activity measured without benzoate. The two transcriptional regulators that are naturally able to sense benzoate (or CCM, as a downstream metabolite) are BenM and CatM, LysR-type transcriptional regulators responsible for the activation of the *ben* and *cat* genes (Craven *et al.*, 2008). They were shown to repress POB degradation in the presence of benzoate (Brzostowicz *et al.*, 2003). The authors showed that these regulators bind to regulatory regions of the *pca* operon in the presence of CCM, possibly blocking the transcription of *pcaK*, encoding a transport protein needed for POB and PCA

uptake. Similar observations were made for *P. putida pcaK*. Its transcription is repressed in the presence of benzoate by BenR, a XylS-type transcriptional regulator (Cowles *et al.*, 2000).

The third regulatory mechanism is observed within the PCA branch of the β-ketoadipate pathway. PCA is consumed prior to vanillate and hydroxycinnamates (Bleichrodt *et al.*, 2010). These compounds are metabolically linked, as vanillate and hydroxycinnamates are degraded to PCA in the β-ketoadipate pathway of *A. baylyi* (Fig. 1.1), and the transcriptional repression of *vanA,B* and *hca* by PCA was termed vertical regulation (Bleichrodt *et al.*, 2010). This mechanism was also shown for the *pobA* gene; its expression is repressed in the presence of PCA (Siehler *et al.*, 2007).

All genes or operons connected with the degradation of aromatic compounds through the β-ketoadipate pathway of *A. baylyi*, are controlled by individual transcriptional regulatory proteins in response to a specific aromatic effector. The expression of the *pca* genes for example, is governed by the IclR-type transcriptional regulator PcaU (Gerischer *et al.*, 1998). PcaU is responsible for activating *pca* expression in the presence of PCA, and to repress gene activity in the absence of PCA. Thus, PcaU is a dual-function transcriptional regulator, able to turn on or off gene activity in response to environmental changes. Table 1.1 gives an overview of the transcriptional regulators involved in aromatic compound degradation in *A. baylyi*.

Table 1.1: Transcriptional regulators of operons involved in aromatic compound degradation.

Name	Type	Genes	Effector	Acting as	Reference
uk	uk	*ant*	anthranilate	uk	Bundy *et al.*, 1998
AreR	XylR	*are*	benzyl esters, benzyl alcohols, benzaldehydes	activator	Jones *et al.*, 1999
BenM	LysR	*ben, catA*	benzoate, CCM	activator	Collier *et al.*, 1998
CatM	LysR	*catA, cat*	CCM	activator	Romero-Arroyo *et al.*, 1995
DcaR	IclR	*dca*	uk	uk	Parke *et al.*, 2001
HcaR	MarR	*hca*	hydroxycinnamoyl-CoA thioesters	repressor	Parke *et al.*, 2003
PcaU	IclR	*pca-qui*	PCA	activator & repressor	Gerischer *et al.*, 1998
PobR	IclR	*pobA*	POB	activator	Di Marco *et al.*, 1993
SalR	LysR	*salA*	salicylate	activator	Jones *et al.*, 2000
VanR	GntR	*vanA,B, vanK*	vanillate	repressor	Morawski *et al.*, 2000

uk: unknown

The analysis of multiple levels governing aromatic compound degradation in *A. baylyi* was of interest in the current study, such as carbon catabolite repression (CCR), cross-regulation, and vertical regulation. Those regulatory mechanisms all have one quality in common: they are of elevated nature and override the specific gene regulation, brought about by specific regulatory proteins in response to a particular aromatic effector (governing the expression of only one operon in most cases).

Since the *pca-qui*, *pobA*, *ben*, *ant*, *are*, *hca*, *dca*, *catA*, *catB,C,I,J,F,D*, and *vanA,B* genes all undergo CCR, it was of interest to know if other genes encoding enzymes involved in aromatic compound degradation are also repressed in the presence of organic acids. To answer this question, transcriptional gene fusion of the *Photinus pyralis luc* gene (Bonin *et al.*, 1994) with the *salA* (involved in salicylate degradation) and *vanK* gene (vanillate transport) were constructed. The activity of the genes was then analyzed in the presence of the organic acids and the aromatic inducer.

Adapted gene expression in bacteria is a consequence of the availability of substrates in the surrounding environment, and components mediating the flow of information are important for the organism. The Crc protein seems to be one component mediating the communication between the environment (with respect to the availability of substrates) and the induction status of genes involved in aromatic compound degradation in *A. baylyi*. Since the *pca-qui* genes are known to undergo a regulation by Crc dependent of the nature of carbon sources present in addition to aromatic compounds, it was an important question if also other genes involved in aromatic compound degradation are subject to a Crc mediated regulation. To test this, the *crc* gene was deleted in strains containing reporter gene fusions in genes involved in the degradation of anthranilate (*ant*), benzyl esters (*are*), benzoate (*ben*), catechol (*catA*), *cis*, *cis*-muconate (*catB,C,I,J,F,D*), dicarboxylates (*dca*), hydroxycinnamates (*hca*), salicylate (*salA*), vanillate (*vanA,B*), and vanillate transport (*vanK*). The activity of the genes was then analyzed in the presence of different carbon sources (succinate, acetate, gluconate, lactate, pyruvate, as well as the substrate combination succinate and acetate) and the specific aromatic inducers.

Two other mechanisms creating a hierarchy of carbon source preference in *A. baylyi* are cross-regulation and vertical regulation. Although of elevated nature, these two regulatory mechanisms govern the order in which aromatic compounds are consumed by the organism. Thus, they seem to be restricted to the β-ketoadipate pathway of *A. baylyi*. Even though the *hca*, *dca*, and *vanA,B* genes were shown to undergo cross-regulation, and the *hca* and *vanA,B* genes vertical regulation, the molecular mechanism forming the basis for these regulations at the *hca*, *dca*, and *vanA,B* operons is not known. The analysis of these mechanisms was a central part of the current thesis.

In some cases adapted gene expression is a consequence of inducer exclusion, with regard to the changing compositions of substrates present to an organism. Transport systems, embedded in the cytoplasmatic membrane of bacteria, play a crucial role in inducer exclusion. The analysis of transport systems is thus necessary to understand adapted gene expression. The analysis of the *vanK* gene (encoding for the vanillate transporter) of *A. baylyi* was chosen as the subject of study in the current thesis. After the introduction of the luciferase reporter gene as a transcriptional fusion into *vanK*, its expression was determined in the presence of different aromatic compounds, to identify substrates that are transported by VanK.

2 Materials and Methods

2.1 Plasmid and strain construction

Standard methods were used for plasmid isolation (Chapter 2.8.1), DNA purification (Chapter 2.8.2), restriction endonuclease cleavage (Chapter 2.8.3.1), ligation (Chapter 2.8.3.2), and transformation (Chapter 2.7).

Strains ADPU97 to 102 and ADPU104 to 106 (Table 2.1) were designed during my diploma thesis in 2007 and constructed as described in Bleichrodt *et al.*, 2010.

Strains ADPU110 to 113 and ADPU120 to 121 (Table 2.1) were constructed in the current study as described in Bleichrodt *et al.* 2010.

The *benM* gene was inactivated in strains ADPU93 to 94, and ADPU102 (Table 2.1), by using a benR1/benR2 (Table 2.3) PCR fragment containing the Δ*benM*-Kn^r region of strain KO_1435 (Table 2.1; (de Berardinis *et al.*, 2008)) for homologous recombination. Obtained strains were selected on kanamycin, and the integration of the Δ*benM*-Kn^r fragment at the right position was verified by PCR using primers benR3 and benR4 (Table 2.3). Obtained strains were designated ADPU135 to 137 (Table 2.1), respectively.

To inactivate the *catM* gene in strains ADPU93 to 94, ADPU102, and ADPU135 to 137 (Table 2.1), a PCR was performed to amplify the *catM* region from chromosomal *Acinetobacter* DNA, using primers catM1 and catM2 (Table 2.3). The obtained fragment was treated with *Sal*I and *Xba*I, and integrated into pBSKII$^+$ (Table 2.2), treated with the same endonucleases, obtaining pAC144 (Table 2.2). The integration of the Ω-cassette (carrying a spectinomycin and streptomycin resistance gene, and leads to premature termination of transcription) into *catM*, was performed by cleaving the Ω-cassette from pHP45Ω (Table 2.2) with *Eco*RI, followed by integration into pAC144 treated with *Eco*RI, yielding plasmid pAC146 (Table 2.2). *A. baylyi* strains ADPU93 to 94, ADPU102, and ADPU135 to 137 (Table 2.1) were transformed by homologous recombination, using an *Xba*I/*Sal*I fragment, containing *catM*Ω, cleaved from pAC146. Obtained clones were selected in the presence of streptomycin and spectinomycin. PCR analysis with primers catM1 and catM2 (Table 2.3) was employed to verify the integration of the Ω-cassette at the right position. Obtained strains were designated as ADPU124 to 126 and ADPU140 to 142 (Table 2.1), respectively.

Plasmid pBAC852 (Table 2.2), containing an inactivated *catA* gene by insertion of a Kn^r-cassette, was used to inactivate the *catA* gene in strains ADPU93 to 94, and ADPU102 (Table 2.1). After plasmid linearization using *Aat*II, the respective *A. baylyi* strains were transformed by homologous recombination, and selected in the presence of kanamycin. PCR analysis with primers catA1 and catA2 (Table 2.3) was

employed to verify the inactivation of *catA*, and the obtained strains were named ADPU156 to 158 (Table 2.1), respectively.

Plasmid pIGG12 (Table 2.2), containing an inactivated *catC* gene, done by the integration of the Ω-cassette, was used to inactivate the *catC* gene in ADPU93 to 94, and ADPU102 (Table 2.1). Therefore, the *Acinetobacter* DNA was cleaved from the vector backbone by *Eco*RI, and the obtained linear DNA fragment harboring *catC*Ω was used to transform the respective *Acinetobacter* strains. Selection was performed in the presence of streptomycin and spectinomycin, and PCR analysis using primers catC1 and catC2 (Table 2.3) was employed to verify the integration at the right position. Strains containing *catC*Ω were designated ADPU159 to 161 (Table 2.1), respectively.

Plasmid pAC94 (Table 2.2; (Jerg & Gerischer, 2008)) was used to generate strains ADPU122 and ADPU123 (Table 2.1), carrying a disrupted *pcaU* gene. pAC94 carries a *pcaU* gene that was rendered non-functional by the insertion of an Ω-cassette, which carries an spectinomycin and streptomycin resistance gene. This construct was cleaved from the vector backbone by the restriction endonucleases *Not*I and *Swa*I and used for transformation of strains ADPU93 and ADPU102 (Table 2.1) by homologous recombination. Selection was performed in the presence of spectinomycin and streptomycin, and the existence of the Ω-cassette within *pcaU* was verified by PCR using primers ΔpcaU_1 and ΔpcaU_2 (Table 2.3).

To inactivate *vanR* in strains ADPU102 and ADPU123 (Table 2.1), strains were transformed with the *vanR*-Kn^r region of strain ADP9300 (Table 2.1; (Morawski *et al.*, 2000)), amplified with primer vanR1 and vanR2 (Table 2.3), obtaining strains ADPU127 and ADPU128 (Table 2.1). Selection of recombinant strains was carried out in the presence of kanamycin, and the mutation was verified by PCR using primers vanA1 and vanR1 (Table 2.3).

Inactivation of *hcaR* in strains ADPU93 and ADPU122 (Table 2.1) was carried out by amplification of the Δ*hcaR*-Kn^r region of strain KO_1728 (Table 2.1; (de Berardinis *et al.*, 2008)), using primers hcaR1 and hcaR2 (Table 2.3), and transformation of strains ADPU93 and ADPU122 by homologous recombination. Strains were selected on minimal medium containing kanamycin, and the integration of the amplified fragment into the chromosome was verified by PCR using primers hcaA4 and hcaR2. Obtained strains were named ADPU138 and ADPU139, respectively.

The deletion of *pcaH* in strains ADPU93 and ADPU102 (Table 2.1) was done accordingly, by amplification of the Δ*pcaH*-Kn^r region from strain KO_1711 (Table 2.1; (de Berardinis *et al.*, 2008)) using primer pcaH1 and pcaH2 (Table 2.3). Recombinant strains were selected using kanamycin and the presence of Δ*pcaH*-Kn^r was verified by PCR using primers pcaH1 and pcaG2 (Table 2.3). Obtained strains were designated ADPU162 and ADPU164 (Table 2.1), respectively.

The *vanB*, *quiC*, or *pobA* gene was inactivated in strain ADPU112 (Table 2.1), using a ΔvanB1/ΔvanB2, Qui606-a/Qui606-b, or pobA1/pobA2 (Table 2.3) PCR fragment containing the Δ*vanB*-Kn^r, Δ*quiC*-Kn^r, or Δ*pobA*-Kn^r region of strain KO_0979, KO_1714, or KO_1719 (Table 2.1(de Berardinis *et al.*, 2008)) for homologous recombination. Obtained strains were selected on kanamycin, and the integration of the inserted fragments at the right position was verified by PCR using primers ΔvanB1 with vanB2, quiC1 with quiC2, or pobA2 with pobA3, respectively. Obtained strains were designated ADPU153 to 155 (Table 2.1), respectively.

Each PCR used to verify the integration of a distinct fragment was carried out using primers targeting loci outside the DNA that has been used for transformation. In addition, the presence of the respective *luc* fusion was confirmed using primers hca3 and luc, dca3 and luc, vanB2 and luc, or vanK1 and luc (Table 2.3), respectively

2.2 Bacterial strains designed and used in this study

Table 2.1 gives an overview of the bacterial strains of *Acinetobacter baylyi* and *Escherichia coli* used and designed in the current thesis.

Table 2.1 Bacterial strains constructed and used in this study.

Strain	Relevant characteristics	Source or reference
A. baylyi		
ADP1	Wild-type (strain BD413; ATCC 33305)	Juni & Janik, 1969
ADP9300	*vanR*-Kn^r	Morawski *et al.* 2000
ADPU92	*benA-luc* fusion, inserted into *benA*	Fischer *et al.*, 2008
ADPU93	*hcaA-luc* fusion, inserted into *hcaA*	Fischer *et al.*, 2008
ADPU94	*dcaA-luc* fusion, inserted into *dcaA*	Fischer *et al.*, 2008
ADPU95	*areA-luc* fusion, inserted into *areA*	Fischer *et al.*, 2008
ADPU96	*antA-luc* fusion, inserted into *antA*	Fischer *et al.*, 2008
ADPU97	*benA-luc* fusion, inserted into *benA*, Δ*crc*Ω, 50 bp *Bsg*I fragment	Bleichrodt *et al.*, 2010
ADPU98	*hcaA-luc* fusion, inserted into *hcaA*, Δ*crc*Ω, 50 bp *Bsg*I fragment	Bleichrodt *et al.*, 2010
ADPU99	*dcaA-luc* fusion, inserted into *dcaA*, Δ*crc*Ω, 50 bp *Bsg*I fragment	Bleichrodt *et al.*, 2010
ADPU100	*catA-luc* fusion, inserted into *catA*	Bleichrodt *et al.*, 2010
ADPU101	*catB,C,I-luc* fusion, inserted into *catI*	Bleichrodt *et al.*, 2010
ADPU102	*vanA,B-luc* fusion, inserted into *vanB*	Bleichrodt *et al.*, 2010
ADPU104	*catA-luc* fusion, inserted into *catA*, Δ*crc*Ω, 50 bp *Bsg*I fragment	Bleichrodt *et al.*, 2010
ADPU105	*catB,C,I-luc* fusion, inserted into *catI*, Δ*crc*Ω, 50 bp *Bsg*I fragment	Bleichrodt *et al.*, 2010
ADPU106	*vanA,B-luc* fusion, inserted into *vanB*, Δ*crc*Ω, 50 bp *Bsg*I fragment	Bleichrodt *et al.*, 2010

ADPU110	*salA-luc* fusion, inserted into *salA*	Bleichrodt *et al.*, 2010
ADPU111	*salA-luc* fusion, inserted into *salA*, Δ*crc*Ω, 50 bp *Bsg*I fragment	Bleichrodt *et al.*, 2010
ADPU112	*vanK-luc* fusion, inserted into *vanK*	Bleichrodt *et al.*, 2010
ADPU113	*vanK-luc* fusion, inserted into *vanK*, Δ*crc*Ω, 50 bp *Bsg*I fragment	Bleichrodt *et al.*, 2010
ADPU120	*areA-luc* fusion, inserted into *areA*, Δ*crc*Ω, 50 bp *Bsg*I fragment	Bleichrodt *et al.*, 2010
ADPU121	*antA-luc* fusion, inserted into *antA*, Δ*crc*Ω, 50 bp *Bsg*I fragment	Bleichrodt *et al.*, 2010
ADPU122	*hcaA-luc* fusion, inserted into *hcaA*, Δ*pcaU*Ω	This work
ADPU123	*vanA,B-luc* fusion, inserted into *vanB*, Δ*pcaU*Ω	This work
ADPU124	*hcaA-luc* fusion, inserted into *hcaA*, *catM*Ω	This work
ADPU125	*dcaA-luc* fusion, inserted into *dcaA*, *catM*Ω	This work
ADPU126	*vanA,B-luc* fusion, inserted into *vanB*, *catM*Ω	This work
ADPU127	*vanA,B-luc* fusion, inserted into *vanB*, *vanR*-Kn^r	This work
ADPU128	*vanA,B-luc* fusion, inserted into *vanB*, Δ*pcaU*Ω, *vanR*-Kn^r	This work
ADPU135	*hcaA-luc* fusion, inserted into *hcaA*, Δ*benM*-Kn^r	This work
ADPU136	*dcaA-luc* fusion, inserted into *dcaA*, Δ*benM*-Kn^r	This work
ADPU137	*vanA,B-luc* fusion, inserted into *vanB*, Δ*benM*-Kn^r	This work
ADPU138	*hcaA-luc* fusion, inserted into *hcaA*, Δ*hcaR*-Kn^r	This work
ADPU139	*hcaA-luc* fusion, inserted into *hcaA*, Δ*pcaU*Ω, Δ*hcaR*-Kn^r	This work
ADPU140	*hcaA-luc* fusion, inserted into *hcaA*, Δ*benM*-Kn^r, *catM*Ω	This work
ADPU141	*dcaA-luc* fusion, inserted into *dcaA*, Δ*benM*-Kn^r, *catM*Ω	This work
ADPU142	*vanA,B-luc* fusion, inserted into *vanB*, Δ*benM*-Kn^r, *catM*Ω	This work
ADPU153	*vanK-luc* fusion, inserted into *vanK*, Δ*vanB*-Kn^r	This work
ADPU154	*vanK-luc* fusion, inserted into *vanK*, Δ*quiC*-Kn^r	This work
ADPU155	*vanK-luc* fusion, inserted into *vanK*, Δ*pobA*-Kn^r	This work
ADPU156	*hcaA-luc* fusion, inserted into *hcaA*, *catA*-Kn^r	This work
ADPU157	*dcaA-luc* fusion, inserted into *dcaA*, *catA*-Kn^r	This work
ADPU158	*vanA,B-luc* fusion, inserted into *vanB*, *catA*-Kn^r	This work
ADPU159	*hcaA-luc* fusion, inserted into *hcaA*, *catC*Ω	This work
ADPU160	*dcaA-luc* fusion, inserted into *dcaA*, *catC*Ω	This work
ADPU161	*vanA,B-luc* fusion, inserted into *vanB*, *catC*Ω	This work
ADPU162	*hcaA-luc* fusion, inserted into *hcaA*, Δ*pcaH*-Kn^r	This work
ADPU164	*vanA,B-luc* fusion, inserted into *vanB*, Δ*pcaH*-Kn^r	This work
KO_0979	Δ*vanB*-Kn^r	de Berardinis *et al.* 2008
KO_1435	Δ*benM*-Kn^r	de Berardinis *et al.* 2008
KO_1709	Δ*pcaK*-Kn^r	de Berardinis *et al.* 2008
KO_1711	Δ*pcaH*-Kn^r	de Berardinis *et al.* 2008

KO_1714	Δ*quiC*-Kn^r	de Berardinis *et al.* 2008
KO_1719	Δ*pobA*-Kn^r	de Berardinis *et al.* 2008
KO_1728	Δ*hcaR*-Kn^r	de Berardinis *et al.* 2008
E. coli		
DH5α	F$^-$, Φ80d*lacZ*ΔM15, Δ(*lacZYA-argF*)U169, *deoR*, *recA*1, *endA*1, *hsdR*17(rk$^-$, mk+), *phoA*, *supE*44, λ$^-$, *thi*-1, *gyrA*96, *relA*1	Hanahan, 1983
BL 21 (DE3)	F$^-$, *ompT*, *hsdS*$_B$ (r_B^- m_B^-), *gal*, *dcm*	Novagen®

2.3 Plasmids constructed and used in this study

All plasmids constructed and used in this study are listed in Table 2.2. Plasmids, which are part of already published experiments are not part of Table 2.2 and are listed in the corresponding publication.

Table 2.2 Plasmids constructed and used in this study.

Plasmid	Relevant characteristics	Source or reference
pBluescript II SK (+)	Ap^r, *lacZ*	Stratagene Europe, Alting-Mees & Short, 1989
pCR®II-TOPO®	Ap^r, Kn^r, *lacZ*	Invitrogen
pDrive	Ap^r, Kn^r, *lacZ*	Qiagen
pHB45Ω	Omega fragment for *in vitro* insertional mutagenesis; *aadA*$^+$ (Spc^r; Sm^r)	Prentki & Krisch, 1984
pAC94	Δ*pcaU*Ω	Jerg *et al.*, 2008
pAC115	pET28(+) containing *pcaU*, producing a C-terminal 6His-tag	Jerg *et al.*, 2008
pAC144	pBSKII containing *catM*	This work
pAC146	*catM*Ω	This work
pAC150	pDrive containing the PcaU binding site upstream of *vanK*	This work
pBAC430	pET21b containing *catM*, producing a C-terminal 6His-tag	Bundy *et al.*, 2002
pBAC433	pET21b containing *benM*, producing a C-terminal 6His-tag	Bundy *et al.*, 2002
pBAC852	*catA*-Kn^r	Provided from E. L. Neidle
pIGG12	*catC*Ω	Gaines *et al.*, 1996

Ap^r: Ampicillin resistance; Kn^r: Kanamycin resistance; Sm^r: Streptomycin resistance; Spc^r: Spectinomycin resistance

2.4 Primers used in this study

Table 2.3 gives an overview of the primers used in this study and their respective application. Primers, which are part of already published experiments are not part of Table 2.3 and are listed in the corresponding publication.

Table 2.3 Primers used in this study and their application.

Primer	Sequence (5´→ 3´)	Application
benAMop#1	CAAGATTTTGAATTTGTCGGC	Amplification of the *benM-benA* promoter region (440 bps) for EMSAs with BenM, used with benAMop#2
benAMop#2	GCTAGTATTAATGACGGGAAT	Amplification of the *benM-benA* promoter region (440 bps) for EMSAs with BenM, used with benAMop#1
benR1	TTTGGCAGGTGTAGGCATTG	Amplification of the Δ*benM*-Kn^r region of strain KO_1435, used with benR2
benR2	CAGCATCGCTTGGATCCTTC	Amplification of the Δ*benM*-Kn^r region of strain KO_1435, used with benR1
benR3	AGTATTCCTGCGGTTCTTGG	Confirmation of the insertion of the Kn^r-cassette in *benM* on the chromosome at the right position, used with benR4
benR4	TCTTGCAGTGACGGTACATC	Confirmation of the insertion of the Kn^r-cassette in *benM* on the chromosome at the right position, used with benR3
catA1	GCGGACTTGAGCAAGAAGGTG	Confirmation of the insertion of the Kn^r-cassette in *catA* on the chromosome at the right position, used with catA2
catA2	CGCTAGACGTGGACGATCAAC	Confirmation of the insertion of the Kn^r-cassette in *catA* on the chromosome at the right position, used with catA1
catB_Start	ACCCAGCAATTCGCTCACAG	Amplification of the *catM-catB* promoter region (884 bps) for EMSAs with CatM, used with catM_Start
catC1	CGGCACATGCCTTTAGTACC	Confirmation of the insertion of the Ω-cassette in *catC* on the chromosome at the right position, used with catC2
catC2	CGATTGAGCGCCATGACTTC	Confirmation of the insertion of the Ω-cassette in *catC* on the chromosome at the right position, used with catC1
catM1	GCGCTATAAGCAGCGTAAAC	Amplification of the *catM* region from chromosomal *A. baylyi* DNA; Confirmation of the insertion of the Ω-cassette in *catM* on the chromosome at the right position, used with catM2
catM2	TCTTCGTCGACCTCAATTCC	Amplification of the *catM* region from chromosomal *A. baylyi* DNA; Confirmation of the insertion of the Ω-cassette in *catM* on the chromosome at the right position, used with catM1

catM_Start	GTGCCGCATTCGATGAGTTC	Amplification of the *catM-catB* promoter region (884 bps) for EMSAs with CatM, used with catB_Start
ΔpcaU_1	GGCTATGCGAGCTTTAAGTG	Confirmation of the insertion of the Ω-cassette in *pcaU* on the chromosome at the right position, used with ΔpcaU_2
ΔpcaU_2	AGGTTCTTGCGACCTAGTTC	Confirmation of the insertion of the Ω-cassette in *pcaU* on the chromosome at the right position, used with ΔpcaU_1
ΔvanB1	AATGTCATCAGGGCACCAAG	Amplification of the Δ*vanB*-Kn^r region of strain KO_0979, used with ΔvanB2
ΔvanB2	CGGTGGGCTGTTTCATATCC	Amplification of the Δ*vanB*-Kn^r region of strain KO_0979, used with ΔvanB; Confirmation of the insertion of the Kn^r-cassette in *vanB* on the chromosome at the right position,used with vanB2
dca3	GATCGACTGGTTGGCTAATGC	Confirmation of the insertion of the *luc-aad9* cassette in *dcaA*, used with luc
dcaA_Start	CCCTTCATCGCGAATCATGC	Amplification of the *dcaA-dcaE* intergentic region (421 bps) for EMSAs with CatM/BenM, used with dcaE_Start
dcaE_Start	TTGAGGCTGGTCGGTTAATC	Amplification of the *dcaA-dcaE* intergentic region (421 bps) for EMSAs with CatM/BenM, used with dcaA_Start
GSP1_dcaA	GGATTGGTGCGTGCCATTAC	5´RACE
GSP2_dcaA	AAAGAGGCAGCATCTGAACC	5´RACE
GSP1_dcaE	GTTAAGCCGGCATTTAAGGG	5´RACE
GSP2_dcaE	TCTTCTGCTGGAACCATGAC	5´RACE
GSP1_hcaA	TGTGCCAGTTCTGTCACTTC	5´RACE
GSP2_hcaA	ACGATGCCCAACCGTATCTG	5´RACE
GSP1_hcaK	ATGGTCGACATCCGTCTTTC	5´RACE
GSP2_hcaK	TCGCCTGCCATAAGCATAGC	5´RACE
GSP1_vanA	ACAGCCCACCGCCATAACTC	5´RACE
GSP2_vanA	CCCATTCGAGTGTGGGTAAG	5´RACE
GSP1_vanK	AAGCGAACAAGTCCGATACG	5´RACE
GSP2_vanK	GTGCTTGCTTCGGTTTCTTC	5´RACE
hca3	GCCTCTTGTCCAATCAGTGATG	Confirmation of the insertion of the *luc-aad9* cassette in *hca*, used with luc
hcaA4	AGTGTGACCCATGCAATTCC	Confirmation of the insertion of the Kn^r-cassette in *hcaR* on the chromosome at the right position, used with hcaR2; Amplification of the *hcaA-hcaK* intergenic region (813 bps) for EMSAs with PcaU, used with hcaK2
hcaA_Start	CACTGCCAGCGACACGAATC	Amplification of the *hcaA-hcaK* intergentic region (902 bps) for EMSAs with CatM/BenM, used with hcaK_Start

hcaK2	ATCGCCTGCCATAAGCATAG	Amplification of the *hcaA-hcaK* intergenic region (813 bps) for EMSAs with PcaU, used with hcaA4
hcaK_Start	GCACCGCCCATACCTAAACC	Amplification of the *hcaA-hcaK* intergentic region (902 bps) for EMSAs with CatM/BenM, used with hcaA_Start
hcaR1	TTCCATTTGGAGGGCTACTG	Amplification of the Δ*hcaR*-Kn^r region of strain KO_1728, used with hcaR2
hcaR2	CCAATGAGCTGCGTTATGAC	Amplification of the Δ*hcaR*-Kn^r region of strain KO_1728, used with hcaR1; Confirmation of the insertion of the Kn^r-cassette in *hcaR* on the chromosome at the right position, used with hcaA4
luc	AAACCGGGAGGTAGATGAGATG	Confirmation of the insertion of the *luc-aad9* cassette in the chromosome at the right position, used with dca3, hca3, vanB2 and vanK1
pcaG2	CACCACCGCACCACTTAGAC	Confirmation of the insertion of the Kn^r-cassette in *pcaH* on the chromosome at the right position, used with pcaH1
pcaH1	AGGCTTACCCGCTTCAAATG	Amplification of the Δ*pcaH*-Kn^r region of strain KO_1711, used with pcaH2; Confirmation of the insertion of the Kn^r-cassette in *pcaH* on the chromosome at the right position, used with pcaG2
pcaH2	TGGACCACCTGTTTGAGATG	Amplification of the Δ*pcaH*-Kn^r region of strain KO_1711, used with pcaH1
pobA1	GGGCAGGCAAACGATTACCC	Amplification of the Δ*pobA*-Kn^r region of strain KO_1719, used with pobA2
pobA2	GTATGCGACCCAGCCTTACG	Amplification of the Δ*pobA*-Kn^r region of strain KO_1719, used with pobA1; Confirmation of the insertion of the Kn^r-cassette in *pobA* on the chromosome at the right position, used with pobA3
pobA3	GCACCCGATTGGTTTGTGAC	Confirmation of the insertion of the Kn^r-cassette in *pobA* on the chromosome at the right position, used with pobA2
Qui606-a	ATTGTCAACGACCTATGCGG	Amplification of the Δ*quiC*-Kn^r region of strain KO_1714, used with Qui606-b
Qui606-b	CAACATCAAGATTAGTGGCG	Amplification of the Δ*quiC*-Kn^r region of strain KO_1714, used with Qui606-a
quiC1	ACTGCAAATATGGGCGGTAG	Confirmation of the insertion of the Kn^r-cassette in *quiC* on the chromosome at the right position, used with quiC2
quiC2	GGGTATTGCCAAGCGTAGTC	Confirmation of the insertion of the Kn^r-cassette in *quiC* on the chromosome at the right position, used with quiC1
RT_dcaA	TCCTCGAGAGCATGAAGTTG	5´RACE
RT_dcaE	CGACCAGCCTCAAAGAATGC	5´RACE
RT_hcaA	ACGTTGGGAAACCGTTGATG	5´RACE

RT_hcaK	AGGCGCGATTATCGGTGGTC	5´RACE
RT_vanA	CCGCCCAGAAGAAATTCAAG	5´RACE
RT_vanK	ATCGGGCTTCTACTTAGTGC	5´RACE
UI-2604	CGTCCATATTTGACCACATTCC	Amplification of a fragment from the *pcaU-pcaI* intergentic region (199 bps) for EMSAs with PcaU, used with UI-2802
UI-2802	CAGTAGAATTCCCTTGTCTG	Amplification of a fragment from the *pcaU-pcaI* intergentic region (199 bps) for EMSAs with PcaU, used with UI-2604
vanA1	GTTACGCCTGAAACAGAAACG	Confirmation of the insertion of the Kn^r-cassette in *vanR* on the chromosome at the right position, used with vanR1
vanA_Start	CAAATCGTACGGCCTAATGG	Amplification of the *vanA-vanK* intergentic region (1195 bps) for EMSAs with CatM/BenM, used with vanK_Start
vanB2	TCCCAATCTGGACAGGAGATAC	Confirmation of the insertion of the Kn^r-cassette in *vanB* on the chromosome at the right position, used with ΔvanB1; Confirmation of the insertion of the *luc-aad9* cassette in *vanB*, used with luc
vanK1	TCATGCGTTGTTCGTCAAG	Confirmation of the insertion of the *luc-aad9* cassette in *vanK*, used with luc
vanK5_*Cla*I	AAGGAGGATCGATTCCCG	Amplification of a fragment from the *vanA-vanK* intergentic region (248 bps) for EMSAs and footprinting assays with PcaU, used with vanK6_*Pvu*I
vanK6_*Pvu*I	AACAGTATGATTCGATCGG	Amplification of a fragment from the *vanA-vanK* intergentic region (248 bps) for EMSAs and footprinting assays with PcaU, used with vanK5_*Cla*I
vanK_Start	CACACGCAAACAACGATCAC	Amplification of the *vanA-vanK* intergentic region (1195 bps) for EMSAs with CatM/BenM, used with vanA_Start
vanR1	CCTACGCAGCAAGAATTACC	Amplification of the *vanR*-Kn^r region of strain ADP9300, used with vanR2; Confirmation of the insertion of the Kn^r-cassette in *vanR* on the chromosome at the right position, used with vanA1
vanR2	GAAGTTTCTGCCCATCAGAC	Amplification of the *vanR*-Kn^r region of strain ADP9300, used with vanR1

2.5 Growth conditions

Strains of *A. baylyi* were grown aerobically in liquid minimal medium at 30 °C and 180 rpm, or on solid minimal media at 30 °C. The minimal media was supplemented with carbon sources as appropriate (Table 2.4). Antibiotics for *A. baylyi* strains were used in the following concentrations: spectinomycin, 100 µg/ml; streptomycin, 20 µg/ml; kanamycin, 15 µg/ml. For growth experiments, *A. baylyi* strains (Table 2.1) with luciferase transcriptional gene fusions were precultured in liquid minimal medium (5 ml) complemented with the carbon source that would later be used in the experiment (except for the aromatic compound). The main culture was then inoculated with 1 to 4 % [v/v] of an overnight culture. Growth experiments were carried out in 300 ml Erlenmeyer flasks featuring closures, containing 60 ml of liquid minimal medium, supplemented with the respective carbon source (Table 2.4) and aromatic compounds (Table 2.5).

Strains of *E. coli* were grown aerobically in liquid LB medium (5 ml) at 37 °C and 185 rpm, or solid LB medium at 37 °C, unless indicated otherwise. Antibiotics were used in the following concentrations: ampicillin, 100 µg/ml; spectinomycin, 100 µg/ml; kanamycin, 50 µg/ml; streptomycin, 20 µg/ml.

Minimal medium

Na_2HPO_4	1.4 g
KH_2PO_4	1.2 g
NH_4Cl	0.5 g
$MgSO_4$ x 7 H_2O	0.2 g
H_2O	ad 1000 ml

$FeSO_4$ (5 mg/ml)	1 ml
$CaCl_2$ x 2 H_2O (5 mg/ml)	1 ml

LB medium

Tryptone	10 g
Yeast extract	5 g
NaCl	10 g
H_2O	ad 1000 ml

For minimal media, $FeSO_4$ and $CaCl_2$ were autoclaved separately and later added to the sterilized medium to avoid side reactions.

Each medium used was sterilized for 20 min at 121 °C. Heat sensitive compounds were filtrated and later added to the medium. Agar (1.5 % [w/v]) was added for solid media.

Table 2.4 Carbon sources used for *A. baylyi* strains

Carbon source		Conc. of stock	Working conc.	Solvent
Acetate		1 M	15 mM	H_2O
Adipate	(light sensitive)	0.5 M	5 - 10 mM	H_2O*
p-Coumarate[a]	(light sensitive)	0.5 M	1 mM	H_2O*
Gluconate		1 M	20 mM	H_2O
Lactate		1 M	20 mM	H_2O
PCA[a]	(light sensitive)	0.5 M	5 mM	H_2O*
POB[a]	(light sensitive)	0.5 M	5 mM	H_2O
Pyruvate	(light sensitive)	1 M	20 mM	H_2O
Succinate		1 M	15 - 30 mM	H_2O
Vanillate[a]	(light sensitive)	0.5 M	5 - 10 mM	H_2O*
Quinate	(light sensitive)	0.5 M	5 mM	H_2O

* pH had to be adjusted with NaOH to dissolve the compound. [a]Compound was stored at -20 °C.

Table 2.5 Aromatic compounds used to influence gene expression of recombinant *A. baylyi* strains.

Carbon source		Conc. of stock	Working conc.	Solvent
Adipate[a]	(light sensitive)	0.5 M	1 mM	H_2O*
Anthranilate[a]	(light sensitive)	0.5 M	1 mM	H_2O
Benzoate	(light sensitive)	0.5 M	0.1 - 5 mM	H_2O
Benzyl alcohol[a]	(light sensitive)	0.5 M	2 mM	DMSO
p-Coumarate[a]	(light sensitive)	0.5 M	1 µM	H_2O*
PCA[a]	(light sensitive)	0.5 M	0.5 - 5 mM	H_2O*
POB	(light sensitive)	0.5 M	0.5 - 5 mM	H_2O*
Salicylate	(light sensitive)	0.5 M	0.5 mM	H_2O
Vanillate[a]	(light sensitive)	0.5 M	0.5 - 5 mM	H_2O*
Quinate	(light sensitive)	0.5 M	0.5 - 5 mM	H_2O

* pH had to be adjusted with NaOH to dissolve the compound. [a]Compound was stored at -20 °C.

2.6 Stock cultures

Each newly designed *E. coli* or *A. baylyi* strain of this study was stored as a stock culture in 10 % [v/v] DMSO at -70 °C two times independently. Strains were registered by serial numbers digitally and in written form.

2.7 Transformation

2.7.1 Transformation of *E. coli*

2.7.1.1 Competent *E. coli* DH5α cells

Cold competent *E. coli* DH5α cells (Table 2.1) for heat shock transformation were obtained following the protocol described by Inoue and colleagues (Inoue *et al.*, 1990). *E. coli* was grown overnight as a 5 ml culture in LB medium, and afterwards inoculated into 250 ml of SOB medium (2 l Erlenmeyer flask containing closures). Then the culture was grown to an OD_{600} of 0.6 at 18 °C and 60 rpm, for 18 to 24 h; followed by incubation on ice for 10 min. Cells were harvested by centrifugation (10 min, 4000 rpm, 4 °C). The pellet was washed using 80 ml ice-cold TB buffer (step repeated). Finally, the cells were resuspended in 20 ml TB buffer containing 7 % [v/v] DMSO, incubated on ice for 10 min, and aliquots were frozen using liquid nitrogen. Aliquots were stored at -70 °C.

SOB medium

Tryptone	20 g
Yeast extract	5 g
NaCl	0.5 g
KCl (0.25 M)	10 ml
H_2O	ad 1000 ml
	→ pH 7.0 with NaOH

TB buffer

PIPES	10 mM
$CaCl_2$ x 2 H_2O	15 mM
KCl	250 mM
$MnCl_2$	55 mM
	→ pH 6.7 with KOH
	filtrated, stored at 4 °C

2.7.1.2 Heat shock transformation

Heat shock transformation was employed to transform *E. coli* DH5α with plasmid DNA. Therefore, 100 µl competent *E. coli* cells were thawed on ice, followed by incubation with plasmid DNA for 30 min on ice. The heat shock was then carried out at 42 °C for 30 sec. After chilling on ice, cells were supplemented with 400 µl LB medium, and incubated for 1 h at 37 °C and 225 rpm, to regenerate. Cells were spread out on selective medium and incubated overnight at 37 °C.

2.7.1.3 Competent *E. coli* BL 21 cells

Electro competent *E. coli* BL 21 (Table 2.1) were obtained by growing an *E. coli* culture to an OD_{600} of 0.5 in 250 ml LB medium (37 °C, 185 rpm, 2 l Erlenmeyer flask containing closures). Cells were harvested by centrifugation (10 min, 5000 rpm, 4 °C) and washed with 250 ml of ice-cold H_2O. The centrifugation and washing step was repeated with 125 ml of ice-cold H_2O. The cells were centrifuged again and dissolved in 25 ml ice-cold 10 % [v/v] glycerol. This centrifugation and washing step was

repeated using 500 µl ice-cold 10 % [v/v] glycerol. Aliquots were frozen using liquid nitrogen and stored at -70 °C.

2.7.1.4 Electroporation

Electroporation of competent *E. coli* BL 21 cells (Table 2.1) was carried out using 50 µl of cells, thawed on ice. After addition of plasmid DNA, the cells were applied to an ice-cold 2 mm cuvette (Biozym). The parameters used for electroporation were: 1700 V, 200 Ohm, and 25 mF. After electroporation, cells were regenerated for 1 h in 1 ml LB medium (37 °C, 185 rpm), spread on selective medium afterwards, and incubated overnight at 37 °C.

2.7.1.5 Blue white screening

Cloning vectors (e. g. pBSKII$^+$; Table 2.2) often carry the multiple cloning site (MCS) within the *lacZ* gene, coding for the β-galactosidase. This enzyme catalyzes the conversion of X-Gal to 5-bromo-4 chloroindole (which is bright blue), in the presence of IPTG (Isopropyl β-D-1-thiogalactopyranoside). Thus, a positive recombination event is indicated by white colonies, as the integration of a DNA fragment into the *lacZ* gene impedes the formation of a functional β-galactosidase, while a negative recombination event is indicated by blue colonies. LB agar plates were used for the screening of recombinant *E. coli* cells, containing 98 µM X-Gal and 200 µM IPTG.

2.7.2 Transformation of *A. baylyi* strain ADP1

A. baylyi strain ADP1 (Table 2.1) was transformed with linear DNA fragments, directly integrating into the chromosome by homologous recombination as described earlier (Gerischer & Ornston, 1995). *A. baylyi* strains were grown overnight (30 °C, 180 rpm) as a 5 ml culture in minimal medium containing succinate (10 mM), and inoculated into fresh medium (5 % [v/v]). After 3 h of incubation (30 °C, 180 rpm), cells were concentrated by centrifugation (5 min; 5000 rpm) and resuspended in 2 ml minimal medium. Cells were then dropped on agar plates (10 mM succinate) and supplemented with the linear DNA fragment. After overnight incubation (30 °C) cells were taken, resuspended in 200 µl minimal medium, and spread on a selective agar plate. Recombinant *A. baylyi* cells were obtained after incubation for 1 to 2 days at 30 °C.

2.8 Working with nucleic acids

Each component used to work with nucleic acids was sterilized for 20 min at 121 °C to avoid contaminations of probes with interfering enzymes, proteins, and bacteria. Heat sensitive solutions were filtrated, other components sterilized by 70 % ethanol.

2.8.1 Nucleic acid isolation

2.8.1.1 Minipreparation of plasmid DNA from *E. coli* - alkaline lysis

E. coli cultures were grown overnight in 5 ml LB medium supplemented with the respective antibiotic and treated according to Birnboim and colleagues (Birnboim & Doly, 1979). First, cells were harvested by centrifugation (5 min, 5000 rpm, RT), and subsequently resuspended in 200 µl solution 1. After 5 min incubation on ice, cells were treated with 400 µl solution 2 (fresh), mixed gently and incubated for 1 min at RT (lysis). Proteins were precipitated for 5 min on ice by adding 300 µl solution 3 and subsequent centrifugation (5 min, 15000 rpm, 4 °C). The supernatant was transferred to a new tube. The DNA was precipitated for 5 min at RT by adding 0.8 vol isopropanol and following centrifugation (20 min, 15000 rpm, 4 °C). The pellet was washed using 70 % ethanol, dried (60 min, 37 °C), resuspended in 200 µl TE buffer containing RNase A (20 µg/ml; Fermentas), and incubated for 30 min at 37 °C. Further purification procedures are explained below (Chapter 2.8.2.1 and 2.8.2.2)

Solution 1

Glucose	50 mM
Tris base	25 mM
EDTA	10 mM
	→ pH 8.0 with HCl

Solution 2

SDS (10 % [w/v])	1 vol
NaOH (1 M)	1 vol
H_2O	8 vol
	→ fresh

Solution 3

Potassium acetate	3 M
→ pH 5.2 with pure acetic acid	

TE buffer

Tris base	10 mM
EDTA	1 mM
	→ pH 8.0 with HCl

2.8.1.2 Plasmid isolation using the Zyppy™ Plasmid Miniprep Kit (Zymo research)

100 µl of 7 x lysis buffer (provided) were added to 600 µl of an overnight grown *E. coli* culture and mixed gently by inverting the tube 4 to 6 times. Within 2 min 350 µl cold neutralization buffer (provided) was added and mixed thoroughly, followed by centrifugation (3 min, 13000 rpm). The supernatant was added to a Zymo-Spin™ IIN column (provided), and centrifuged (15 sec, 13000 rpm). After discarding the flow-through, 200 µl endo-wash buffer (provided) were added to the column, followed by centrifugation (15 sec, 13000 rpm), adding of 400 µl Zyppy™ wash buffer (provided), and centrifugation (30 sec, 13000 rpm). Then the column was transferred to a fresh microcentrifuge tube, followed by adding 30 µl of Zyppy™ elution buffer (provided), and incubation for 1 min at RT. DNA was eluted by centrifugation (15 sec, 13000 rpm).

2.8.1.3 Plasmid isolation using the QIAGEN Plasmid Mini Kit

5 ml of an overnight grown *E. coli* culture were harvested by centrifugation (5 min, 5000 rpm). The pellet was resuspended in 250 µl buffer P1 (provided), supplemented with RNase A (provided), followed by adding 250 µl buffer P2 (provided). The solution was briefly but thoroughly mixed by inverting the tube 4 to 6 times. After adding 350 µl buffer N3 (provided) and mixing, the solution was centrifuged (10 min, 13000 rpm), the supernatant applied to a QIAprep Spin column (provided), and the column centrifuged (30 sec, 13000 rpm). After discarding the flow-through, the column was washed by adding 750 µl buffer PE (provided), and subsequently centrifuged (30 sec, 13000 rpm). The column then was transferred to a new microcentrifuge tube, 50 µl buffer EB (provided) was applied to the column, followed by incubation for 5 min at RT. Elution of DNA then was performed by centrifugation (1 min, 13000 rpm).

2.8.1.4 Total RNA extraction using TriReagent® (Molecular Research Center, Inc.)

5 ml of an overnight grown *A. baylyi* culture were harvested by centrifugation (5 min, 5000 rpm). The pellet was resuspended in 1 ml TriReagent containing phenol (provided), and incubated for 5 min at RT. 200 µl chloroform were added, thoroughly mixed, followed by incubation for 15 min at RT. The solution was centrifuged (15 min, 8800 rpm, 4 °C) to complete the phase separation, and the aqueous phase was transferred to a fresh tube. The RNA was precipitated by adding 500 µl isopropanol, followed by incubation for 10 min at RT, and another centrifugation step (8 min, 8800 rpm, 4 °C). The RNA then was washed with 75 % ethanol, mixed, centrifuged (5 min, 5500 rpm, 4 °C), and air dried (5 min, 37 °C) to fully remove ethanol. RNA solubilization was done by dissolving the pellet in 50 µl RNase-free water, and incubation at 55 °C for 15 min. The RNA was stored at -20 °C.

2.8.2 Nucleic acid enrichment and purification

2.8.2.1 Phenol chloroform extraction

This method was used to remove proteins from a nucleic acid solution, e. g. after plasmid isolation, PCR, or other enzyme treatments. Therefore, the volume of the DNA-containing solution was adjusted to 200 µl, before the addition of 200 µl phenol/chloroform/isoamyl alcohol (25:24:1 [v/v/v]). The solution was mixed thoroughly and centrifuged (10 min, 13000 rpm) to enhance the phase separation. After transferring the aqueous phase to a new tube, carryovers of phenol were removed by adding 200 µl chloroform/isoamyl alcohol (24:1 [v/v]), followed by centrifugation (10 min, 13000 rpm) to enhance phase separation. The DNA-containing aqueous phase was transferred to a fresh tube, and treated further by ethanol-precipitation (Chapter 2.8.2.2).

2.8.2.2 Ethanol precipitation

To concentrate a DNA-containing solution, ethanol precipitation was employed, by adding 0.1 vol sodium acetate (3 M, pH 5.2) and 2 vol 100 % ethanol. Precipitation was done after incubation for 20 min at

-20 °C, and subsequent centrifugation (20 min, 15000 rpm, 4 °C). The DNA pellet was ethanol (70 %) washed, air dried (60 min, 37 °C), and resolved in 20 to 50 µl TE buffer.

2.8.2.3 Purification of PCR products using the NucleoSpin® Extract Kit (Macherey & Nagel)

The volume of the PCR sample was adjusted to 200 µl using TE buffer or water, applied to a NucleoSpin® column (provided), and centrifuged (1 min, 13000 rpm) to bind the DNA. After discarding the flow-through, 600 µl NT3 buffer (provided) were added to the column, followed by centrifugation (1 min, 13000 rpm), to wash the DNA. The flow-through was discarded, and the membrane dried by centrifugation (2 min, 13000 rpm). The membrane then was air dried (5 min, 60 °C) to fully remove buffer NT3. Elution of the DNA was performed by adding 15 to 50 µl NE buffer (provided) or water, followed by centrifugation (1 min, 13000 rpm).

2.8.2.4 Purification of radiolabled DNA fragments using MicroSpin™ G-25 columns (GE Healthcare)

Radiolabeled DNA fragments were purified using MicroSpin™ G-25 columns to remove non-incorporated radiolabeled nucleotides (e. g. [γ ^{32}P]-ATP), slats and proteins. The radiolabeled probe was applied to a resuspended column and centrifuged (2 min, 3000 rpm). The flow-through contained the purified probe, and was used for further experiments.

2.8.3 Enzymatic modification of nucleic acids

2.8.3.1 Restriction

Restriction endonucleases (Fermentas) were used to cleave DNA at a specific position. Buffers, temperatures, incubation times, and inactivation steps were applied due to manufacturers instructions (Fermentas). The enzyme concentration used was maximal 1/10th of the reaction volume, to avoid glycerol to interfere in the reaction (Fuchs & Blakesley, 1983). Restricted DNA was checked by an agarose gel electrophoresis, and purified by phenol chloroform extraction (Chapter 2.8.2.1), if necessary.

2.8.3.2 Ligation

Ligation of linear DNA fragments was performed to integrate the DNA fragment of interest into a vector molecule (plasmid). DNA fragment and vector DNA were cut with the same restriction enzymes (or enzymes creating compatible ends) and ligated using T4-DNA-ligase (Fermentas). Incubation was performed overnight in a water bath providing a linear temperature gradient, ranging from 25 to 4 °C. The enzyme was maximal 1/10th of the reaction volume, and the proportion of DNA fragment to vector DNA was 3:1.

2.8.3.3 End-labeling

Linear DNA fragments were 5´end-labeled using the T4 polynucleotide kinase (Fermentas), catalyzing the transfer of γ-phosphate from ATP to the 5´-OH group of DNA. The enzyme was used for radioactive labeling of DNA probes used in DNase I footprinting assays (Chapter 2.10.5).

2.8.4 Polymerase chain reaction (PCR)

PCR was basically used to amplify specific DNA fragments which were later used in electro mobility shift assays (Chapter 2.10.4), DNase I footprinting assays (Chapter 2.10.5), ligation procedures (Chapter 2.8.3.2), and transformation techniques (Chapter 2.7.2), or to detect mutations. In the current thesis, exclusively chromosomal DNA of *A. baylyi* strains was used as PCR template. Therefore, cells of an overnight culture were harvested by centrifugation (5 min, 5000 rpm), suspended in water, boiled for 10 min, cooled on ice and centrifuged (1 min, 13000 rpm). The supernatant contained the chromosomal DNA and was used as template. The conditions using *Taq* DNA polymerase (Genaxxon) were 95 °C for 3 min, followed by 30 cycles of denaturation for 1 min at 95 °C, annealing for 1 min at 46 to 68 °C (depending on the primers (Table 2.3)), and elongation at 72 °C for a variable period (depending on the length of the amplified fragment; 1 kb per min). PCR samples were used at a final volume of 50 µl and were composed of:

Template	2 µl
10 x PCR buffer (without $MgCl_2$)	0.1 vol
$MgCl_2$	2.5 mM
Primer 1	100 pM
Primer 2	100 pM
dNTP mix	200 µM
Taq DNA polymerase	0.5-2 U
H_2O	ad 50 µl

Obtained PCR products were analyzed running an agarose gel electrophoresis, and purified by phenol chloroform extraction (Chapter 2.8.2.1) or NucleoSpin® (Chapter 2.8.2.3), if necessary.

2.8.5 Direct cloning of PCR products

Direct cloning of PCR products was employed using the QIAGEN PCR cloning kit (vector pDRIVE), or the TOPO TA® Cloning Kit (Invitrogen™; vector pCR®II-TOPO®). Kits provided by QIAGEN and Invitrogen™ are based on linearized plasmid DNA, exhibiting a single 3´-thymidine overhang. PCR products amplified with *Taq* DNA polymerase contain a single 3´-deoxyadenosine, which allows to ligate

efficiently with the vector. As a feature, successful insertion can be tested by blue white screening, as described in Chapter 2.7.1.5.

2.8.6 Rapid amplification of cDNA ends (5´RACE)

5´RACE (Invitrogen™) is a fast and reliable method to identify the transcriptional start point of a distinct gene. The method is based on transcribing a distinct mRNA into cDNA (reverse transcription; SuperScript™ II RT; provided), using a gene specific primer 1 (GSP1; Table 2.3), followed by polydC-tailing of cDNA by the enzyme terminal deoxynucleotidyl transferase (TdT; provided). The dC-tailed cDNA is then amplified in a PCR using the abridged anchor primer (provided) and a nested gene specific primer (GSP2; Table 2.3). The obtained PCR product is then cloned into a vector as described (Chapter 2.8.5) and sequenced.

2.8.7 DNA sequencing

DNA sequencing was performed by the companies GENEWIZ Inc. or GATC Biotech AG, from plasmid DNA.

2.9 Electrophoresis

2.9.1 Agarose gel electrophoresis

Agarose gels (0.8 to 2 %) were used to analyze DNA fragments over 200 bps in size. Gels were made by melting agarose in 0.5 x TBE or TAE buffer, and pouring into a horizontal electrophoresis chamber. DNA samples mixed with 5 x loading buffer were applied to the gel after polymerization and run at 50 to 120 V in running buffer (0.5 x TBE or TAE buffer), for a variable time period. Staining was done by ethidium bromide, SYBRgreen or SYBRgold to visualize the DNA using an UV illuminator.

5 x TBE buffer

Tris base	54 g
Boric acid	27.5 g
EDTA (0.5 M; pH 8.0)	20 ml
H_2O	ad 1000 ml

5 x TAE buffer

Tris base	24.2 g
Pure acetic acid	5.71 ml
EDTA (0.5 M; pH 8.0)	20 ml
H2O	ad 1000 ml

5 x loading buffer

Ficoll 400	15 % [w/v]
Bromophenol blue	0.25 % [w/v]
Xylene cyanol	0.25 % [w/v]

2.9.2 Polyacrylamide gel electrophoresis (PAGE)

Polyacrylamide gels (6 to 8 %) were used in electro mobility shift assays (Chapter 2.10.4) to analyze protein-DNA complexes. The gel matrix contained:

	6 %	8 %
0.5 x TBE buffer	1.56 ml	2.08 ml
Rotiphorese (40 %; Bio-Rad)	1.25 ml	1.67 ml
APS (10 % [w/v])	56.3 µl	75 µl
TEMED	5.6 µl	7.5 µl
H_2O	3.44 ml	4.58 ml

Polymerization of the gel was started with the addition of APS, followed by pouring the gel into a vertical gel chamber. Samples were supplemented with 5 x loading buffer (Chapter 2.9.1) and run for a variable time period at 50 to 100 V in 0.5 TBE running buffer. Staining was done by ethidium bromide, SYBRgreen or SYBRgold to visualize the DNA using a UV illuminator.

2.9.3 Denaturing polyacrylamide gel electrophoresis

Denaturing polyacrylamide gels were used in radioactive DNase I footprinting assays (Chapter 2.10.5) to analyze DNA fragments protected from DNase I cleavage by a bound protein. To set up a denaturaing PAGE, 42.06 g urea were dissolved in 10 ml 10 x TBE and 30 ml H_2O by stirring at 80 °C in a glass beaker. The volume of the solution was adjusted to 100 ml after adding 15 ml Rotiphorese (40 %; Bio-Rad), and filtrated. TEMED (50 µl) and APS (10 % [w/v], 500 µl) were added to start the polymerization. The gel was poured into a vertical gel chamber, and incubated overnight at RT to ensure complete polymerization. DNA samples were mixed with loading buffer containing formamide and loaded. The gel run was carried out in 1 x TBE buffer at 1500 V (46 mA, 60 W) for 1.5 to 8 hours. The gel then was transferred to Whatman paper and vacuum dried for 1 h at 70 °C. Radioactivity was detected with a Bio Imager BAS (Fuji Photo Film Co., Ltd.).

Loading buffer (footprints)

Bromophenol blue	30 mg
Xylene cyanol	30 mg
EDTA (0.5 M; pH 8)	200 µl
Formamide	ad 10 ml

2.9.4 SDS polyacrylamide gel electrophoresis (SDS-PAGE)

SDS polyacrylamide gels (12 %) were used in order to analyze purity and size of proteins. The gel matrix contained:

Resolving gel

Resolving gel buffer	2.08 ml
Rotiphorese (40 %; Bio-Rad)	2.5 ml
APS (10 % [w/v])	75 µl
TEMED	7.5 µl
H_2O	2.08 ml

Stacking gel

Stacking gel buffer	1.25 ml
Rotiphorese (40 %; Bio-Rad)	1.5 ml
APS (10 % [w/v])	30 µl
TEMED	15 µl
H_2O	3.25 ml

Resolving buffer

Tris base	1.5 M
SDS	0.4 % [w/v]
H_2O	ad 1000 ml
	→ pH 8.8 with HCl

Stacking buffer

Tris base	0.5 M
SDS	0.4 % [w/v]
H_2O	ad 1000 ml
	→ pH 6.8 with HCl

Polymerization of the gel was started with the addition of APS, followed by pouring the gel into a vertical gel chamber. Samples were supplemented with 4 x SDS loading buffer and run for a variable time period at 50 to 100 V in 1 x SDS running buffer. Staining was done by coomassie or silver (Chapter 2.9.4.1 and 2.9.4.2).

10 x SDS running buffer

Glycin	2 M
Tris base	0.25 M
SDS	1 % [w/v]
H_2O	ad 1000 ml

4 x SDS loading buffer

Tris-HCl (1.25 M; pH 6.8)	10 ml
β-mercaptoethanol	10 ml
Glycerol	20 ml
SDS	2 g
Bromophenol blue	0.02 g
H_2O	ad 50 ml

2.9.4.1 Coomassie staining

SDS gels were incubated overnight in staining solution, followed by destaining in destaining solution until protein bands were visible. The two components of the staining solution were prepared separately and put together afterwards.

Staining solution component 1

G250 Brilliant Blue (Fisher-Biotech)	0.08 g
Ethanol (100 %)	20 ml
H_2O	30 ml

Staining solution component 2

Ammonium sulfate	8 g
Phosphoric acid	1.6 ml
H_2O	40.4 ml

Destaining solution

Ethanol (100 %)	16.5 ml
Acetic acid	5 ml
H_2O	78.5 ml

2.9.4.2 Silver staining

SDS gels were incubated for 30 min in fixative solution, and afterwards incubated twice with 50 % ethanol for 10 min. Thiosulfate solution was then applied to the gel for 1 min followed by three washing steps in H_2O for 5 to 10 sec. The staining solution (fresh) was added for 15 min followed by three washing steps in H_2O for 5 to 10 sec. Afterwards the gel was developed for maximal 15 min in developer solution, and the reaction was stopped by adding stop solution for 10 min.

Fixative solution

Methanol	500 ml
Formaldehyde (37 %)	0.5 ml
Acetic acid	120 ml
H_2O	ad 1000 ml

Developer solution

Na_2CO_3	6 g
Formaldehyde (37 %)	50 µl
$Na_2S_2O_3$ x 5 H_2O	0.4 mg
H_2O	ad 1000 ml

Thiosulfate solution

$Na_2S_2O_3$ x 5 H_2O	0.025 g
H_2O	500 ml

Stop solution

EDTA	14.6 g
H_2O	1000 ml

Staining solution (fresh)

Formaldehyde (37 %)	50 µl
$AgNO_3$	0.2 g
H_2O	100 ml

2.9.5 Size standards

Size standards were run alongside DNA or protein samples to directly determine their size after electrophoretic separation. For DNA size standards, λ DNA was cut with *Pst*I or *Bgl*I, creating fragments of known size. Protein samples were run alongside the PAGE-Ruler Prestained Protein-ladder (Fermentas).

2.10 Working with proteins

2.10.1 Overproduction of recombinant proteins with *E. coli* BL 21

E. coli BL 21 was transformed by electroporation (Chapter 2.7.4) with overexpression plasmids pBAC430, pBAC433, or pAC115 (Table 2.2) to produce CatM-6His, BenM-6His, or PcaU-6His, respectively. 20 ml of an overnight culture containing pBAC430 or pBAC433 were inoculated into 500 ml of autoinduction medium PA-5052 (Studier, 2005) containing ampicillin (100 µg/ml) and incubated for 13 h at 37 °C and 140 rpm. Cells then were harvested by centrifugation (10 min, 5000 rpm, 4 °C). *E. coli* cells harboring expression plasmid pAC115 were grown in 500 ml TB medium supplemented with kanamycin (50 µg/ml) at 37 °C, 140 rpm to an OD_{600} of ~3.0, and isopropyl-β-D-thiogalactopyranosite (1 mM) was added for induction. Cells were harvested after an additional 2 h incubation by centrifugation (10 min, 5000 rpm, 4 °C). Harvested cells were resolved in ice cold binding buffer, disrupted by French Press at 4 °C and subsequently centrifuged at 45000 rpm for 1.5 h at 4 °C. The supernatant was used for further treatment (Chapter 2.10.2).

Autoinduction medium (PA-5052)

$MgSO_4$ (1M)	0.5 ml
1000 x metals mix	0.5 ml
50 x 5052	10 ml
20 x NPS	25 ml
Methionine (25 mg/ml)	4 ml
17aa (each 10 mg/ml)	10 ml
H_2O	ad 500ml

TB medium (terrific broth)

Tryptone	12 g
Yeast extract	24 g
Glycerol 100 %	8 ml
Na_2HPO_4 x 2 H_2O	11.8 g
NaH_2PO_4 x 2 H_2O	2.2 g
H_2O	ad 1000 ml

17aa (amino acids); contains no Cys, Tyr, Met

1 g of each amino acid was given to 90 ml water in a glass beaker on a magnetic stirrer in the order: Glu, Asp, Lys, Arg, His, Ala, Pro, Gly, Thr, Ser, Gln, Asn, Val, Leu, Ile, Phe, Trp. The solution was then filter sterilized and kept at 4 °C.

1000 x trace metals mix

$FeSO_4$ (0.1 M)	50 ml
$CaCl_2$ (1 M)	2 ml
$MnCl_2$ (1 M)	1 ml
$ZnSO_4$ (1M)	1 ml
$CoCl_2$ (0.2 M)	1 ml
$CuCl_2$ (0.1 M)	2 ml
$NiCl_2$ (0.2 M)	1 ml
Na_2MoO_4 (0.1 M)	2 ml
Na_2SeO_4 (0.1 M)	2 ml
H_3BO_3 (0.1 M)	2 ml
H_2O	36 ml

20 x NPS

$(NH_4)_2SO_4$	6.6 g
KH_2PO_4	13.6 g
Na_2HPO_4	14.2 g
H_2O	ad 100 ml

50 x 5052

Glycerol	25 g
Glucose	2.5 g
α-Lactose	10 g
H_2O	ad 100 ml

Binding buffer

Tris base	30 mM
NaCl	500 mM
Imidazole	5 mM
Glycerol	10 mM
H_2O	ad 1000
	→ pH 7.9 with HCl

2.10.2 Purification of His-tagged recombinant proteins by high performance liquid chromatography (HPLC)

Cell extracts containing His-tagged proteins were applied to a HisTrap™ FF 1 ml Column (GE Healthcare) charged with Ni^{2+} and purified using a linear imidazole (5 mM to 500 mM) gradient against elution buffer. Desalting of purified 6His-tagged proteins was accomplished against storage buffer, using a HiTrap™ 5 ml Desalting Column (GE Healthcare). Purity of protein fractions was confirmed by running a 12 % SDS-PAGE (Chapter 2.9.4) and protein solutions were stored in 50 % [v/v] glycerol at -20 °C.

Elution buffer

Tris base	30 mM
NaCl	500 mM
Imidazole	500 mM
Glycerol	10 mM
H_2O	ad 1000
	→ pH 7.9 with HCl

Storage buffer

Tris base	50 mM
NaCl	100 mM
$MgCl_2$	10 mM
EDTA	1 mM
Glycerol	10 % [v/v]
H_2O	ad 500 ml
	→ pH 7.9 with HCl

2.10.3 Determination of protein concentrations

Protein concentration was determined using the BCA™ protein assay kit (Thermo Fisher Scientific Inc.), or the method by Bradford (Bradford, 1976) using the Bio-Rad Protein Assay Dye Reagent Concentrate, according to manufacturers instructions. Both methods required a preparation of a BSA standard curve, using defined concentrations of BSA, ranging from 0 to 2 mg/ml BSA. The protein concentrations then were determined by measuring the absorption at 562 nm (BCA™) or 595 nm (Bradford).

2.10.4 Electro mobility shift assays (EMSAs)

Electro mobility shifts assays (EMSAs) were performed to analyze the formation of protein-DNA complexes. DNA probes used in the assays were generated by PCR (Chapter 2.8.4) and purified using the NucleoSpin™ Extract Kit (Chapter 2.8.2.4). Binding of the protein to the DNA fragment was performed at 30 °C for 15 to 30 min. Samples then were applied to an agarose (Chapter 2.9.1) or polyacrylamide gel (Chapter 2.9.2), and finally analyzed after staining.

Binding reaction

10 x binding buffer + BSA	2 µl
Glycerol (100 %)	2 µl
DTT (20 mM)	1 µl
Poly [dI/dC] (1 µg/ml)	2 µl
DNA fragment	1 to 25 nM
Protein	0 to 2000 nM
H_2O	ad 20 µl

10 x binding buffer

Tris base	0.5 M
KCl	0.5 M
MgCl2	50 mM
EDTA	10 mM
H2O	ad 100 ml
	→ pH 8.0 with HCl

0.1 % BSA (100 mg/ml) was added to 10 x binding buffer right before starting the experiment.

2.10.5 DNase I footprinting assays

DNase I footprinting assays were performed to exactly identify the binding site of a DNA binding protein (e. g. transcriptional regulator). The enzyme DNase I randomly cuts DNA into fragments varying in size, creating a specific banding pattern after electrophoretic separation. In contrast, a DNA sequence can be protected by a DNA binding protein, by impeding access of DNase I to a distinct DNA region. After electrophoretic separation, this protected region is visible as a footprint in the banding pattern, where DNase I was unable to cleave (Brenowitz *et al.*, 1986).

2.10.5.1 Footprint

DNA fragments under study were radioactively end-labeled (Chapter 2.8.3.3), purified by G25 columns (Chapter 2.8.2.4), and one end removed by a specific restriction endonuclease. After second purification with G25 columns, the binding reaction was done as described (Chapter 2.10.4) using 15000 cpm of radiolabeled probe in a total volume of 200 µl. DNase I digestion was performed with 0.02 U of enzyme in buffer R1. After incubation for 1 min at room temperature digestion was stopped by adding EDTA (0.025 M), 2 vol 100 % ethanol, and 1/10 vol NaAcetate (3M, pH 5.2). DNA was precipitated for 30 min at -20 °C, centrifuged (30 min, 13000 rpm), washed with 70 % ethanol and dried. The pellet was dissolved in loading buffer and denatured for 2 min at 80 °C prior to electrophoresis. Samples were run alongside a dideoxy sequencing ladder of the same fragment on a 6 % denaturing polyacrylamide gel (Chapter 2.9.3). The gel was dried and radioactivity was detected with a Bio Imager BAS (Fuji Photo Film Co., Ltd.).

Buffer R1

$MgCl_2$	120 mM
$CaCl_2$	120 mM

2.10.5.2 Sequencing reaction

The sequencing reaction of a fragment used in footprinting assays was a need to obtain a dideoxy sequencing ladder. This sequencing ladder was run alongside of samples cleaved by DNase I, and was used to accuracy determine the regions protected by the protein. The sequencing ladder was obtained using the T7 Sequencing Kit (USB Corporation), based on the method described by Sanger (Sanger *et al.*, 1977). Plasmids containing the fragments used in the footprinting assays were used as the template. To obtain the sequencing ladder, 1.5 to 2 µg of template was incubated for 10 min at RT in a total volume of 40 µl containing 1/5 vol of NaOH (2 M). Plasmid DNA was precipitated by adding 3 vol of 100 % ethanol and 1/10 vol NaAcetate (3 M, pH 4.8) for 15 min at -20 °C and subsequent centrifugation (15 min, 15000 rpm, 4 °C). After a washing step using 70 % ethanol, the pellet was air dried at 37 °C and resolved in 10 µl H_2O. The primer annealing was carried out in a total volume of 14 µl, containing 5-10 pmol of

primer (defining the starting position of the sequencing reaction) and 1/7 vol annealing buffer (provided). The primer annealing was done after three incubation steps: 5 min at 65 °C, 10 min at 37 °C, and 5 min at RT. The prepared template was then incubated for 5 min at 37 °C, after the addition of 2 µl T7 DNA polymerase (provided), 3 µl Labeling Mix A (provided), and 1 µl [α ^{32}P]-dATP (10 µCi). This labeling reaction was then incubated for 5 min at 37 °C in four independent reactions (4.5 µl each) containing 1 µl ddATP, ddCTP, ddGTP, or ddTTP. The reaction was stopped by adding 5 µl stop solution (provided). The samples were diluted 1:10 using loading buffer (Chapter 2.9.3) and denatured at 80 °C for 2 min prior to electrophoresis.

2.11 Determination of luciferase activity

The luciferase reporter gene (*luc; Photinus pyralis*) was used to directly detect expression of several genes in recombinant *A. baylyi* strains, carrying a transcriptional luciferase reporter gene fusion (Table 2.1). Luciferase activity was detected *in vivo* using a Luminometer (flash´n glow; Berthold Detection Systems), by mixing 150 µl *Acinetobacter* cells with 150 µl luciferase buffer, followed by 4.5 sec of incubation, and addition of D-luciferin (working solution). Light emission was measured for 15 sec at 526 nm (given in RLU; relative light units). The OD_{600} of the culture was determined simultaneously, and normalization of results was done by dividing the RLU with the respective OD_{600} (specific luciferase activity). A value from the mid-logarithmic growth was read as characteristic for each strain and condition.

D-luciferin stock solution

D-luciferin (p·j·k GmbH)	9.2 mg
NaOH (33 mM)	1 ml

D-luciferin working solution

D-luciferin stock solution	0.1 ml
H_2O	10 ml

Luciferase buffer

Glycyl-Glycin	62.5 mM
$MgCl_2$	25 mM
H_2O	ad 500 ml
	→ pH 7.6 with KOH

The D-luciferin stock solution was stored in aliquots at -20 °C protected from light. The luciferase buffer was filter sterilized and stored at 4 °C. The D-luciferin working solution was prepared fresh right before starting the experiment and kept on ice protected from light.

2.12 Software tools and data banks

- NCBI Databank (http://www.ncbi.nlm.nih.gov/)
- Pattern locator (http://www.cmbl.uga.edu/software.html)
- Prodoric (http://prodoric.tu-bs.de/)

2.13 Chemicals and instruments

2.13.1 Instruments

AEG Nürnberg	Micromat 15; Microwave
Amersham Pharmacia Biotech GmbH, Freiburg	Electrophoresis Power Supply EPS 600, and 601
Appligene Heidelberg	Gel chambers
B. Braun Biotech Inter. Melsungen	Certomat ®; Incubator
Berthold Detection Systems, Pforzheim	Luminometer flash´n glow
Bio Imager Fujix BAS100	Phosphoimager
GE Healthcare GmbH, Freiburg	Electrophoresis power supply, Äkta purifier
Heidolph Instruments GmbH & Co. KG, Schwabach	Magnetic Stirrer MR2000
Heraeus Instruments GmbH, Osterode	Laminar Flow, Biofuge pico, Incubator B6
Integra Biosciences, Fernwald	Fireboy plus
Memmert GmbH & Co. KG, Schwabach	Water bath
MWG Biotech AG, Ebersberg	PCR Primus Thermocycler, Gelprint 2000i
Perkin-Elmer GmbH, Überlingen	Photometer λ 11
Sartorius AG, Göttingen	Sterile Filter (0.2 µm)
Scientific Industries INC, Bohemia, USA	Vortex-Genie
Sigma GmbH, Osterode	Laborzentrifuge Sigma 2K15
Syngene, Cambridge, UK	Gene Flash Bioimaging
Whatman, Biometra, Göttingen	T-Personal PCR Maschine
Wissenschaftliche Werkstätten, Weilheim	pH-Meter WTW pH521
Zirbus, Bad Grund	Autoclave

2.13.2 Chemicals

Serva Feinbiochemica GmbH & Co. KG, Heidelberg

Fluka, Sigma Aldrich Chemie GmbH, Deisendorf

Biomers GmbH, Ulm	Primer

Biomol Feinchem., GmbH, Hamburg	IPTG, X-Gal
Bio-Rad Laboratories, München	Rotiphorese
Carl Roth GmbH, Karlsruhe	SDS, DMSO
Difco Laboratories, Detroit, USA	Bacto-Agar, Bacto-Trypton, Yeast Extract
GE Healthcare GmbH, Freiburg	FF Column, Desalting Column, MicroSpin™ G-25 Columns
GIBCO/BRL life technologies GmbH, Eggenstein	Agarose, TEMED, Nucleotides
Invitrogen, Carlsbad, CA, USA	TOPO TA® Cloning Kit, 5´RACE Kit
Machery-Nagel GmbH, St. Leon-Rot	NucleoSpin® Extract II-Kit
MBI Fermentas GmbH, St. Leon-Rot	λ DNA, Restriction enzymes, T4 DNA-Ligase, T4-PNK, PAGE Ruler prestained protein ladder, RNase
Molecular Research Center, Inc, Cincinnati, OH, USA	TriReagent®
p·j·k GmbH, Kleinblittersdorf	D-Luciferin
Roche Diagnostics GmbH, Mannheim	Ampicillin, Kanamycin, Spectinomycin, Streptomycin
USB Corporation, Fremont, CA, USA	T7 Sequencing Kit
QIAGEN, Hilden	QIAGEN Plasmid Mini Kit, PCR Cloning Kit
Zymo Research Corporation	Zyppy™ Plasmid Miniprep Kit

3 Results

3.1 Analysis of carbon catabolite repression

Carbon catabolite repression (CCR) in *Acinetobacter baylyi* is observed in the presence of the organic acids succinate and acetate, in addition to a second carbon source (e. g. an aromatic compound; (Neidle & Ornston, 1987)). Glucose was never shown to induce CCR in *A. baylyi*, as it is the case for many Gram-negatives and Gram-positives. A lot of genes encoding enzymes involved in aromatic compound degradation through the β-ketoadipate pathway of *A. baylyi* were shown to undergo CCR by succinate and acetate in several investigations (Dal *et al.*, 2002, Siehler *et al.*, 2007, Fischer *et al.*, 2008, Bleichrodt *et al.*, 2010). Thus, CCR is considered to be of global nature, overriding the specific regulation of genes connected with the β-ketoadipate pathway. An example is the *vanA,B* operon, encoding the vanillate O-demethylase oxidoreductase. The enzyme is responsible for the degradation of vanillate to protocatechuate (PCA), and expression of *vanA,B* is activated in the presence of vanillate (Segura *et al.*, 1999, Morawski *et al.*, 2000). After introduction of the luciferase reporter gene (*luc*; *Photinus pyralis* (Bonin *et al.*, 1994)) as a transcriptional fusion into *vanB*, the operon was shown to undergo a strong repression in the presence of succinate and/or acetate although vanillate was present (Bleichrodt *et al.*, 2010). The repression was strongest, when succinate and acetate were added simultaneously (down to 10 %), compared to the activity measured in the presence of the non repressing carbon source pyruvate with the addition of vanillate.

In the current thesis, the expression of the *salA* and *vanK* genes was analyzed regarding CCR in the presence of succinate and/or acetate in addition to the specific aromatic inducer (salicylate, vanillate; Table 3.1). *salA* encodes the salicylate 1-monooxygenase required for the breakdown of salicylate to catechol ((Jones *et al.*, 2000); Fig 1.1), and *vanK* encodes a transport protein considered to be involved in vanillate uptake (Segura *et al.*, 1999, D'Argenio *et al.*, 1999). The luciferase gene was introduced as a transcriptional fusion into named genes (Fig. 3.8 and 3.9) and subsequently their expression was determined in the presence of succinate and/or acetate plus aromatic inducer or pyruvate (considered as a non repressing carbon source) plus aromatic inducer. Results obtained showed that luciferase activity of the *salA* and *vanK* operon was strongest in the presence of succinate and acetate when added in combination plus aromatic inducer, compared to the activity in the presence of pyruvate plus aromatic inducer (down to 58 % and 12 %, respectively). The presence of succinate or acetate (plus aromatic inducer), also led to a repressed expression, but to a lesser extent; down to 61 and 75 % for *salA*, and 19 and 15 % for *vanK* (published in Bleichrodt *et al*, 2010).

The knowledge of the molecular mechanism leading to this repression is still limited, but there is evidence for the involvement of a protein called Crc (catabolite repression control), originally discovered in *Pseudomonas aeruginosa* (MacGregor *et al.*, 1991, Wolff *et al.*, 1991). The *crc* gene was identified in *A. baylyi* (Zimmermann *et al.*, 2009), but how Crc operates is still not clear.

One possibility is that Crc acts at the transcriptional level. Operons encoding enzymes required for anthranilate (*ant*), benzyl esters (*are*), benzoate (*ben*), catechol (*catA*), *cis*, *cis*-muconate (*catB,C,I,J,F,D*), dicarboxylates (*dca*), hydroxycinnamates (*hca*), salicylate (*sal*), and vanillate (*vanA,B*) degradation, as well as vanillate transport (*vanK*) were shown to undergo strong CCR by succinate and acetate although the specific aromatic inducer is present (Table 3.1), using strains carrying the luciferase gene as a transcriptional fusion ((Fischer *et al.*, 2008, Bleichrodt *et al.*, 2010) Fig. 3.1 to 3.9 gives an overview of the transcriptional fusions between *A. baylyi* genes and the luciferase reporter gene, and indicates their positions on the chromosome). The repression by succinate and acetate was diminished in the absence of the *crc* gene. This was shown first for strains carrying a *benA-luc*, *catA-luc*, *catB,C,I-luc*, *dcaA-luc*, *hcaA-luc*, and *vanA,B-luc* transcriptional fusion in the presence of the substrate combination succinate and acetate in addition to the aromatic inducer (Bleichrodt, 2007), and extended for strains carrying a *antA-luc*, *areA-luc*, *salA-luc*, and *vanK-luc* transcriptional fusion and a deleted *crc* gene, in the current study. In addition, the analysis was extended using either succinate or acetate in addition to the aromatic inducer. The activity of operons in a *crc* negative background in the presence of succinate and/or acetate plus specific aromatic inducer (Table 3.1) was therefore compared to the activity shown by the respective *crc* positive strain. Results obtained showed that almost all the operons (with the exception of *catA*) responded with a derepression of promoter activity on the substrate combination succinate and acetate to various degrees (from 3-fold for the *sal* operon, up to 28-fold for the *ben* operon) in comparison to the *crc* positive strain. Results obtained in the presence of succinate or acetate, were comparable to those on the substrate combination, except for a few cases. The most notably here was the *ben* operon, as the absence of *crc* led to a repression on succinate (down to 13 %), while no significant effect was detected on acetate. Regarding the activity of the *ben* operon on succinate, Crc seems to have an activating effect. This activating effect was not observed until now and could be the subject of future investigations. However, the observation of a derepression in the absence of Crc first made for *pca-qui*, can now be extended to almost all operons investigated here.

Results described above were completely published in 2010 (Bleichrodt *et al.*, 2010), and the corresponding publication is attached to this work.

Table 3.1. Aromatic compounds used for induction of analyzed operons.

Operon	Aromatic compound	Concentration
ant	Anthranilate	1.0 mM
are	Benzyl alcohol	2.0 mM
ben	Benzoate	0.5 mM
catA	Benzoate	0.5 mM
catB,C,I,J,F,D	Benzoate	0.5 mM
dca	Adipate	1.0 mM
hca	*p*-Coumarate	1.0 µM
sal	Salicylate	0.5 mM
vanA,B	Vanillate	0.5 mM
vanK	Vanillate	0.5 mM

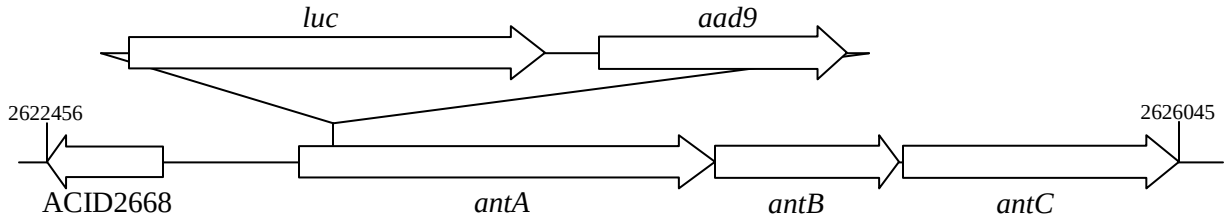

Figure 3.1. *ant* region (the position on the chromosome is given). *antA:* anthranilate dioxygenase large subunit; *antB*: anthranilate dioxygenase small subunit; *antC*: anthranilate dioxygenase reductase; ACID2668: hypothetical protein; *luc*: luciferase reporter gene; *aad9*: spectinomycin resistance cassette. *antA-luc* fusion in strain ADPU96 (Fischer *et al.*, 2008).

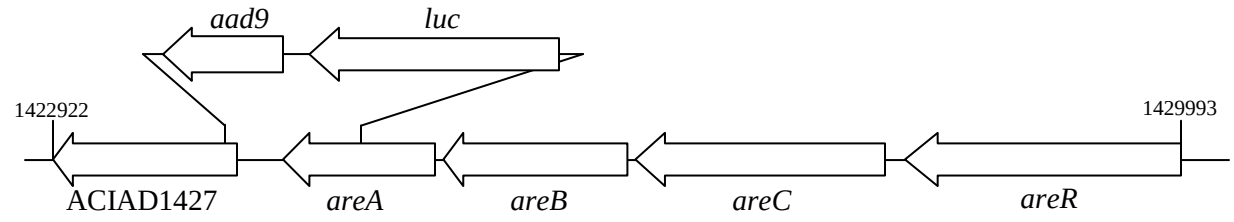

Figure 3.2. *are* region (the position on the chromosome is given). ACIAD1427: putative fatty acid and hydrocarbon transporter; *areA*: esterase; *areB*: aryl-alcohol dehydrogenase; *areC*: benzaldehyde dehydrogenase II; *areR*: transcriptionnal regulator for *areCBA* operon; *luc*: luciferase reporter gene; *aad9*: spectinomycin resistance cassette. *areA-luc* fusion in strain ADPU95 (Fischer *et al.*, 2008).

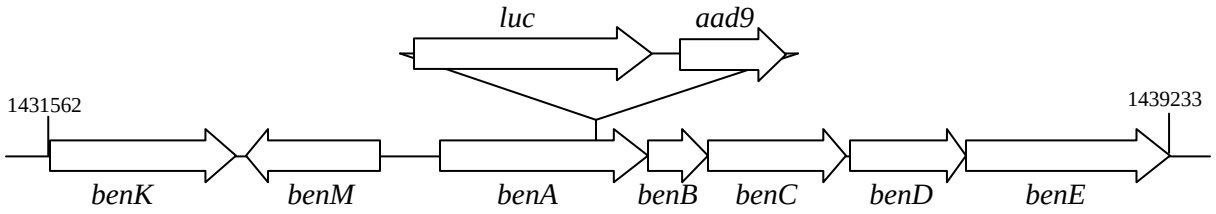

Figure 3.3. *ben* region (the position on the chromosome is given). *benK*: benzoate membrane transporter; *benM*: transcriptional regulator for benzoate metabolism; *benA*: benzoate 1,2 dioxygenase α subunit; *benB*: benzoate 1,2 dioxygenase β subunit; *benC*: benzoate 1,2 dioxygenase ferredoxin reductase subunit; *benD*: 1,6-dihydroxycyclohexa-2,4-diene-1-carboxylate dehydrogenase; *benE*: benzoate membrane transporter (MFS); *luc*: luciferase reporter gene; *aad9*: spectinomycin resistance cassette. *benA-luc* fusion in strain ADPU92 (Fischer *et al.*, 2008).

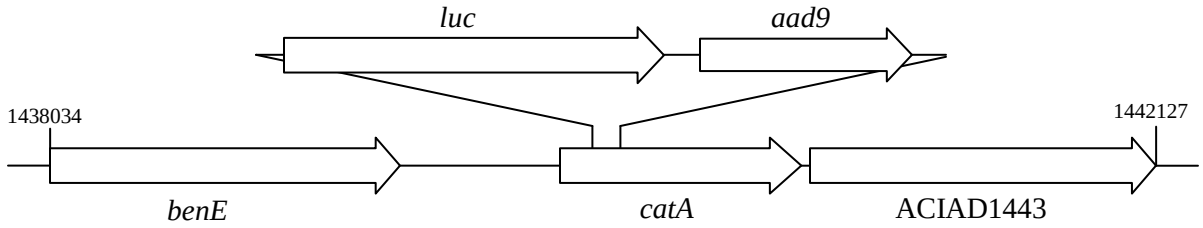

Figure 3.4. *catA* region (the position on the chromosome is given). *benE*: benzoate membrane transporter (major facilitator superfamily); *catA*: catechol 1,2 dioxygenase; ACID1443: hypothetical protein; *luc*: luciferase reporter gene; *aad9*: spectinomycin resistance cassette. *catA-luc* fusion in strain ADPU100 (Bleichrodt *et al.*, 2010).

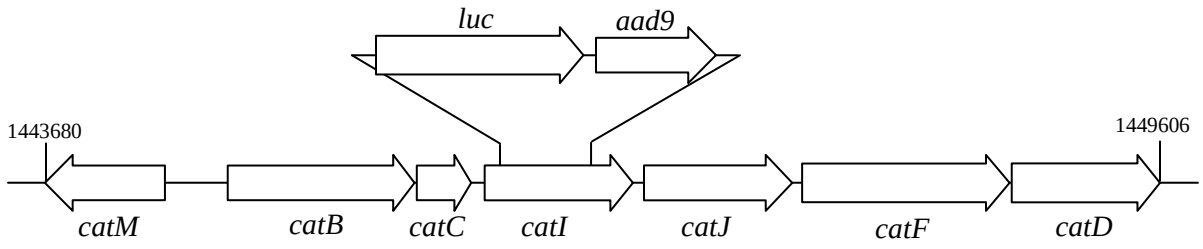

Figure 3.5. *catB,C,I,J,F,D* region (the position on the chromosome is given). *catM*: transcriptional regulator for catechol metabolism; *catB*: *cis,cis*-muconate lactonizing enzyme I; *catC*: muconate delta-isomerase; *catI*: β-ketoadipate:succinyl-CoA transferase subunit A; *catJ*: β-ketoadipate:succinyl-CoA transferase subunit B; *catF*: β-ketoadipyl CoA thiolase; *catD*: β-ketoadipate enol-lactone hydrolase II; *luc*: luciferase reporter gene; *aad9*: spectinomycin resistance cassette. *catB,C,I-luc* fusion in strain ADPU101 (Bleichrodt *et al.*, 2010).

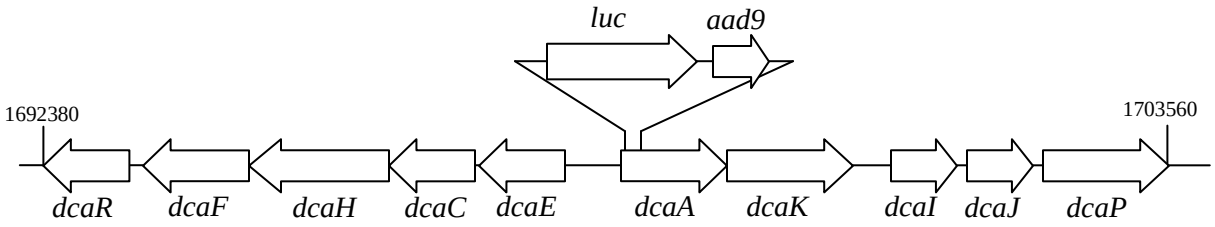

Figure 3.6. *dca* region (the position on the chromosome is given). *dcaR*: transcriptional regulator; *dcaF*: acetyl-CoA acetyltransferase; *dcaH*: 3-hydroxybutyryl-CoA dehydrogenase; *dcaC*: 3-ketoacyl-(acyl-carrier-protein) reductase; *dcaE*: enoyl-CoA hydratase; *dcaA*: acyl-CoA dehydrogenase; *dcaK*: dicarboxylic acid transport protein (MFS); *dcaI*: acyl-CoA-transferase subunit A; *dcaJ*: acyl-CoA-transferase subunit B; *dcaP*: porin precursor in catabolism of dicarboxylic acids; *luc*: luciferase reporter gene; *aad9*: spectinomycin resistance cassette. *dcaA-luc* fusion in strain ADPU94 (Fischer *et al.*, 2008).

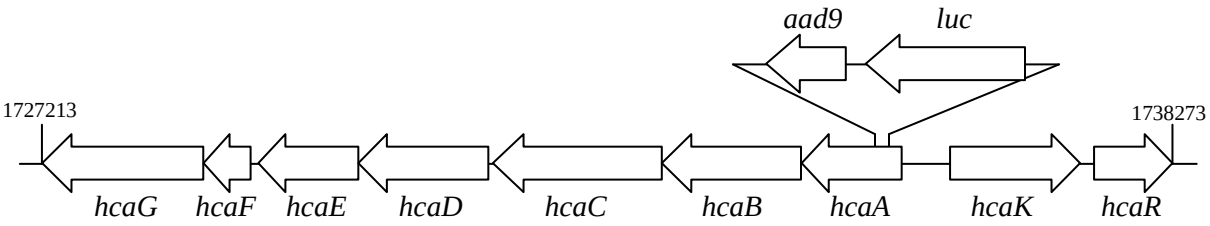

Figure 3.7. *hca* region (the position on the chromosome is given). *hcaG*: chlorogenate esterase; *hcaF*: hypothetical protein; *hcaE*: putative porin; *hcaD*: acyl-CoA dehydrogenase; *hcaC*: acyl-CoA ligase; *hcaB*: aldehyde dehydrogenase; *hcaA*: hydroxycinnamoyl-CoA hydratase/lyase; *hcaK*: putative hydroxycinnamate transporter; *hcaR*: transcriptional regulator for hydroxycinnamate metabolism; *luc*: luciferase reporter gene; *aad9*: spectinomycin resistance cassette. *hcaA-luc* fusion in strain ADPU93 (Fischer *et al.*, 2008).

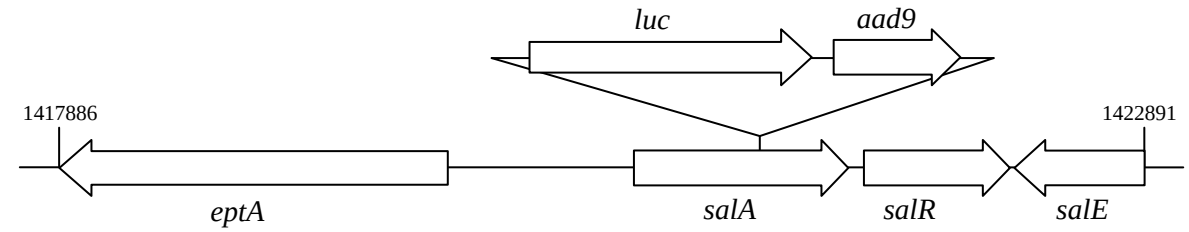

Figure 3.8. *sal* region (the position on the chromosome is given). *eptA*: lipid A phosphoethanolamine transferase (associated with polymyxin resistance); *salA*: salicylate 1-monooxygenase; *salR*: transcriptional regulator for salicylate metabolism; *salE*: salicylate esterase; *luc*: luciferase reporter gene; *aad9*: spectinomycin resistance cassette. *salA-luc* fusion in strain ADPU110 (Bleichrodt *et al.*, 2010).

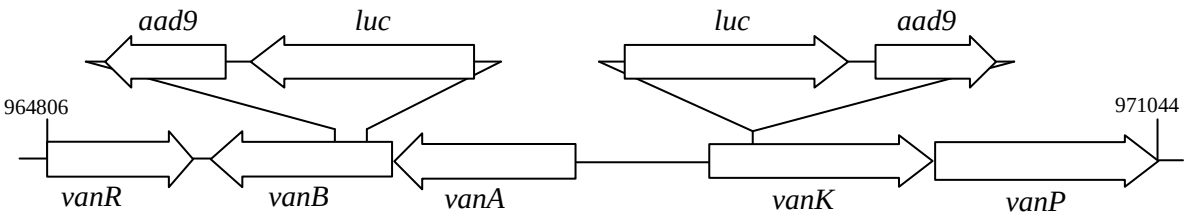

Figure 3.9. *van* region (the position on the chromosome is given). *vanR*: transcriptional regulator for vanillate metabolism; *vanB*: vanillate O-demethylase oxidoreductase; *vanA*: vanillate O-demethylase oxygenase subunit; *vanK*: vanillate transporter (major facilitator superfamily); *vanP*: putative porin for vanillate trafficking; *luc*: luciferase reporter gene; *aad9*: spectinomycin resistance cassette. *vanA,B-luc* fusion in strain ADPU102; *vanK-luc* fusion in strain ADPU112 (Bleichrodt *et al.*, 2010).

3.2 Expression pattern in the presence of lactate and gluconate

A. baylyi is able to grow with pyruvate, lactate, glucose, gluconate, succinate, and acetate. Succinate and acetate were shown to repress expression of several operons involved in aromatic compound degradation through the β-ketoadipate pathway, when added simultaneously with the respective aromatic compound ((Dal *et al.*, 2002, Siehler *et al.*, 2007, Fischer *et al.*, 2008, Bleichrodt *et al.*, 2010), Chapter 3.1). In contrast, pyruvate is considered to be a non-repressing carbon source regarding those operons. Lactate can easily be converted to pyruvate by the action of lactate/pyruvate dehydrogenase, and may thus have related effects. Glucose leads to CCR in many bacteria (e. g. *E. coli*); it is the precursor of gluconate in glucose metabolism in *A. baylyi*; it was thus interesting to investigate its effect. However, gluconate turned out to be a better growth substrate for *A. baylyi* and was chosen instead of glucose.

To analyze the nature of lactate and gluconate of being a repressing or non repressing carbon source in addition to the respective aromatic inducer (Table 3.1), the expression of the *ant*, *are*, *catA*, *catB,C,I,J,F,D*, *vanA,B*, *salA*, and *vanK* operons was analyzed using luciferase reporter gene strains (Fig. 3.1 to 3.9). The transcriptional activity of operons under study in the presence of lactate or gluconate in addition to the aromatic inducer was compared to the activity shown in the presence of pyruvate (considered as non-repressing) plus aromatic inducer. Results identified lactate as a non-repressing carbon source for the *catB,C,I,J,F,D* and *salA* genes, while a slight repressing effect was observed for *vanA,B* and *vanK* (down to 58 and 46 %), as previously shown for *antA* and *areA* (Fischer *et al.*, 2008). Gluconate turned out to have no repressing effect on the *salA* gene, a slight repressing effect on the *areA* gene (down to 63 %), and a moderate repressing effect on the *vanA,B*, *vanK*, *catB,C,I,J,F,D*, and *antA* genes (down to 48, 36, 35, and 16 %). The results obtained for *catA* were most remarkable; lactate turned out to be a repressing carbon source (*catA* activity was down to 10 %), whereas gluconate caused an increased

expression (up to 2.4-fold). Taken together, lactate and gluconate seem to be a repressing or non repressing carbon source for the operons analyzed (with the exception of *catA* on gluconate).

These findings were completely published in 2010, and the corresponding publication is attached to this work.

It was further interesting to analyze if the Crc protein affects the expression of operons involved in aromatic compound degradation in the presence of pyruvate, lactate, and gluconate in addition to the aromatic inducer (Induced activity; Table 3.1). Strains analyzed in luciferase assays (Chapter 2.11) carried a transcriptional luciferase fusion in genes *antA*, *areA*, *benA*, *catA*, *catI*, *dcaA*, *hcaA*, *salA*, *vanB*, or *vanK* (Fig. 3.1 to 3.9) and a deleted *crc* gene, and were constructed as described by Bleichrodt *et al.*, 2010. The impact of Crc on the expression of operons was determined by comparing the transcriptional activity in the *crc* positive strain, with the one of the *crc* negative strain. In addition to the determination of the induced activity, the basal activity (no aromatic compound) of the operons was measured, basically to ensure an induction of the operons by the specific inducer, by comparing the basal activity with the induced activity. Results obtained are shown in Fig. 3.10 (and in tabular form in Chapter 10.1).

Using pyruvate as the carbon source in addition to the aromatic inducer, expression of the *catB,C,I,J,F,D*, *dca*, and *salA* operons did not change significantly with the deletion of *crc*, suggesting that Crc does not influence gene expression of these operons under these conditions. The activity of the *ben*, *catA*, *hca*, *vanA,B*, and *vanK* operons increased to various degrees in the absence of Crc, suggesting that Crc negatively affects gene expression in the presence of pyruvate. In contrast, the *ant* and *are* operons responded with a decrease in expression to the absence of Crc. This observation of a decrease in activity in a *crc* negative background was previously observed for the *ben* operon in the presence of succinate and specific inducer (Chapter 3.1). Here, Crc seems to have an activating effect, and the analysis of this effect could be the subject of future investigations.

Using lactate as the carbon source in addition to the aromatic inducer, the absence of Crc led to an increase of promoter activity of the *dca*, *salA*, *vanA,B*, and *vanK* operons, while a decrease of promoter activity was observed for the *ant*, *are*, and *ben* operons. This effect was previously seen for the activity of the *ben* operon on succinate (Chapter 3.1), and for the activity of the *ant* and *are* operons in the presence of pyruvate. Again, Crc seems to have an activating effect, and the analysis of this effect could be the subject of future investigations. In contrast, Crc does not seem to affect the expression of the *catA*, *catB,C,I,J,F,D*, and *hca* operons significantly in the presence of lactate.

Expression of the *ant*, *ben*, *catA*, *dca*, *hca*, and *vanK* operons turned out to be independent of Crc in the presence of gluconate in addition to the aromatic inducer, as expression did not change significantly with

the deletion of *crc*. However, a slight decrease in transcriptional activity was determined for the *catB,C,I,J,F,D* operon in a *crc* negative background. Interestingly, strains carrying a *areA-luc*, *salA-luc*, and *vanA,B-luc* transcriptional fusion and a deleted *crc* gene, did not show any growth in the presence of gluconate. This effect was not observed until now and could be the subject of future investigations. Nevertheless, results presented for the *ant*, *ben*, *catA*, *catB,C,I,J,F,D*, *dca*, *hca*, and *vanK* operons suggest that expression of most operons is independent of Crc when gluconate is the sole carbon source.

Taken together, Crc seems to have no effect on the expression of the *catB,C,I,J,F,D* operon under any condition tested; only a slight decrease of promoter activity was observed in the presence of gluconate. The other operons (with the exception of *ben*), either showed an increased/unmodified (*catA*, *dca*, *hca*, *salA*, *vanA,B*, *vanK*) or a decreased/unmodified (*ant*, *are*) expression in the absence of Crc. The expression of the *ben* operon was ambivalent, as it responded with an increased activity in the presence of pyruvate, a decreased activity in the presence of lactate, and no change in the presence of gluconate when *crc* was silenced.

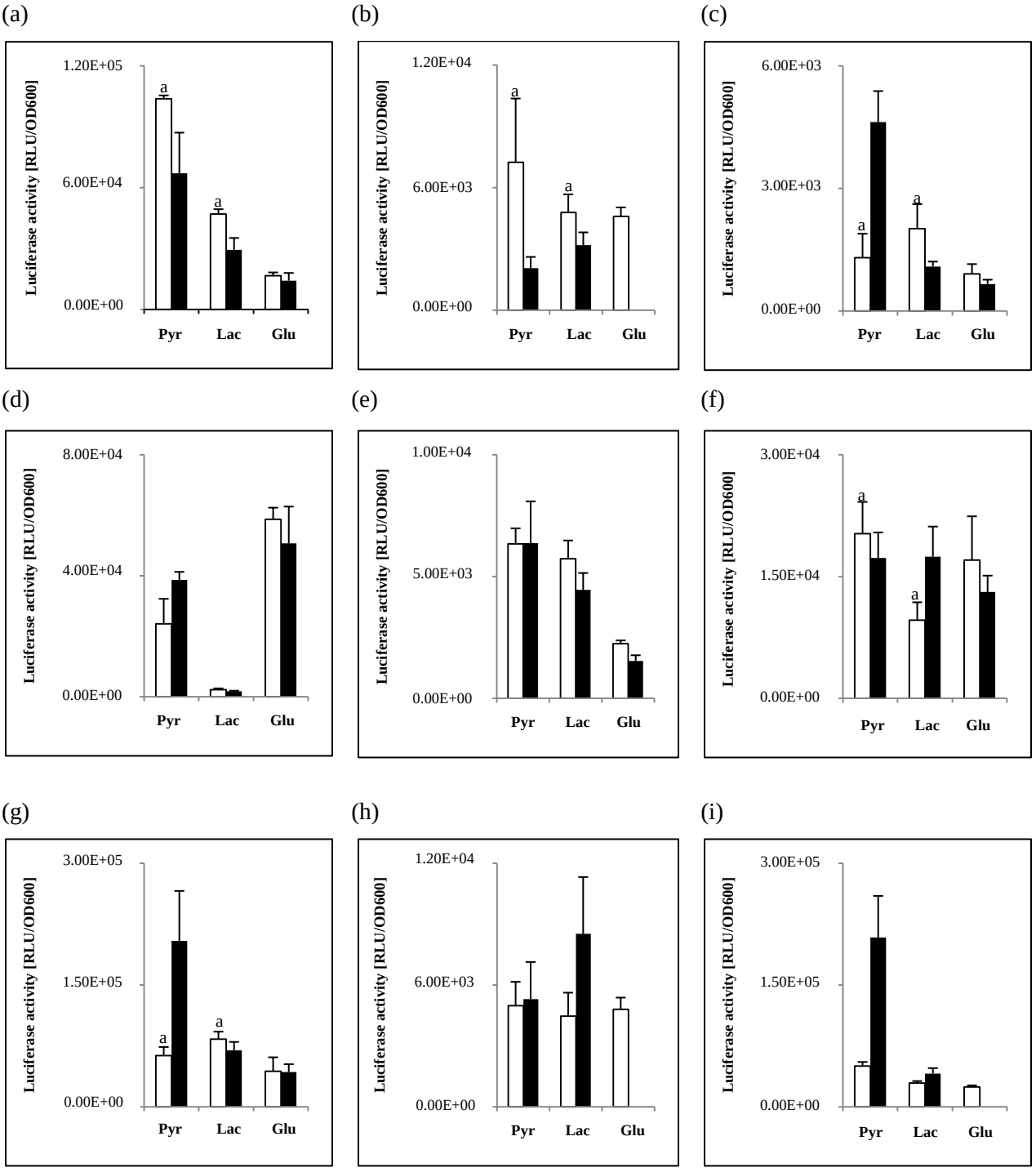
(a)
(b)
(c)
(d)
(e)
(f)
(g)
(h)
(i)
Luciferase activity [RLU/OD600]
1.20E+05
6.00E+04
0.00E+00
1.20E+04
6.00E+03
6.00E+03
3.00E+03
8.00E+04
4.00E+04
1.00E+04
5.00E+03
3.00E+04
1.50E+04
3.00E+05
1.50E+05
a
Pyr
Lac
Glu

(j)

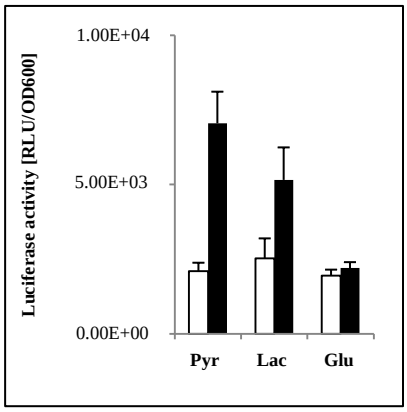

Figure 3.10. Expression pattern in the presence of pyruvate, lactate, and gluconate in addition to the aromatic inducer, depending on the presence of Crc. Expression of the (a) *ant*, (b) *are*, (c) *ben*, (d) *catA*, (e) *catB,C,I,J,F,D*, (f) *dca*, (g) *hca*, (h) *salA*, (i) *vanA,B*, and (j) *vanK* operons is shown as specific luciferase activity in the presence of pyruvate (Pyr), lactate (Lac), or gluconate (Glu; 20 mM each) with the addition of the specific aromatic inducer (anthranilate, 1 mM (*ant*); benzyl alcohol, 2 mM (*are*); benzoate, 0.5 mM (*ben*, *catA*, *catB,C,I,J,F,D*); adipate, 1 mM (*dca*); *p*-coumarate, 1 µM (*hca*); salicylate, 0.5 mM (*salA*); vanillate, 0.5 mM (*vanA,B, vanK*)), in a crc^+ (white bars) or crc^- (black bars) background. Values are means of at least three independent experiments. Error bars indicate standard deviation. [a] Fischer *et al.*, 2008.

The results presented in Fig. 3.10 for the *ant*, *are*, *ben*, *catA*, *catB,C,I,J,F,D*, *dca*, *hca*, *salA*, *vanA,B*, and *vanK* operons were obtained under inducing conditions (pyruvate, lactate, gluconate plus aromatic inducer), in a *crc* positive vs. a *crc* negative background. In addition, the expression of operons was checked on pyruvate, lactate, and gluconate under uninducing conditions (without the addition of the aromatic compound; basal activity), in the *crc* positive and the *crc* negative strains (see supplementary data in Chapter 10.1). This was done basically, to assure an induction of the operons by the aromatic inducer, by comparing the basal activity with the induced activity. This was true in each case, since the expression in the presence of the aromatic inducer was higher than the basal activity for each operon and condition. Interestingly, a difference in the basal activity was seen for some operons by comparing the activity seen in a *crc* positive with the respective activity seen in a *crc* negative background. For example, the basal activity observed for the *hca* operon was strongly repressed in a *crc* negative background in the presence of pyruvate, lactate, and gluconate, compared to the one measured in a *crc* positive background (Table 10.7). That was also true for the *ant* operon in the presence of pyruvate (Table 10.1). A slight decrease of the basal activity was determined for *catA* on gluconate (Table 10.4), *vanA,B* on pyruvate and lactate (Table 10.9), and *vanK* on pyruvate (Table 10.1). Thus again, an activating effect was observed for Crc. The opposite was seen for the *are* operon, since its basal expression was increased in the presence of pyruvate and lactate in a *crc* negative background (n. g. on gluconate; Table 10.2). No change was observed for the basal activity of the *ben*, *catB,C,I,J,F,D*, and *sal* oerons (Table 10.3, 10.5, and 10.8).

Taken together, Crc seems to affect gene expression not only in the presence of pyruvate, lactate, and gluconate in the presence of an aromatic inducer (induced conditions), since a change in the basal activity is also visible. However, the effects determined for Crc under uninducing conditions do not correspond with the effects seen under inducing conditions. An exception is the *catB,C,I,J,F,D* operon, since its expression was never affected by Crc, independent of the induction status. These results may indicate that

Crc is a true global regulator, acting independent of the presence of aromatic compounds in addition to a second carbon source. The analysis of these findings could be subject of future investigations.

3.3 Analysis of cross-regulation

Cross-regulation was first described in *P. putida* in 1995, where POB uptake and degradation is repressed in the presence of benzoate (Nichols & Harwood, 1995), a substrate that is degraded through the catechol branch of the β-ketoadipate pathway, while POB is degraded through the PCA branch. Studies dealing with cross-regulation in *A. baylyi* showed that the presence of benzoate in addition to POB leads to a repressed expression of *pobA*, compared to the induced activity (only POB), and preferred benzoate degradation (Gaines *et al.*, 1996, Brzostowicz *et al.*, 2003). This repression was further observed for the *pca* genes (Siehler *et al.*, 2007), as well as for the *hca*, *vanA,B*, and *dca* genes (Bleichrodt *et al.*, 2010).

Almost all operons under cross-regulation encode enzymes dealing with the degradation of aromatic compounds through the PCA branch of the β-ketoadipate pathway (Fig. 1.1; *pca-qui*, *pobA*, *hca*, *vanA,B*). However, the *dca* genes do not; they form a short funneling pathway feeding dicarboxylates into the pathway at the level of β-ketoadipyl-CoA (Fig. 1.1). Nevertheless, cross-regulation is commonly described as a cross-talk between the two main branches of the pathway, creating a priority of benzoate consumption through the catechol branch over any substrate of the PCA branch.

Questions arose about the molecular mechanism leading to cross-regulation, and a study focused on the two transcriptional regulators BenM and CatM, LysR-type transcriptional regulators responsible for activating *ben* and *cat* gene expression in response to benzoate and/or CCM. In addition, they control their own expression by autoregulation, acting as repressors (Ezezika *et al.*, 2006, Craven *et al.*, 2008). In cross-regulation, they were shown to be involved in repression of the *pobA* gene, since *benM* and *catM* negative strains did not show preferred benzoate consumption (Brzostowicz *et al.*, 2003). But rather than binding to the *pobA* promoter repressing expression, they were shown to bind within regulatory regions of the *pca* genes. The authors suggested that binding of BenM and CatM to those regions is repressing *pcaK* gene expression (as a part of the *pca* operon), encoding the PCA and POB uptake protein. Exclusion of POB from the cell would inhibit *pobA* activation by PobR in response to POB. Similar observations were made for *P. putida pcaK* (Cowles *et al.*, 2000).

The analysis of the molecular mechanisms leading to cross-regulation of the *hca*, *dca*, and *vanA,B* operons is described in the following chapters. The effector leading to cross-regulation at *hca* and *vanA,B* was identified, as well as the regulatory proteins mediating repression. Hints about how cross-regulation could

work for the *hca* and *vanA,B* operons, were derived from bioinformatical and molecular approaches including electro mobility shift assays, and 5´RACE.

3.3.1 Searching the effector

While BenM is able to respond to benzoate and CCM, CatM is only able to bind CCM (Ezezika *et al.*, 2006, Craven *et al.*, 2009), a metabolite of benzoate degradation through the catechol branch (Fig. 1.1). Since there was evidence for CCM being the effector for cross-regulation of *pobA* (Brzostowicz *et al.*, 2003), CCM was supposed to also be involved in repression of the *hca*, *dca*, and *vanA,B* genes. To test this hypothesis, a block in CCM formation was constructed in several luciferase reporter gene strains (ADPU93, *hcaA-luc*; ADPU94, *dcaA-luc* (Fischer *et al.*, 2008); ADPU102, *vanA,B-luc* (Bleichrodt *et al.*, 2010); Table 2.1), by inactivating *catA* as described in methods (Chapter 2.1). Strains were designated ADPU156 (*hcaA-luc, catA*-Kn^r), ADPU157 (*dcaA-luc, catA*-Kn^r), and ADPU158 (*vanA,B-luc, catA*-Kn^r) (Table 2.1). The parental strains (ADPU93, ADPU94, ADPU102) showed a strong repression of promoter activity in the presence of benzoate in addition to the specific aromatic inducer (*p*-coumarate, adipate, vanillate), compared to the induced conditions without benzoate (Bleichrodt *et al.*, 2010). The newly designed strains were analyzed using the same conditions. Pyruvate was used as the carbon source, since it was shown to have no repressing effect on expression of operons connected with aromatic compound degradation (Dal *et al.*, 2002, Fischer *et al.*, 2008, Bleichrodt *et al.*, 2010). Luciferase activity (directly reflecting gene activity) was measured upon growth (Chapter 2.11) in the presence of the aromatic inducer (*p*-coumarate, 1 µM; adipate, 1 mM; vanillate, 0.5 mM) with or without the addition of benzoate (1 mM for ADPU156 and ADPU158; 3 mM for ADPU157). A concentration of 3 mM benzoate was chosen for *dca*, since the operon did not show a repression by benzoate at concentrations lower than 2 mM. In contrast, a concentration of 1 mM benzoate was sufficient to repress *hca* and *vanA,B* activity (Bleichrodt *et al.*, 2010). The basal activity (no aromatic compound) of each gene was determined without any aromatic compound added, to assure an induction of the operons by the aromatic inducer, by comparing the basal activity with the induced activity

An inactivation of *catA* resulted in a loss of repression in the presence of benzoate with regard to the *hca* and *vanA,B* genes, as shown in Fig. 3.11 (a), (b), and Table 3.2. Here, gene activity in the presence of benzoate was at least as high as the induced activity measured without benzoate. Thus, blocking CCM formation in the *hcaA-luc* and *vanA,B-luc* strains resulted in a complete loss of cross-regulation at these operons, indicating that CCM is the effector mediating *hca* and *vanA,B* repression. However, the *dca* operon still showed repression by benzoate after inactivation of *catA*, and this repression appears to be independent of CCM formation (Fig. 3.11 (c), Table 3.2).

To further support the hypothesis of CCM being the effector releasing cross-regulation and to exclude down-stream metabolites, an inactivation of *catC* was constructed based on strains ADPU93 (*hcaA-luc*), ADPU94 (*dcaA-luc*), and ADPU102 (*vanA,B-luc*), as described (Chapter 2.1). Strains obtained were designated ADPU159 (*hcaA-luc*, *catC*Ω), ADPU160 (*dcaA-luc*, *catC*Ω), and ADPU161 (*vanA,B-luc*, *catC*Ω) (Table 2.1). The expression of the respective genes was expected to be the same as for the parental strain, since CCM formation is not impeded, otherwise as in the *catA* negative strains. In contrast to this expectation, strains blocked in CCM degradation did not show any growth in the presence of benzoate, possibly due to the toxic accumulation of CCM.

The basal activity (absence of any aromatic compound) of the *hca*, *dca*, and *vanA,B* operons in a *catA* negative background (Table 3.2) was also determined, basically to assure an induction of the operons by the aromatic inducer, by comparing the basal activity with the induced activity. This was true in each case, since the expression in the presence of the aromatic inducer was higher than the basal activity for each operon. Interestingly, a slightly but significant increase of the basal activity was seen for the *dca* and *vanA,B* operons by comparing the basal activity seen in a *catA* positive with the respective activity seen in a *catA* negative background, which was unexpected. However, this increase is negligible compared to the increase of promoter activity in the presence of the specific aromatic inducer. The molecular basis of this observation remains hidden so far, and could be the subject of future investigations.

Taken together, the block in CCM formation led to a complete loss of cross-regulation (transcriptional repression) of the *hca* and *vanA,B* operons in the presence of benzoate and aromatic inducer (*p*-coumarate, vanillate). This was not observed for the *dca* operon. Table 3.2 summarizes these results; benzoate led to a repressed activity of *hca* and *vanA,B* (ADPU93 and ADPU102) although the specific aromatic inducer is present. This repression is completely lost by inactivating *catA* (resulting in a block in CCM formation; ADPU156 and ADPU158), since the activity of the *hca* and *vanA,B* operon measured in a *catA* negative background in the presence of benzoate in addition to the specific aromatic inducer is as high as in the absence of benzoate. These findings may refer to the conclusion, that CCM is the effector releasing cross-regulation at *hca* and *vanA,B*. However, downstream metabolites cannot be excluded at this point. The repression observed for *dca* seems to be independent of CCM.

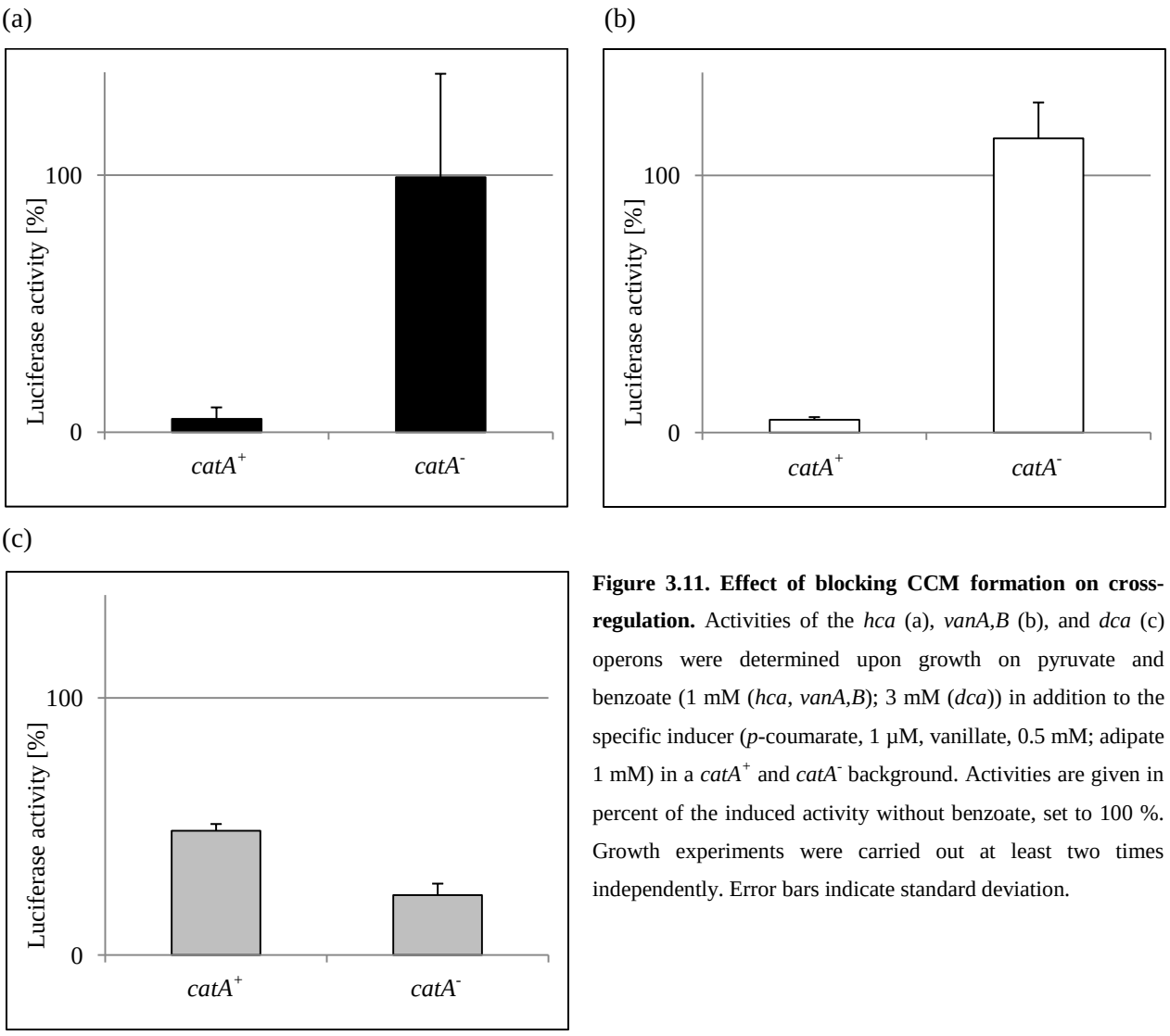

Figure 3.11. Effect of blocking CCM formation on cross-regulation. Activities of the *hca* (a), *vanA,B* (b), and *dca* (c) operons were determined upon growth on pyruvate and benzoate (1 mM (*hca*, *vanA,B*); 3 mM (*dca*)) in addition to the specific inducer (*p*-coumarate, 1 µM, vanillate, 0.5 mM; adipate 1 mM) in a *catA*$^+$ and *catA*$^-$ background. Activities are given in percent of the induced activity without benzoate, set to 100 %. Growth experiments were carried out at least two times independently. Error bars indicate standard deviation.

Table 3.2. Effect of blocking CCM formation on cross-regulation

		Luciferase activity[a]		
Strain	**Characteristics**	**Basal activity**	**Inducer**	**Inducer & benzoate**
ADPU93	*hcaA-luc*	1768 ± 789 [b]	63060 ± 10533 [b]	3282 ± 945
ADPU156	*hcaA-luc*, *catA*-Kn	3057 ± 828	28704 ± 10069	28486 ± 11538
ADPU94	*dcaA-luc*	155 ± 51 [b]	11698 ± 859 [b]	5645 ± 320
ADPU157	*dcaA-luc*, *catA*-Kn	358 ± 61	15887 ± 396	3707 ± 714
ADPU102	*vanA,B-luc*	1670 ± 340 [c]	50241 ± 4932 [c]	2689 ± 584
ADPU158	*vanA,B-luc*, *catA*-Kn	6116 ± 669	45124 ± 8533	51633 ± 6301

[a] Values are given as specific luciferase activity [RLU/OD_{600}], and are averages of at least two independent experiments, standard deviation is given. [b] Fischer *et al.*, 2008. [c] Bleichrodt *et al.*, 2010.

3.3.2 Identification of the regulators mediating cross-regulation

CCM was identified as the effector mediating cross-regulation at least for the *hca* and *vanA,B* operons. The transcriptional regulators naturally able to sense and bind CCM are BenM and CatM, and therefore their involvement in cross-regulation observed for the *hca*, *dca*, and *vanA,B* genes was tested by inactivating the *benM* and/or *catM* genes in the respective luciferase reporter gene strains as described in methods (Chapter 2.1). Strains constructed for this purpose were designated ADPU135 (*hcaA-luc*, Δ*benM*-Kn^r), ADPU136 (*dcaA-luc*, Δ*benM*-Kn^r), ADPU137 (*vanA,B-luc*, Δ*benM*-Kn^r), ADPU124 (*hcaA-luc*, *catM*Ω), ADPU125 (*dcaA-luc*, *catM*Ω), ADPU126 (*vanA,B-luc*, *catM*Ω), ADPU140 (*hcaA-luc*, Δ*benM*-Kn^r, *catM*Ω), ADPU141 (*dcaA-luc*, Δ*benM*-Kn^r, *catM*Ω), and ADPU142 (*vanA,B-luc*, Δ*benM*-Kn^r, *catM*Ω) (Table 2.1).

Strains containing an inactivated *benM* and/or *catM* gene were subsequently used to analyze *hca*, *vanA,B*, and *dca* gene expression under cross-regulation conditions in luciferase assays (Chapter 2.11). Again, pyruvate was used as non-repressing carbon source and benzoate in increasing concentrations (0.5 to 5.0 mM) was added in addition to the aromatic compound inducing gene expression (*p*-coumarate, 1 µM; vanillate, 0.5 mM; adipate, 1 mM). Luciferase activity was measured upon growth, directly reflecting gene expression. The activity shown by the operons in the presence of benzoate and aromatic inducer, was compared to the induced activity of the operon (no benzoate), set to 100 %. The basal activity (no aromatic compound) of each gene was determined without any aromatic compound added, to assure an induction of the operons by the aromatic inducer, by comparing the basal activity with the induced activity.

As shown in Fig. 3.12 (a) and (b) for the *hca* and *vanA,B* operons, repression by benzoate is not completely lost until both, BenM and CatM are absent. For *hca*, the loss of either one transcriptional regulator led to an intermediate repression at high benzoate concentrations (3.0 and 5.0 mM), compared to the native situation. At benzoate concentrations below 3.0 mM, the loss of one transcriptional regulator was sufficient to restore full *hca* expression. For *vanA,B*, the loss of BenM led to increased but still repressed expression. Here, the loss of BenM was sufficient to restore full *vanA,B* expression at benzoate concentrations below 2.0 mM, while benzoate concentrations higher than 2.0 mM led to a partially repressed activity. Furthermore, repression was not as strong as observed in a *benM* and *catM* positive background. Interestingly, the loss of CatM did not influence repression of *vanA,B* by benzoate under any condition tested. Taken together, *hca* and *vanA,B* expression was completely restored in the absence of both transcriptional regulators under any condition tested. These results indicate that both transcriptional regulators are needed to completely shut off *hca* and *vanA,B* expression in the presence of benzoate, and are therefore necessary to induce cross-regulation. Nevertheless, for the *vanA,B* operon, regulation by

CatM seems to be dependent on BenM, Results presented in Fig. 3.12 (a) and (b) are also given in specific luciferase activity in tabular form in chapter 10.2.

In contrast, the repression observed for *dca* expression, was not affected under any condition (Fig. 3.12 (c)). In addition, growth of the *dcaA-luc* strain containing an inactivation of *catM*, was prohibited at benzoate concentrations above 2 mM, and *dcaA-luc* strains containing any mutations in *benM* and/or *catM* showed a strongly reduced growth rate at benzoate concentrations above 2 mM. Keeping that in mind, it is worth to note that repression by benzoate is first observed at concentrations above 2 mM. However, the analysis of the molecular mechanisms forming the basis for these observations remains unknown, and may be evaluated in the future. Results presented in Fig. 3.12 (c) are also given in specific luciferase activity in tabular form in chapter 10.2

The basal activity (no aromatic compound) of the *hca*, *vanA,B*, and *dca* operons was also determined in a *benM* and/or *catM* negative background (given in tabular form in chapter 10.2), basically to ensure an induction of the operons by the aromatic inducer, by comparing the basal activity with the induced activity. This was true for each operon and condition except for a few cases. Regarding the basal activity of the *hca* and *vanA,B* operons, there were some unexpected but interesting details discovered that should not be overlooked at this point: the basal activity of both operons in a *benM* negative background drastically increased compared to the activity measured in a native background. For the *vanA,B* operon (Table 10.2), this increased activity was comparable to the induced activity of the operon in the presence of vanillate. For the *hca* operon (Table 10.1) the basal activity in a *benM* negative background was even higher than the induced activity. This increase of basal activity was not seen in strains lacking CatM, but in strains lacking both, BenM and CatM. Thus, it might be speculated that BenM is involved in repressing promoter activity of *hca* and *vanA,B* also in the absence of any aromatic inducer. Whether this is true or not, has to be confirmed in the future.

Taken together, cross-regulation observed at the *hca* and *vanA,B* operons seems to depend on the action of both, BenM and CatM, since repression in the presence of benzoate in addition to the aromatic inducer is not lost until both, *benM* and *catM* are nonfunctional. The absence of either one regulator led to an intermediate effect (*hca* operon in the absence of BenM or CatM; *vanA,B* operon in the absence of BenM), or no effect (*vanA,B* in the absence of CatM) on repression strength by benzoate. In addition, BenM seems to be involved in repressing *hca* and *vanA,B* activity also in the absence of any aromatic inducer, and not only under the conditions of cross-regulation (presence of benzoate in addition to the aromatic inducer). In contrast, expression of the *dca* operon seems to be completely independent of BenM and CatM.

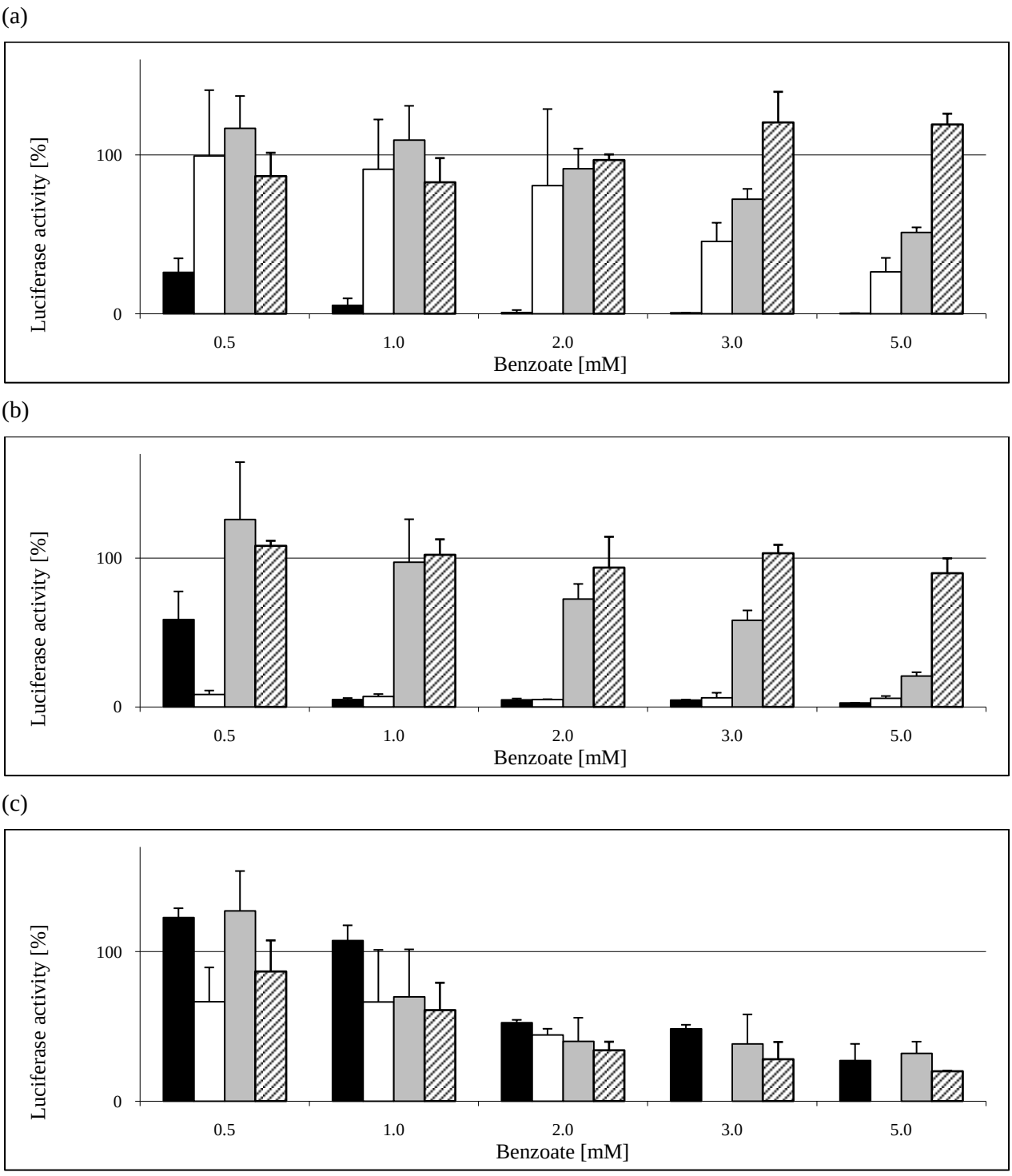

Figure 3.12. Effect of BenM and CatM on cross-regulation of the *hca* (a), *vanA,B* (b), and *dca* (c) operons. Expression was determined by luciferase reporter gene assays in the presence of the specific aromatic inducer (*p*-coumarate, 1 µM; vanillate, 0.5 mM, adipate, 1 mM) with benzoate in increasing concentrations (0.5-5.0 mM) in a $catM^+/benM^+$ (black bars; Bleichrodt *et al.*, 2010), a $catM^-$(white bars), a $benM^-$ (gray bars), or a $catM^-/benM^-$ (shaded bars) background. Activities are given in percent of the induced activity without benzoate. Values are means of at least three independent experiments. Error bars are showing standard deviation. Source data are enlisted in chapter 10.2.

3.3.3 Bioinformatic exploration of regulatory regions

The results presented in chapter 3.3.1 and 3.3.2 identified BenM and CatM as mediators of cross-regulation in response to CCM for the *hca* and *vanA,B* operon. In this chapter, the molecular mechanism of this regulation was further analyzed in detail.

BenM and CatM were shown to bind to regulatory regions of the *pca* genes (Brzostowicz *et al.*, 2003), blocking their transcription by likely hindering RNA polymerase (RNAP) from binding. The binding of BenM and CatM to a DNA region calls for the presence of a specific sequence; the BenM and CatM binding motif. To determine if putative BenM and CatM binding sites are present within the intergenic *hcaA-hcaK*, *dcaA-dcaE*, and *vanA-vanK* regions (Fig. 3.7, 3.6, and 3.9), a bioinformatic approach was employed using the software tool "pattern locator" (Mrazek & Xie, 2006). Since the sequence of the binding sites of BenM and CatM is conserved and well known (Fig. 3.13), it was used as a query sequence. This bioinformatic approach was successful and Fig. 3.14 indicates the new sites found within the intergenic *hcaA-hcaK*, *dcaA-dcaE*, and *vanA-vanK* regions.

3.3.4 Binding of BenM and CatM to intergenic regions

To test the functionality of the putative new binding sites of BenM and CatM within the intergenic *hcaA-hcaK*, *dcaA-dcaE*, and *vanA-vanK* regions (Fig. 3.14), electro mobility shift assays (EMSAs) were performed.

Therefore, BenM-6His and CatM-6His were overproduced and purified as described in methods (Chapter 2.10.1 to 2.10.3) using plasmids pBAC433 or pBAC430 (Table 2.2 (Bundy *et al.*, 2002)), respectively. The desalting step was skipped for CatM-6His, since the protein tends to fall out of solution afterwards. Fig. 3.15 (a) and (b) shows the chromatogram of CatM-6His and BenM-6His purification after His-tag nickel affinity chromatography. After protein purification, size (~ 35 kDa) and purity of the obtained BenM-6His and CatM-6His were checked using a 12 % SDS-PAGE (Chapter 2.9.4; Fig. 3.16), and protein concentration was determined according to Bradford (Bradford, 1976) using the Bio-Rad Protein Assay Dye Reagent Concentrate (Chapter 2.10.3).

For EMSA experiments, DNA fragments were amplified by PCR using the primers listed in Table 2.3. DNA fragments contained either the putative new BenM/CatM binding sites as indicated in Fig. 3.14, or the native binding sites located in the intergenic regions of *benM-benA* (positive control for BenM-6His; 440 bps), and *catM-catB* (positive control for CatM-6His; 884 bps) (Ezezika *et al.*, 2006).

EMSA experiments with CatM-6His were carried out as explained in methods (Chapter 2.10.4), using 4.57 nM of DNA fragment, incubated with increasing amounts of protein, ranging from 0 to 696 nM. The DNA-protein complexes were analyzed by a 2 % agarose gel (*catM-catB* fragment) or a 6 % PAGE (*hcaA-hcaK*, *dcaA-dcaE*, *vanA-vanK* fragments), stained with SYBRgreen (Fig. 3.17).

Figure 3.13. The BenM and CatM binding site (prepared by weblogo.berkeley.edu). The profile summarizes nucleotide occurrence of five known binding sites of BenM and CatM (Brzostowicz *et al.*, 2003, Tropel & van der Meer, 2004, Ezezika *et al.*, 2006, Craven *et al.*, 2008). The size of letters corresponds to the frequency of occurrence of this nucleotide at this position.

(a)

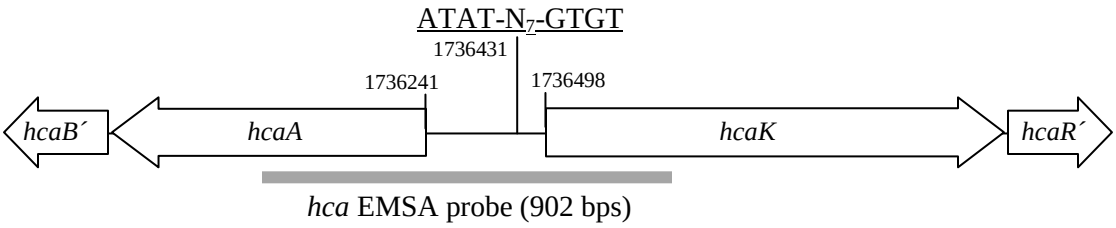

(b)

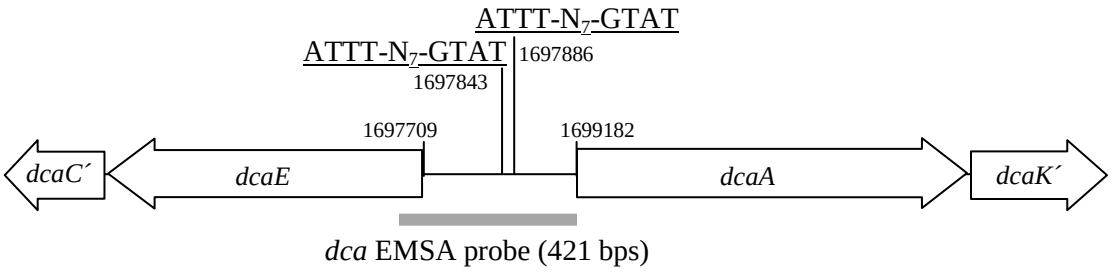

(c)

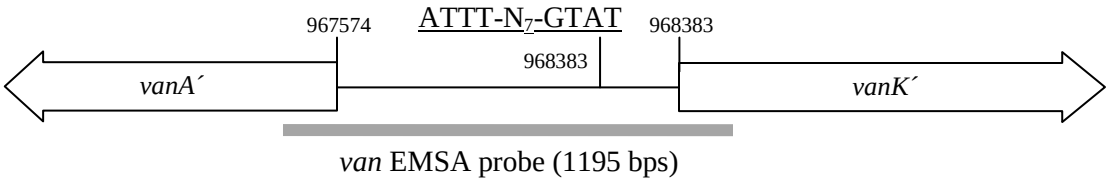

Figure 3.14. Putative BenM/CatM binding sites found within the intergenic regions of *hcaA-hcaK, dcaE-dcaA*, and *vanA-vanK*. The sequence of new sites found and the position in the chromosome is given. Genes and gene names are indicated by white arrows. Probes used in EMSA experiments are illustrated as gray bars.

(a)

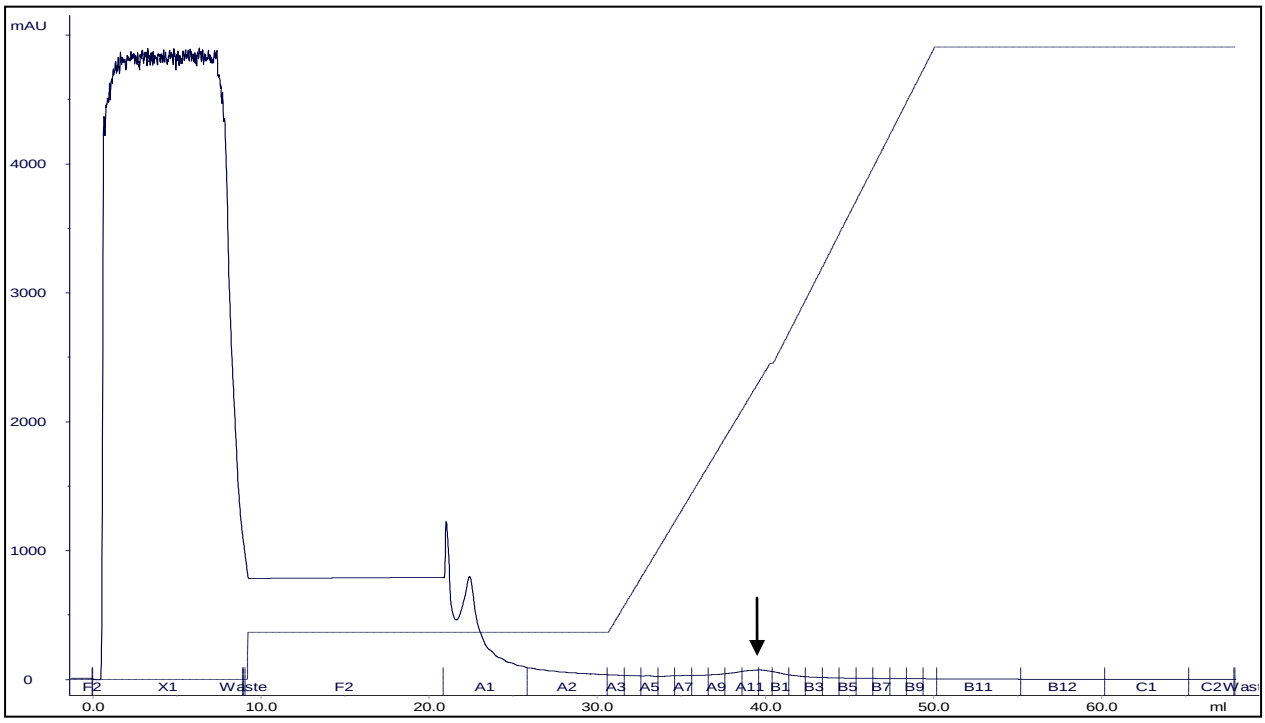

(b)

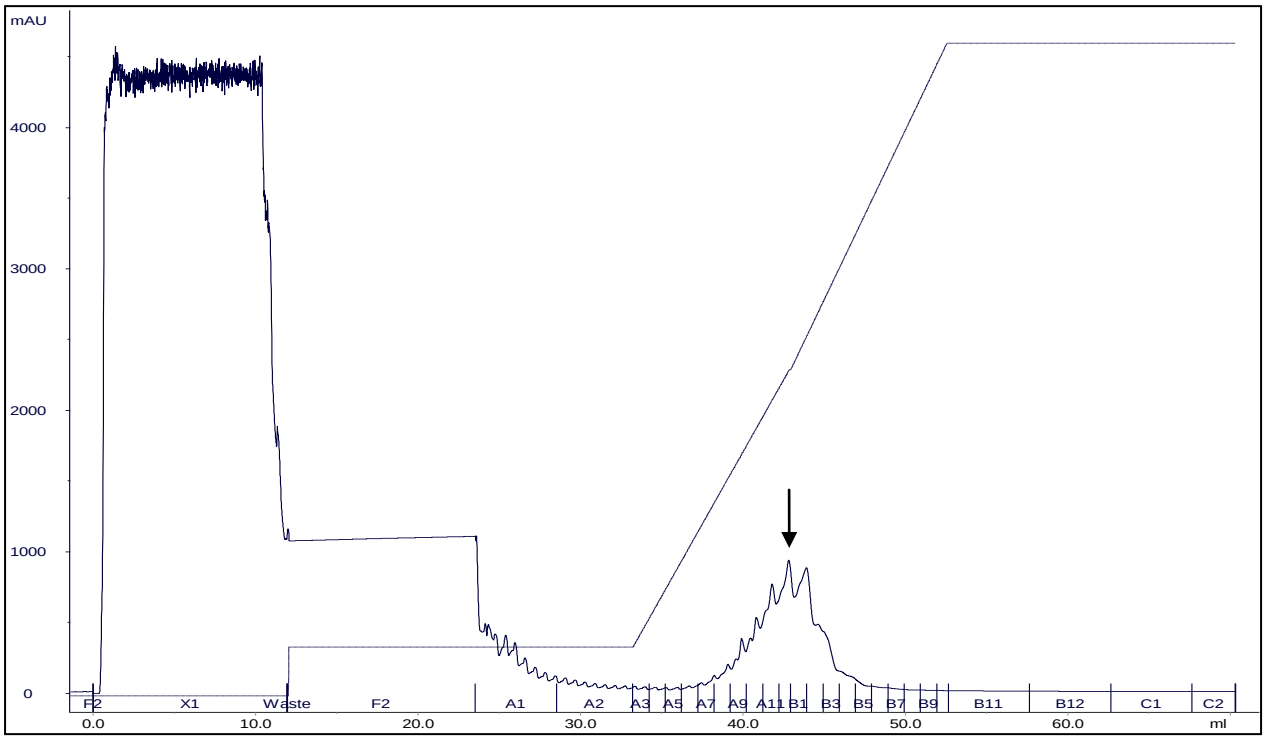

Figure 3.15. Chromatogram of CatM-6His (a) and BenM-6His (b) purification after Ni^{2+} affinity chromatography. The protein peaks are marked by an arrow. Proteins were detected my measuring the absorption at 280 nm (mAU, y-axis, solid line). Proteins were eluted by applying a linear imidazole gradient, ranging from 5 to 500 mM (0 to 100 % elution buffer; dashed line). Fractions collected are indicated (A1 to C2; above x-axis).

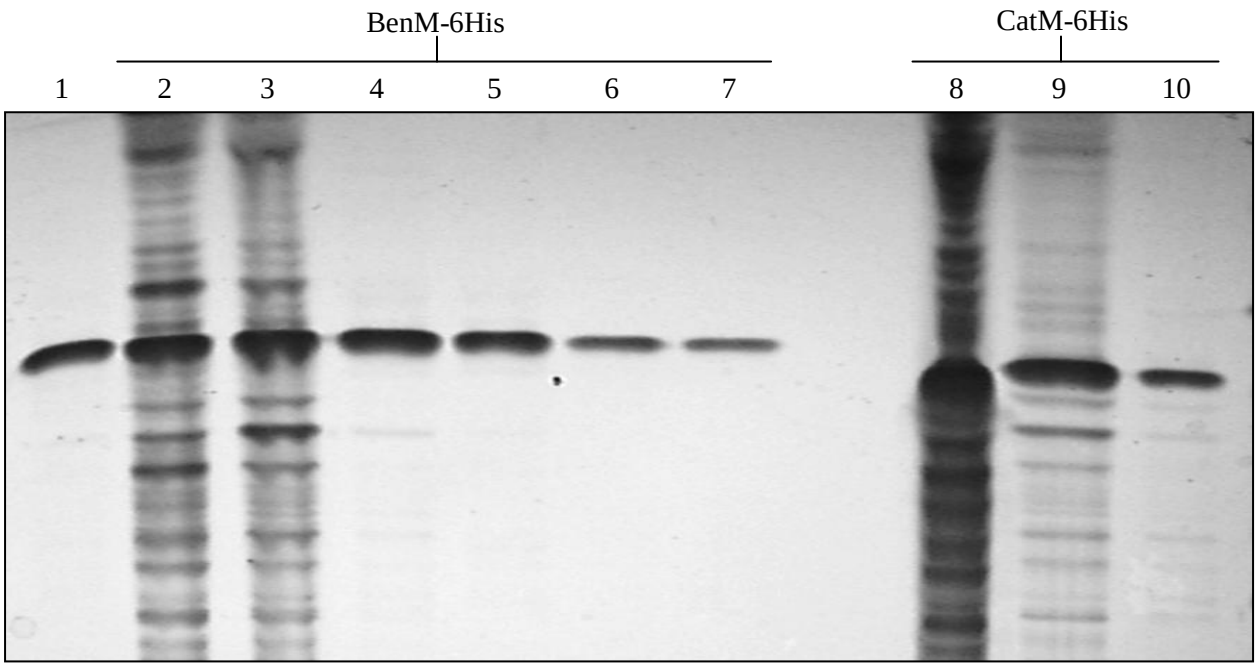

Figure 3.16. 12 % SDS-PAGE of purified BenM-6His and CatM-6His. Lane 1: BenM-6His (used as size standard); Lane 2: culture supernatant after French press and centrifugation (BenM-6His); Lane 3: cell pellet after French press and centrifugation (BenM-6His); Lane 4 and 5: fraction A12 and B1 after HisTrap™ FF column (BenM-6His); Lane 6 and 7: fraction A12 and B1 after Desalting column (BenM-6His); Lane 8: culture supernatant after French press and centrifugation (CatM-6His); Lane 9: cell pellet after French press and centrifugation (CatM-6His); Lane 10: fraction A11 after HisTrap™ FF column (CatM-6His).

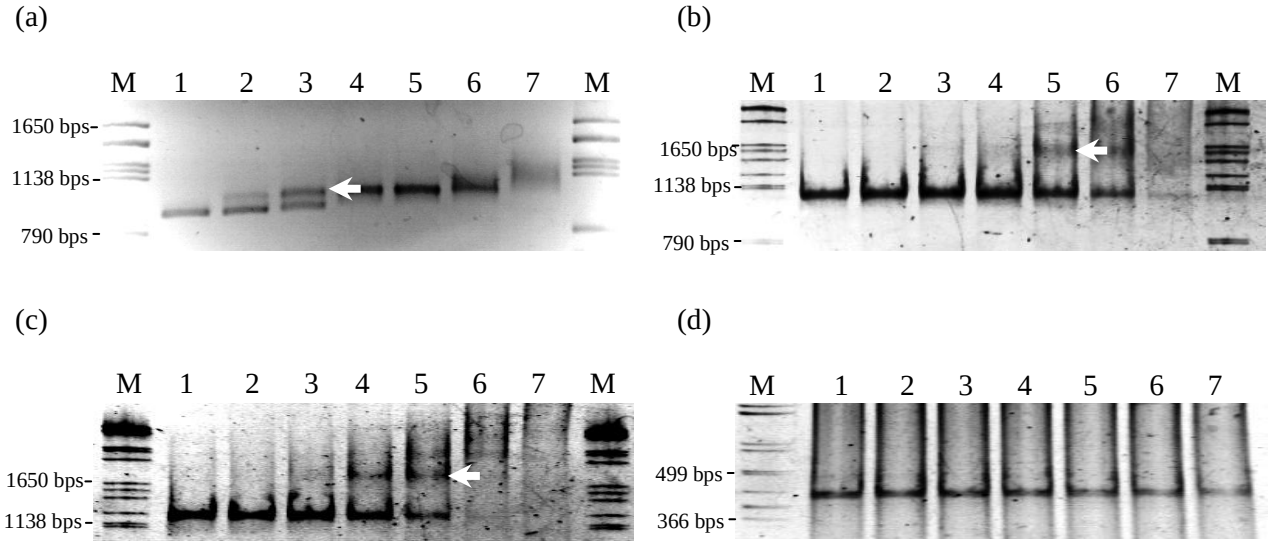

Figure 3.17. Electro mobility shift assays (EMSAs) to show interaction of CatM with DNA fragments containing (putative) CatM binding sites. (a) *catM-catB* region (positive control), (b) *hcaA-hcaK* region, (c) *vanA-vanK* region, (d) *dcaA-dcaE* region. CatM-6His was added in increasing concentrations (0, 22, 44, 87, 174, 348, 696 nM; lanes 1 to 7). M: λ *Bgl*I DNA ladder. Retarded protein-DNA complexes are marked by white arrows.

EMSA experiments clearly confirmed an interaction of CatM-6His with the *hca* and *van* probe (Fig. 3.17 (b) and (c)), as it was seen for the positive control (Fig. 3.17 (a)). This interaction is visible as a retarded DNA-protein complex with respect to the unbound fragment. In addition, BenM-6His was able to interact with the *hca* and *van* probes in a comparable manner (supplementary data in chapter 10.3). However, the binding of CatM-6His to the *hca* and *van* probes seems to be weaker compared to the native site, as CatM-6His is able to bind the positive control at lower concentrations. This suggests a higher affinity of CatM-6His to the native site (retardation is visible at CatM-6His concentrations of 22, 174, and 87 nM, respectively; Fig. 3.17 (a), (b), and (c)). Interestingly, no interaction was observed for the *dca* probe, although putative binding sites are present. This finding corresponds with the reporter gene results described in chapters 3.3.1 and 3.3.2.

To summarize the results presented in chapter 3.3.3 and 3.3.4: putative new binding sites for BenM and CatM were identified within intergenic *hcaA-hcaK*, *dcaA-dcaE*, and *vanA-vanK* regions using a bioinformatical approach. The functionality of the sites between *hcaA* and *hcaK*, as well as between *vanA* and *vanK* was proved in EMSAs, since purified CatM-6His and BenM-6His were able to bind DNA fragments containing these sites. In contrast, no binding was observed using a DNA fragment containing the sites between *dcaA* and *dcaE*. The findings presented here are in line with the reporter gene results described in chapter 3.3.1 and 3.3.2.

3.3.5 Determination of transcriptional start sites

In order to deeper analyze the molecular mechanism leading to cross-regulation at the *hca* and *vanA,B* operons, 5´RACE (Chapter 2.8.6) was performed to identify the transcriptional start sites (TSSs) of *hcaA*, *hcaK*, *vanA*, and *vanK*. The knowledge of the position of the TSS with respect to the predicted BenM/CatM binding sites would then give information about possible interactions of bound regulatory protein with e. g. RNAP.

Therefore, *A. baylyi* strain ADP1 was grown to late-exponential growth phase, using *p*-coumarate (1 mM) or vanillate (10 mM) as sole carbon source to induce *hca* or *van* gene expression (Fig. 3.18 (a)). Cells were harvested before entering the stationary phase, followed by total RNA isolation using TriReagent® (Molecular Research Center, Inc; Chapter 2.8.1.4). After DNase I digestion, the absence of genomic DNA was confirmed by PCR using primers RT_hcaA and GSP2_hcaA or RT_hcaK and GSP2_hcaK (Table 2.3) for the *p*-coumarate grown cells, and RT_vanA and GSP2_vanA or RT_vanK and GSP2_vanK (Table 2.3) for the vanillate grown cells. RT-PCR was performed using SuperScript™ II RT (Invitrogen™), primers GSP1_hcaA, GSP1_hcaK, GSP1_vanA, or GSP1_vanK (Table 2.3) and 1-5 µg of total RNA as template according to manufacturers instructions. Followed by polydC-tailing and PCR with

the corresponding GSP2 primers (Table 2.3). The 5´RACE products were analyzed by agarose gel electrophoresis (Chapter 2.9.1), purified (Chapter 2.8.2), and cloned using the TOPO® TA Cloning® Kit (Invitrogen™; Chapter 2.8.5). Obtained plasmids were analyzed by a sequencing reaction with the standard primer (M13R) provided by the company (GENEWIZ, Inc.).

Using this method, it was possible to confidently identify the TSS of the *hcaK* and *vanK* genes (4 times independently) and putative promoter regions are suggested for *hcaK* and *vanK*. (Fig. 3.18 (b) and (c)). Unfortunately, results obtained for the *hcaA* and *vanA* genes were not reliable. The same method explained above was used to identify the TSSs of *dcaE* and *dcaA*, but without success (*A. baylyi* grown on adipate, the respective primers are listed in Table 2.3.).

Nevertheless, the comparison of the position of the predicted BenM/CatM binding sites with the location of the TSSs and putative promoter regions identified for *hcaK* and *vanK*, shed some light on the molecular mechanism of cross-regulation. As shown in Fig. 3.18 (b), the predicted BenM/CatM binding site upstream of *hcaK* is directly sitting on the TSS of this gene and overlaps in parts with the supposed -10 promoter region, possibly indicating interactions of BenM/CatM with components of the transcriptional machinery. The predicted BenM/CatM binding site upstream of *vanK* is separated by 106 bps from the TSS of *vanK* (Fig. 3.18 (c)) and 61 bps from the supposed -35 promoter region. This is in contrast to the ~ 350 bp distance to the start codon of *vanA*.

(a)

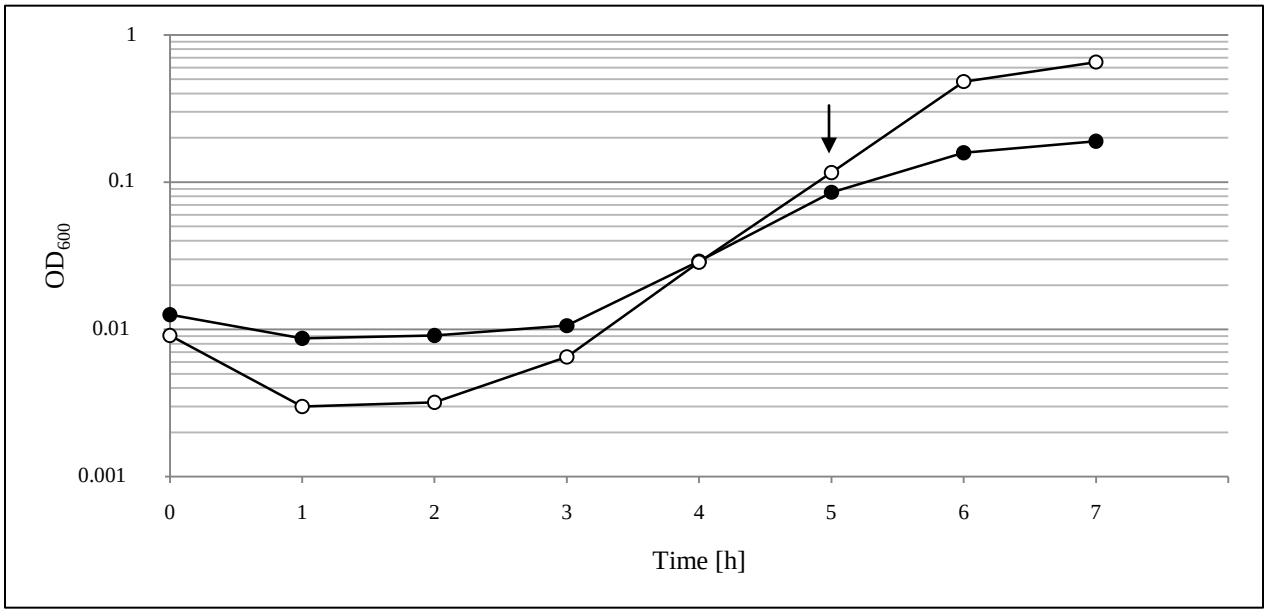

(b)

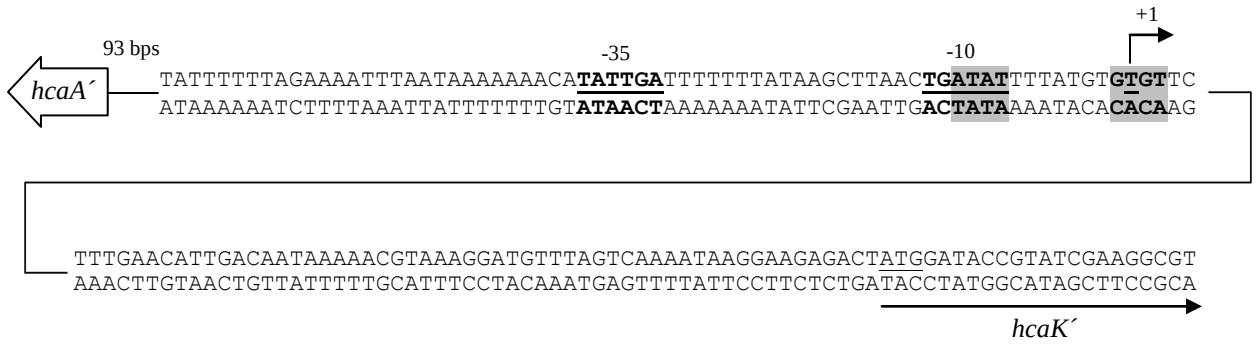

(c)

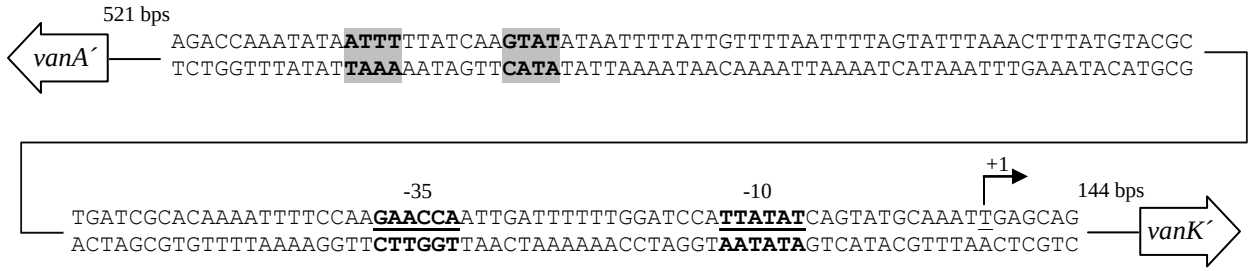

Figure 3.18. (a) Growth of *A. baylyi* strain ADP1 on *p*-coumarate (1 mM; open circles), or vanillate (10 mM; solid circles). Cells were harvested before entering the stationary phase; time point indicated by an arrow. **Transcriptional start sites determined by 5´RACE of the (b) *hcaK* and (c) *vanK* gene.** The positions of the TSSs are indicated by an arrow and +1, first base underlined. Putative promoter regions are indicated (-10; -35). The predicted BenM/CatM binding sites are marked with a gray background. Distances to coding regions are given above the sequence. Genes are illustrated by white arrows, and by a black underline arrow for *hcaK*.

3.4 Analysis of vertical regulation

Vertical regulation is observed within the PCA branch of the β-ketoadipate pathway. Here,, repression of the *pobA* (Siehler *et al.*, 2007), the *vanA,B*, and the *hca* genes (Bleichrodt *et al.*, 2010) is observed when PCA is present in addition to the specific aromatic compound, which should induce gene expression. These genes encode enzymes needed for the degradation of POB, vanillate, and hydroxycinnamate to PCA, and the corresponding compounds are thus metabolically linked. However, the molecular mechanism forming the basis of vertical regulation is unknown.

The transcriptional regulator naturally able to sense and bind PCA is PcaU, an IclR-type transcriptional regulator (Gerischer *et al.*, 1998, Gerischer *et al.*, 2008). This regulator is responsible for activating expression of the *pca* genes (needed for PCA breakdown) in the presence of PCA, and to repress their expression in the absence of PCA (Dal *et al.*, 2005). Thus, PcaU can be both an activator and a repressor, and maybe it is also involved in repressing the *vanA,B* and *hca* genes.

The *vanA,B* and *hca* genes were shown to undergo a specific regulation triggered by vanillate and hydroxycinnamoyl-CoA thioesters. The regulatory proteins mediating this regulation are VanR (GntR-type (Morawski *et al.*, 2000)) and HcaR (MarR-type (Parke & Ornston, 2003)). Both regulators were shown to act as repressors, repressing *vanA,B* and *hca* expression in the absence of their inducers. Both, *vanR* and *hcaR* are transcribed divergently from the structural genes, which encode enzymes for the breakdown of vanillate and hydroxycinnamates, respectively (Fig. 3.9 and 3.7). Since HcaR and VanR were shown to govern expression of the *hca* and *vanA,B* genes, they may be also involved in their repression observed in the presence of PCA.

The analysis of the molecular mechanisms leading to vertical regulation of the *hca* and *vanA,B* operons is described in the following chapters. The effector leading to vertical regulation at *hca* and *vanA,B* was identified, as well as the regulatory protein mediating repression. Hints about how vertical regulation could function for the *hca* and *vanA,B* operons, were derived from bioinformatical and molecular approaches including electro mobility shift assays, 5´RACE, and DNase I footprinting.

3.4.1 Searching the effector mediating vertical regulation

The *vanA,B* and *hca* genes are induced in the presence of vanillate and hydroxycinnamates (e. g. *p*-coumarate). The addition of PCA to the aromatic inducers resulted in a repressed *vanA,B* and *hca* expression (Bleichrodt, 2007, Bleichrodt *et al.*, 2010). Since this repression is observed in the presence of

PCA, PCA is suggested to be the mediator causing vertical regulation. However, downstream metabolites formed in PCA degradation, possibly mediating repression, were not excluded until now. To identify PCA as mediator, a block in PCA degradation was constructed by deleting *pcaH*, encoding the first enzyme needed for PCA breakdown, in the *vanA,B-luc* (ADPU102; Table 2.1 (Bleichrodt *et al.*, 2010)) and *hcaA-luc* (ADPU93; Table 2.1 (Fischer *et al.*, 2008)) strains, as described in methods (Chapter 2.1). Obtained strains carried either a *vanA,B-luc* transcriptional fusion and a deleted *pcaH* gene (ADPU164; Table 2.1) or a *hcaA-luc* transcriptional fusion and a deleted *pcaH* gene (ADPU162; Table 2.1). *vanA,B* and *hca* transcriptional activity was then determined in luciferase assays (Chapter 2.11) in the presence of the specific aromatic inducer (vanillate, 0.5 mM; *p*-coumarate, 1 µM), with or without PCA in increasing concentrations (0.5 to 5.0 mM), compared to the parental strains (ADPU102 (*vanA,B-luc*) and ADPU93 (*hcaA-luc*)). The basal activity (no aromatic compound) of each gene was determined without any aromatic compound added, to assure an induction of the operons by the aromatic inducer, by comparing the basal activity with the induced activity

As shown in Fig. 3.19, a block in PCA degradation did not lead to a loss of vertical regulation in the presence of PCA. Activity of *hcaA-luc* (Fig. 3.19 (a)) and *vanA,B-luc* (Fig. 3.19 (b)) in a *pcaH* negative background (ADPU162 and ADPU164) was down to 38 and 20 % of the original induced activity at PCA concentrations of 5 mM. This finding is comparable to the repressed activity shown by the parental strain, which was down to 46 and 10 %, respectively. Interestingly, regarding the *vanA,B-luc*, Δ*pcaH* strain (ADPU164), vertical regulation seems to be less strong compared to the parental strain (ADPU102) under all conditions tested. Results presented in Fig. 3.19 are also given in specific luciferase activity in tabular form in chapter 10.4.

The basal activity (no aromatic compound) of the *hca* and *vanA,B* genes was also determined in a *pcaH* negative background (given in tabular form in chapter 10.4). Unexpectedly, the basal activity of the *vanA,B* operon in a *pcaH* negative background was as high as the induced activity (plus vanillate). This was not seen for the *hca* operon. How the absence of *pcaH* should influence the basal expression of *vanA,B* remains to be elucidated and could be subject for future investigations.

Anyway, the block in PCA breakdown did not abolish vertical regulation of the *hca* and *vanA,B* operon in the presence of PCA in addition to the specific aromatic inducer. Thus, PCA is identified as the main effector mediating vertical regulation of the *hca* and *vanA,B* genes. Interestingly, the repression of *vanA,B* was not that strong in a *pcaH* negative background compared to a *pcaH* positive background. Since PCA is not degraded by this strain (due to a nonfunctional *pcaH*), it might be possible that the *vanA,B* genes are also induced by PCA, what is tested in the following chapter.

3.4.2 Induction of *hca* and *vanA,B* expression by PCA alone

Strain ADPU164 (*vanA,B-luc*, Δ*pcaH*) did show an increase of gene activity in the presence of vanillate and PCA compared to the parental strain ADPU102 (*vanA,B-luc*; Fig. 3.19 (b)). This was not observed for the *hcaA-luc* strains (ADPU93, ADPU162; Fig. 3.19 (a)). Howeve,r ADPU162 and ADPU164 differ from the parental strains as they accumulate PCA, because PCA degradation is blocked. This may suggest that PCA is also able to induce the *vanA,B* genes. To test this hypothesis, *hca* and *vanA,B* activity was determined in the presence of PCA in increasing concentrations without aromatic inducer, using strains ADPU93 and ADPU102 (*hcaA-luc*; *vanA,B-luc*; Table 2.1) in luciferase assays (Chapter 2.11).

While the *hca* operon did not respond to the addition of PCA as expected (Fig. 3.20 (a)), the *vanA,B* operon showed induced activity in the presence of low PCA concentrations (0.5 and 1 mM), while high PCA concentrations (above 1 mM) did not induce *vanA,B* expression (Fig. 3.20 (b)). As a reference parameter, the basal activity of *vanA,B* is 3.3 % of the vanillate induced activity.

However, it is worth to note that PCA induced activity of the *vanA,B* genes never reached the strength of vanillate induced activity. The activity in the presence of 0.5 mM PCA was only 61 % of the induced activity by 0.5 mM vanillate (Fig. 3.20 (b)). Interestingly, PCA concentrations above 1 mM did not induce the *vanA,B* genes at all, as activity measured here was below the basal activity of the operon. Thus, it seems that there is an induction of *vanA,B* by PCA, which is visible under very low concentrations. Results presented in Fig. 3.20 (b) are also given in specific luciferase activity in tabular form in chapter 10.4 (Table 10.16).

The activity measured for the *hca* operon in the presence of PCA was in any case in the range of the basal activity of the operon: ca. 3 % of the induced activity by *p*-coumarate (Fig. 3.20 (a)). Thus, *hca* expression is not inducible by PCA under any condition tested. Results presented in Fig. 3.20 (a) are also given in specific luciferase activity in tabular form in chapter 10.4 (Table 10.16).

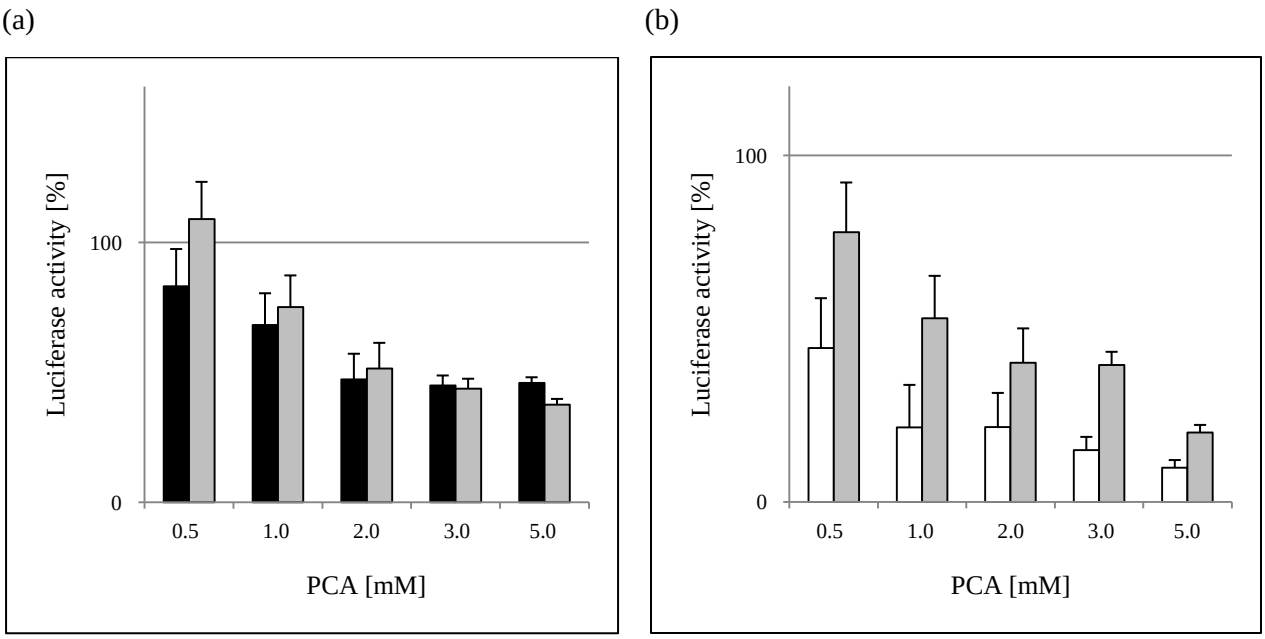

Figure 3.19. Effect of blocking PCA degradation on vertical regulation. Expression of the (a) *hca* and (b) *vanA,B* genes in the presence of PCA (0.5 to 5.0 mM) in the parental strains (ADPU93 (black bars); ADPU102 (white bars)) compared to strains blocked in PCA degradation (ADPU162; ADPU164 (gray bars)). Luciferase activity is given in percent of the induced activity only by *p*-coumarate or vanillate, set to 100 %. Each growth experiment was carried out at least three times independently. Error bars indicate standard deviation.

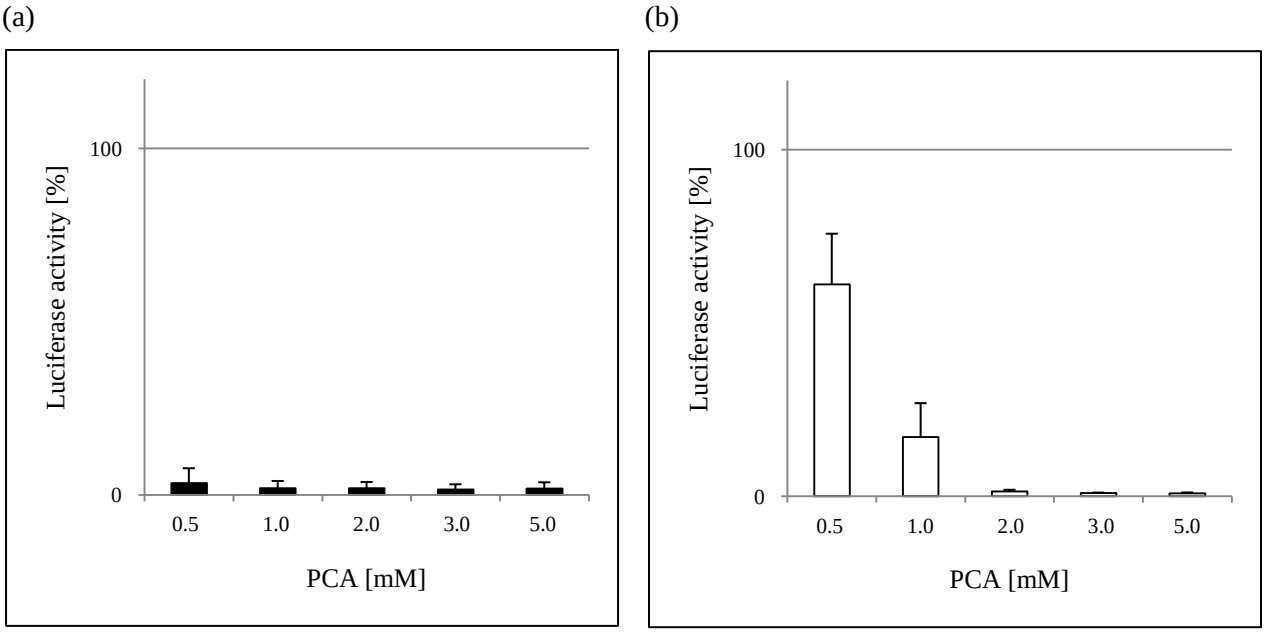

Figure 3.20. *hcaA* (a) and *vanA,B* (b) expression in the presence of PCA (0.5 to 5.0 mM). Luciferase activity is given in percent of the induced activity by *p*-coumarate (*hca-luc*, ADPU93) or vanillate (*vanA,B-luc*, ADPU102), set to 100 %. Each growth experiment was carried out at least three times independently. Error bars indicate standard deviation.

3.4.3 Identification of the regulator mediating vertical regulation

Vertical regulation of the *hca* and *vanA,B* genes seems to be dependent on the presence of PCA as shown in chapter 3.4.1. The only known regulator naturally able to sense and bind PCA is PcaU (Gerischer *et al.*, 1998, Gerischer *et al.*, 2008), acting as a dual function transcriptional regulator at promoter $pcaI_P$ (Trautwein & Gerischer, 2001, Dal *et al.*, 2005). Thus, PcaU was tested for its ability to regulate also the *hca* and *vanA,B* genes. The *pcaU* gene was therefore deleted in ADPU93 and ADPU102 (*hcaA-luc*; *vanA,B-luc*; Table 2.1), as described in methods (Chapter 2.1), generating the strains ADPU122 (*hcaA-luc*, Δ*pcaU*Ω) and ADPU123 (*vanA,B-luc*, Δ*pcaU*Ω), respectively (Table 2.1). Since the *hca* and *vanA,B* genes undergo a specific induction by their specific transcriptional regulators HcaR (Parke & Ornston, 2003) and VanR (Morawski *et al.*, 2000), their possible involvement in vertical regulation was also tested by deleting the *hcaR* and *vanR* genes in strains ADPU93 or ADPU122, and ADPU102 or ADPU123, respectively (Chapter 2.1.; Table 2.1). Obtained strains were named ADPU138 (*hcaA-luc*, *ΔhcaR*-Kn^r), ADPU139 (*hcaA-luc*, Δ*pcaU*Ω, *ΔhcaR*-Kn^r). ADPU127 (*vanA,B-luc, vanR*-Kn^r), and ADPU128 (*vanA,B-luc,* Δ*pcaU*Ω, *vanR*-Kn^r) (Table 2.1).

All strains designed, containing the respective luciferase fusions and deletions of genes, were tested in luciferase assays (Chapter 2.11) in the presence of the specific aromatic inducer (vanillate, 0.5 mM; *p*-coumarate, 1 µM), with or without the addition of PCA in increasing concentrations. PCA concentrations used ranged from 0.5 to 5.0 mM, according to experiments described by Bleichrodt *et al.*, 2010. In addition, the basal activity of the *hca* and *vanA,B* operons was determined (no aromatic compound).

The activity of the *vanA,B* genes is shown in Fig. 3.21, in a *pcaU* negative, a *vanR* negative, or *pcaU* and *vanR* negative background, compared to a *pcaU* and *vanR* positive background. Results presented in Fig. 3.21 clearly identified PcaU as the regulator mediating vertical regulation of the *vanA,B* genes. The strain carrying a deleted *pcaU* gene (ADPU123) did show high activity in the presence of vanillate and PCA under any condition, which is comparable to the induced activity of this strain (only vanillate), while the parental strain ADPU102 did show repression in the presence of increasing concentrations of PCA. The deletion of *vanR* (ADPU127) did not lead to a loss of vertical regulation, but the *vanA,B* genes showed high activity in the absence of any aromatic compound (basal activity; Table 3.3). Thus, VanR was confirmed as being a repressor of *vanA,B* expression (Morawski *et al.*, 2000). The double mutant in *vanR* and *pcaU* did show high luciferase activity under all conditions tested, reflecting the action of VanR as repressor of *vanA,B* expression, and corroborating PcaU as the mediator causing vertical regulation in the presence of PCA (Fig. 3.21, Table 3.3). Table 3.3 summarizes these findings for ADPU102, ADPU123, ADPU127, and ADPU128, showing the basal activity (no aromatic compound), the induced activity (0.5 mM vanillate), and the activity in the presence of vanillate (0.5 mM) and PCA (5.0 mM).

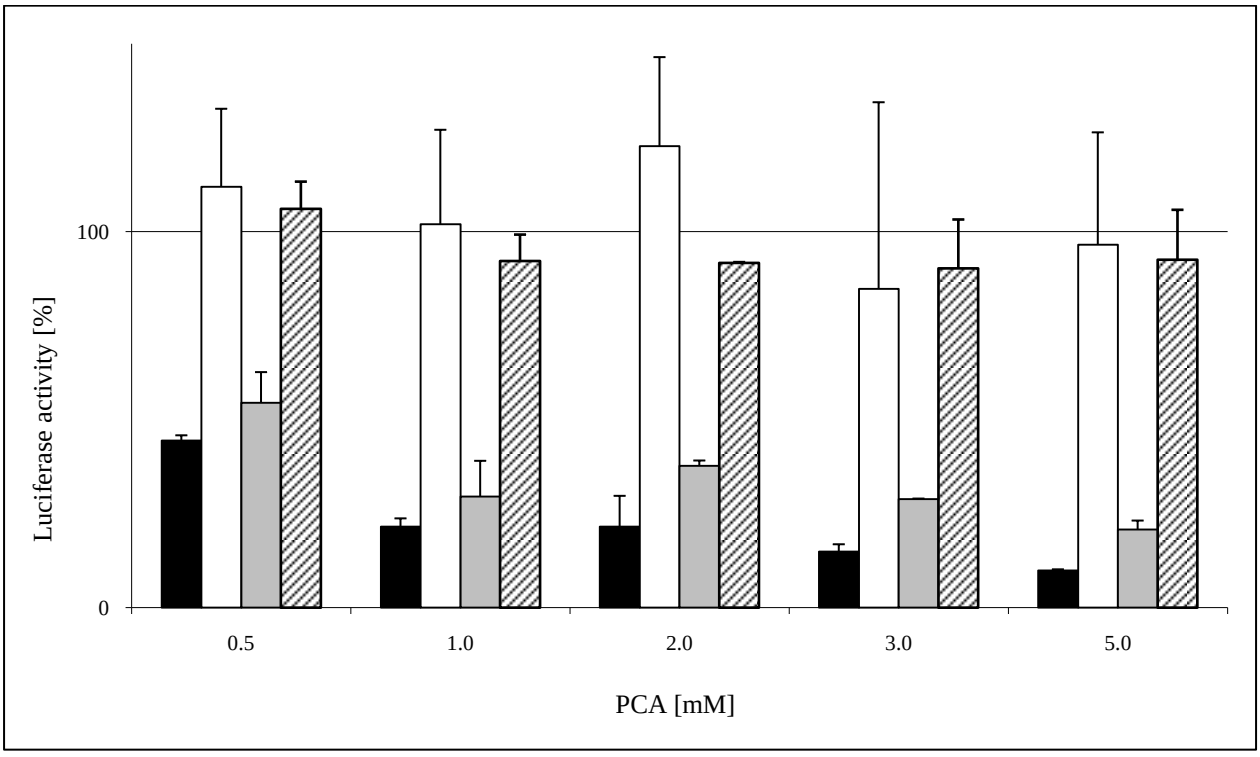

Figure 3.21. Effect of PcaU and VanR on the expression of the *vanA,B* genes. *vanA,B-luc* activity in a *pcaU* and *vanR* positive background (ADPU102; black bars; Bleichrodt *et al.*, 2010), compared to a *pcaU* negative (ADPU123; white bars), a *vanR* negative (ADPU127; gray bars), or a *pcaU* and *vanR* negative background (ADPU128; shaded bars). Activity was determined in the presence of vanillate (0.5 mM) and PCA in increasing concentrations (0.5 to 5.0 mM). Luciferase activities are given in percent of the induced activity of the respective strain only by vanillate, set to 100 %. Each growth experiment was carried out at least three times independently. Error bars indicate standard deviation. Source data are enlisted in chapter 10.5.

Table 3.3. Effect of PcaU and VanR on the expression of *vanA,B-luc*

		Luciferase activity[a]		
Strain	**Characteristic**	**Basal activity**	**Vanillate**	**Vanillate & PCA**
ADPU102	*vanA,B-luc*	1670 ± 340 [b]	50241 ± 4932 [b]	5427 ± 158 [b]
ADPU123	*vanA,B-luc*, Δ*pcaU*Ω	118 ± 13	42021 ± 8144	40564 ± 9067
ADPU127	*vanA,B-luc*, *vanR*-Kn^r	40214 ± 1292	41322 ± 5798	8581 ± 992
ADPU128	*vanA,B-luc*, Δ*pcaU*Ω, *vanR*-Kn^r	47399 ± 8129	55933 ± 3077	51754 ± 7429

[a] Values are given as specific luciferase activity [RLU/OD_{600}], and are averages of at least three independent experiments, standard deviation is given. [b] Bleichrodt *et al.*, 2010

The activity of the *hca* genes is shown in Fig. 3.22, in a *pcaU* negative, an *hcaR* negative, or *pcaU* and *hcaR* negative background, compared to a *pcaU* and *hcaR* positive background. Results obtained are partially comparable to those obtained for the *vanA,B-luc* strains.

The strain carrying a deleted *pcaU* gene (ADPU122) did respond with an increase of promoter activity in the presence of PCA and specific inducer, compared to the parental strain (ADPU93). The observed activity of *hcaA-luc* in a *pcaU* negative background with the highest PCA concentration (5.0 mM) was down to 67 % compared to the induced activity (only *p*-coumarate). As the parental strain ADPU93 showed a repressed activity with 5.0 mM PCA down to 45 %, the lack of PcaU obviously diminishes vertical regulation. This effect was visible more clearly at low PCA concentrations ranging from 0.5 to 2.0 mM (Fig. 3.22), since *hcaA-luc* activity was not significantly impaired.

HcaR was confirmed as repressor for *hca* expression (Parke & Ornston, 2003), since the basal activity in the strain lacking HcaR (ADPU138) was comparable to the induced activity by *p*-coumarate (Table 3.4). Nevertheless, this strain still showed the phenotype of vertical regulation as seen for the parental strain ADPU93 (Fig. 3.22; Table 3.4). Thus, HcaR can be excluded as mediator for vertical regulation.

However, results obtained with ADPU139 (*hcaA-luc*, Δ*pcaU*Ω, Δ*hcaR*-Kn^r) were unexpected, since the activity of *hca* was still repressed in the presence of PCA and *p*-coumarate, while it was not repressed in the absence of any aromatic compound or with *p*-coumarate alone (Fig. 3.22; Table 3.4). In addition, ADPU139 was strongly restricted in growth when *p*-coumarate and PCA were added simultaneously. This fact may influence luciferase activity, and results presented for this strain and condition should be regarded as barely preliminary. Still, there could be an additional mediator for vertical regulation of *hca*.

Table 3.4 summarizes the findings for ADPU93, ADPU122, ADPU138, and ADPU139, showing the basal activity (no aromatic compound), the induced activity (1 µM *p*-coumarate), and the activity in the presence of *p*-coumarate (1 µM) and PCA (5.0 mM).

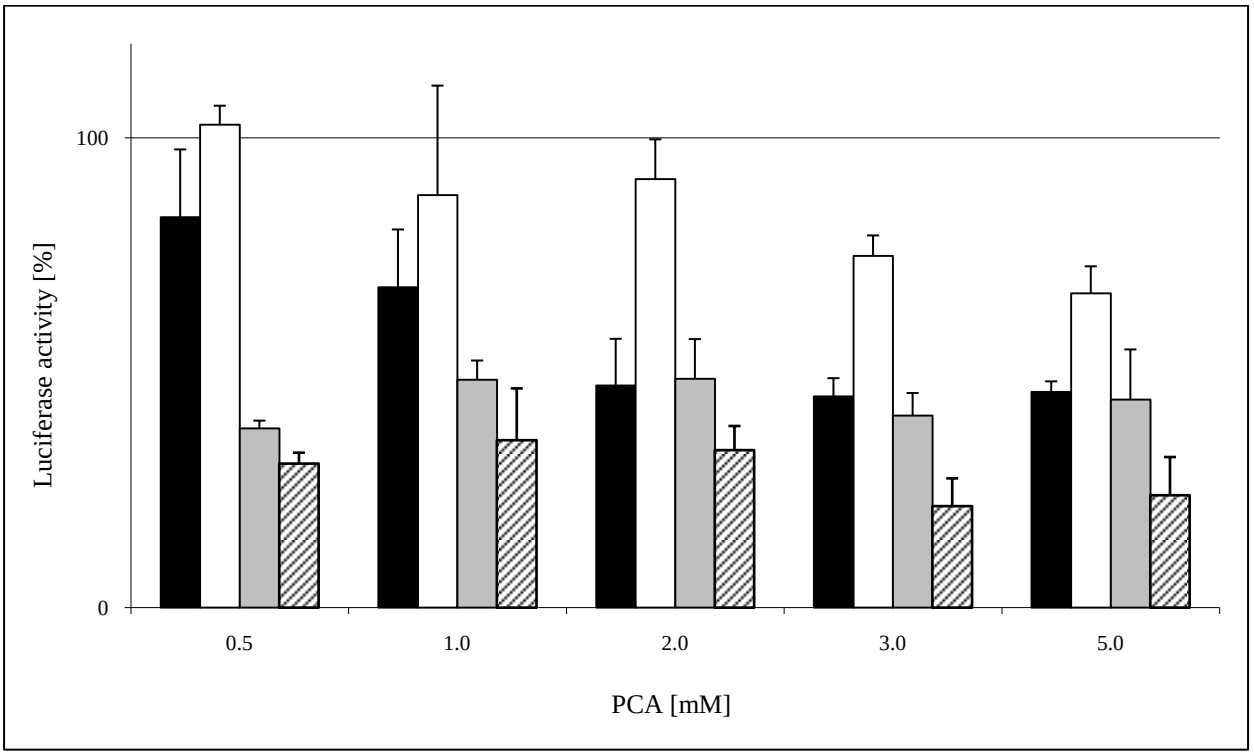

Figure. 3.22. Effect of PcaU and HcaR on the expression of the *hca* genes. *hcaA-luc* activity in a *pcaU* and *hcaR* positive background (ADPU93; black bars; Bleichrodt *et al.*, 2010), compared to a *pcaU* negative (ADPU122; white bars), an *hcaR* negative (ADPU138; gray bars), or a *pcaU* and *hcaR* negative background (ADPU139; shaded bars). Activity was determined in the presence of *p*-coumarate (1.0 µM) and PCA in increasing concentrations (0.5 to 5.0 mM). Luciferase activities are given in percent of the induced activity of the respective strain only by *p*-coumarate, set to 100 %. Each growth experiment was carried out at least three times independently. Error bars indicate standard deviation. Source data are enlisted in chapter 10.5.

Table 3.4. Effect of PcaU and HcaR on the expression of *hcaA-luc*

		Luciferase activity[a]		
Strain	**Characteristic**	**Basal activity**	***p*-coumarate**	***p*-coumarate & PCA**
ADPU93	*hcaA-luc*	1768 ± 789[b]	63060 ± 10533[b]	28955 ± 1410[c]
ADPU122	*hcaA-luc*, Δ*pcaU*Ω	417 ± 16	47992 ± 7970	32514 ± 4430
ADPU138	*hcaA-luc*, Δ*hcaR*-Kn^r	79796 ± 14704	52179 ± 16146	23088 ± 5582
ADPU139	*hcaA-luc*, Δ*pcaU*Ω, Δ*hcaR*-Kn^r	111820 ± 18059	75284 ± 21935	(17995 ± 6130)

[a] Values are given as specific luciferase activity [RLU/OD_{600}], and are averages of at least two independent experiments, standard deviation is given. [b] Fischer *et al.*, 2008; [c] Bleichrodt *et al.*, 2010. Bracketed values: preliminary result.

Results presented in chapter 3.4.3 showed that vertical regulation of *vanA,B* and *hca* is independent of the specific transcriptional regulators VanR and HcaR, since the inactivation of their genes did not influence repression in the presence of PCA in addition to the aromatic inducer. The observation that VanR and HcaR act as repressors of *vanA,B* and *hca* expression was confirmed (high basal activity in a *vanR* negative and *hcaR* negative background). Vertical regulation seems to rely on the action of PcaU, since repression of *vanA,B* is completely lost in strains lacking *pcaU*, and repression of *hca* is strongly diminished in the absence of *pcaU*.

Results presented in Fig. 3.21 and Fig. 3.22 are also given as specific luciferase activity in tabular form in chapter 10.5 (Table 10.17 and Table 10.18).

3.4.4 Bioinformatic exploration of regulatory regions

Results presented in Chapter 3.4.1 and 3.4.3 confirmed the hypothesis of PcaU being the mediator of vertical regulation in response to PCA at the *vanA,B* and *hca* genes. To further identify the molecular mechanism in more detail, it was searched for the well known consensus sequence of the binding site of PcaU (Fig. 3.23 (a) (Gerischer *et al.*, 1998, Popp *et al.*, 2002, Gerischer *et al.*, 2008)) within the intergenic *vanA-vanK* and *hcaA-hcaK* regions. The native PcaU binding motif found in the intergenic region *pcaU-pcaI* of *A. baylyi* consists of three perfect 10 bp sequence repetitions (R1, R2, and R3), two of which are forming a palindrome (R1, R2). The spacer between R2 and R3 is spanning 10 bps, and the whole motif is separated by 4 and 15 bps from the -35 promoter region of *pcaU* and *pcaI*, respectively (Fig. 3.23 (b)).

To search for putative new binding sites of PcaU in the intergenic regions *vanA-vanK* and *hcaA-hcaK*, the software tool "Prodoric release 2" (Münch *et al.*, 2005) was used. The search profile was a consensus sequence of nine binding sites of a subgroup of IclR-type transcriptional regulators (PcaU, PobR (*A. baylyi*), PobR and PcaR (*P. putida*)), which are well conserved (Gerischer *et al.*, 2008, Jerg & Gerischer, 2008). As shown in Fig. 3.23 (a), the consensus focuses on the internal palindrome (R1, R2) of the binding site. It is worth to note that some nucleotides within this consensus sequence are particularly well conserved: positions 5, 6, 7, 8, 13, and 15. It was also shown that the two guanine nucleotides within R1 (positions 2 and 6 in Fig. 3.23 (a)), which are separated by 3 bps, are highly important for the binding of PcaU (Jerg & Gerischer, 2008).

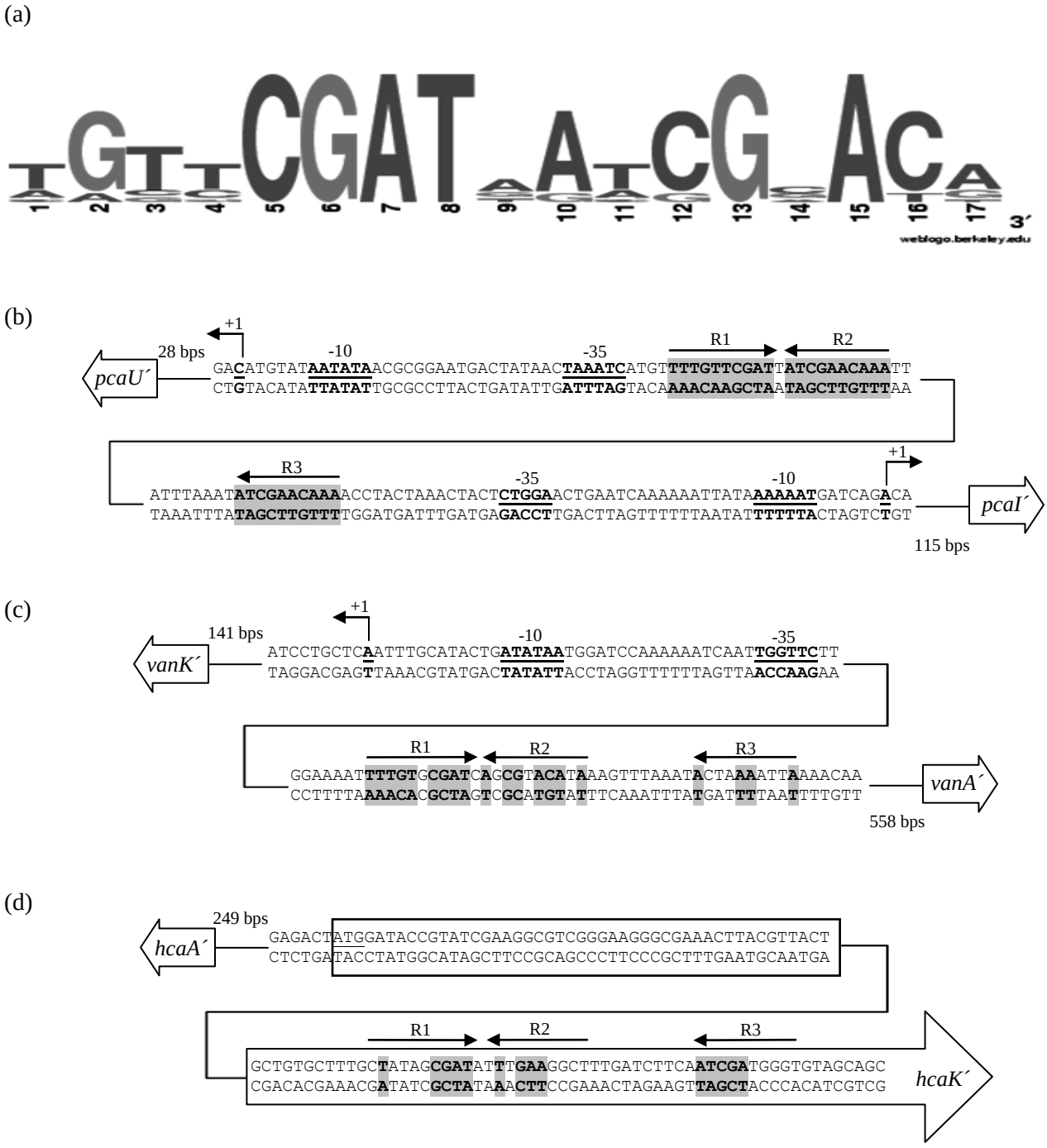

Figure 3.23. PcaU binding sites. (a) Profile summarizing nucleotide occurrence in the palindrome of nine known binding sites of PcaU, PobR (*A. baylyi*), PobR and PcaR (*P. putida*). The size of letters corresponds to the frequency of occurrence of this nucleotide at this position (Jerg & Gerischer, 2008). PcaU binding motifs within the intergenic *pcaU-pcaI* (b; confirmed), *vanA-vanK*; (c; putative), and *hcaA-hcaK* (d; putative) regions of *A. baylyi*. The repeated regions of the putative PcaU binding sites are indicated by R1, R2, and R3. Genes and gene names are indicated by white arrows. Relevant promoter regions are indicated (-10; -35), as well as the transcriptional start points (+1). The translational start point of *hcaK* is indicated (ATG; underlined). The distance of the sequence shown to the respective translational start points is given in bps. Conserved residues regarding the binding motif of the intergenic *pcaU-pcaI* region are highlighted.

Using "Prodoric release 2", one potential new binding site for PcaU was found in the intergenic region between *vanA* and *vanK* (Fig. 3.23 (c)). This motif is located directly upstream of the transcriptional start point of *vanK*, encoding the vanillate transport protein. However, the site is not exactly homologous to the original motif between *pcaU* and *pcaI* (Fig. 3.23 (b)). Particularly R3 shows only 40 % sequence similarity, while R1 and R2 are 90 and 70 % identical to R1 and R2 of the original binding site, respectively. The transcriptional start site of *vanK* was identified by 5´RACE (Chapter 2.8.6) as described in chapter 3.3.5, and a putative -10 and -35 region is suggested (Fig. 3.23 (c)). Here, the newly suggested PcaU binding site is separated by 9 bps from the predicted -35 promoter region of *vanK*. This genetic organization is similar to the situation found in the *pcaU-pcaI* intergenic region (Fig. 3.23 (b)). The conserved nucleotides at positions 5, 6, 7, 8, 13, and 15 (Fig 3.23 (a)) are present in the new site found upstream of *vanK*, as well as the two guanine nucleotides within R1. Furthermore, a putative PcaU binding site was found at the 5´end of the *hcaK* gene, 56 bps downstream of the translational start site (Fig. 3.23 (d)). The transcriptional start site of *hcaK* was determined by 5´RACE (Chapter 3.3.5) as well, and is located 60 bps upstream of the translational start site. The motif found in *hcaK* (Fig. 3.23 (d)) does show 50 % (R1) and 40 % (R2; R3) sequence similarity to the original motif (Fig. 3.23 (b)), and does contain the conserved nucleotides of the consensus binding site (Fig. 3.23 (a)) at positions 5, 6, 7, 8, 13 and 15. However, only one of the two conserved guanine residues within R1 is present.

3.4.5 Binding of PcaU to its putative binding sites

Functionality of the putative PcaU binding sites shown in Fig. 3.23 (c) and (d) was tested by means of EMSAs (Chapter 2.10.4). PcaU was purified as described (2.10.1 to 2.10.2) using *E. coli* BL21 and plasmid pAC115 (Table 2.2; (Jerg & Gerischer, 2008)). Fig. 3.24 (a) shows the chromatogram of PcaU-6His purification after His-Tag nickel affinity chromatography. After protein purification, size and purity of PcaU-6His (native PcaU monomer: ~ 28 kDa) was analyzed by running a 12 % SDS-PAGE (Chapter 2.9.4; Fig 3.24 (b)), and protein concentration was determined with the BCA™ Protein Assay Kit (Thermo Fisher Scientific Inc.; Chapter 2.10.3).

For EMSA experiments, DNA probes were amplified by PCR using the respective primers listed in Table 2.3. DNA fragments contained either the putative new PcaU binding sites found for the *hca* and *van* regions as indicated in Fig. 3.25 (a) and (b), or the native binding site located in the intergenic region between *pcaU* and *pcaI* (199 bps). EMSA experiments were carried out as explained in methods (Chapter 2.10.4), using 1.58 nM of the DNA fragment containing the native site between *pcaI* and *pcaU* (positive control), the *van* EMSA probe (248 bps; Fig 3.25 (b)), or the negative control. 20.86 nM DNA were used for the *hca* EMSA probe (813 bps; Fig 3.25 (a)). The negative control used was a PCR product (490 bps)

from the *sucCD* promoter region of *C. glutamicum*, showing no sequence similarity to the PcaU binding site. DNA probes were incubated with increasing amounts of PcaU-6His, ranging from 0 to 1122 nM.

The DNA-protein complexes were analyzed by running a 2 % agarose gel (*hca* probe) stained with ethidium bromide, or a 6 % PAGE (positive control, *van* probe, negative control), stained with SYBRgold (Fig. 3.25 (c) to (f)).

As shown in Fig. 3.25 (d) and (e), an interaction of PcaU was evident with the *van* and the *hca* probes, as it was for the positive control (Fig. 3.25 (c)), resulting in a retarded mobility of the DNA-protein complex in comparison to the unbound DNA fragment.

However, two positions of retardation (Fig. 3.25 (c)) are visible for the *pca* region, but only one is observed using *van* as probe (Fig. 3.25 (d)). Furthermore, PcaU is able to bind the *pca* probe at lower concentrations as compared to the *van* probe, suggesting a higher affinity of PcaU to its native site (retardation is visible at PcaU concentrations of 187 nM and 374 nM, respectively; Fig. 3.25 (c) and (d)).

The *hca* probe was used in higher concentrations than the positive control (20.86 nM versus 1.58 nM), and conclusions regarding binding strength cannot be drawn at this point. Nevertheless, PcaU-6His specifically bound the *hca* probe, producing at least one retardation step (Fig. 3.25 (e)).

To summarize the results presented in chapters 3.4.4 and 3.4.5: putative new binding sites for PcaU were identified within the *hcaK* coding region and between *vanA* and *vanK* using a bioinformatical approach. The functionality of the sites was proved in EMSAs, since purified PcaU-6His was able to bind DNA fragments containing these sites specifically. The findings presented here are in line with the reporter gene results described in chapters 3.4.1 and 3.4.3.

(a)

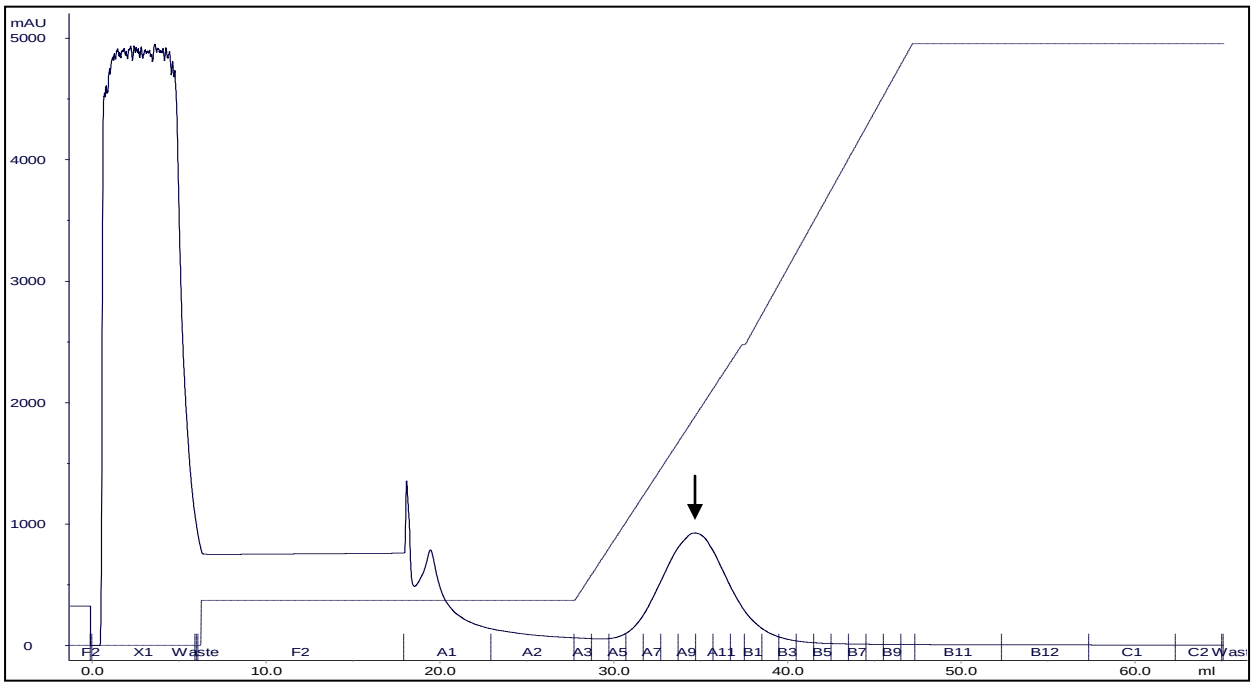

(b)

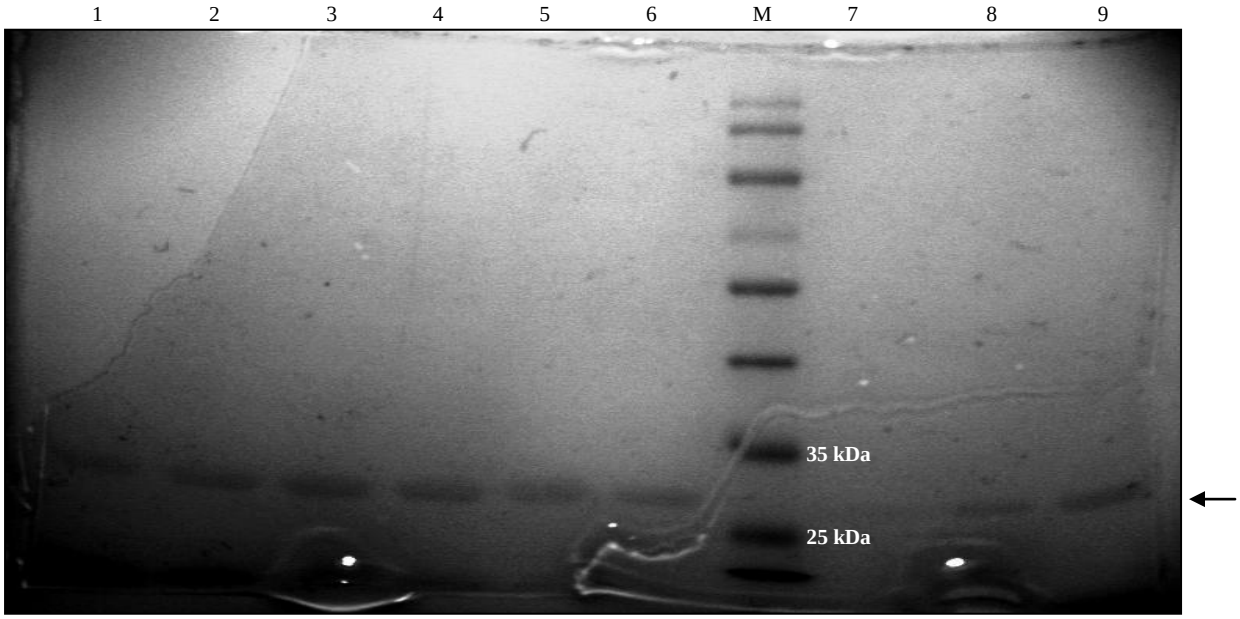

Figure 3.24. Purification of PcaU-6His. (a) Chromatogram of PcaU-6His after Ni^{2+} affinity chromatography. The protein peak is marked by an arrow. Proteins were detected my measuring the absorption at 280 nm (mAU, y-axis, solid line). PcaU-6His was eluted by applying a linear imidazole gradient, ranging from 5 to 500 mM (0 to 100 % elution buffer; dashed line). Fractions collected are indicated (A1 to C2; above x-axis). (b) 12 % SDS-PAGE of purified PcaU-6His. Lane 1 to 6: protein fractions A7 to A12, after HisTrap™ FF column. M: PAGE Ruler Prestained protein-ladder (Fermentas). Lane 7: protein fraction A9 after Desalting column. Lane 8 and 9: protein fraction A10 after Desalting column. PcaU-6His is marked by an arrow next to the gel.

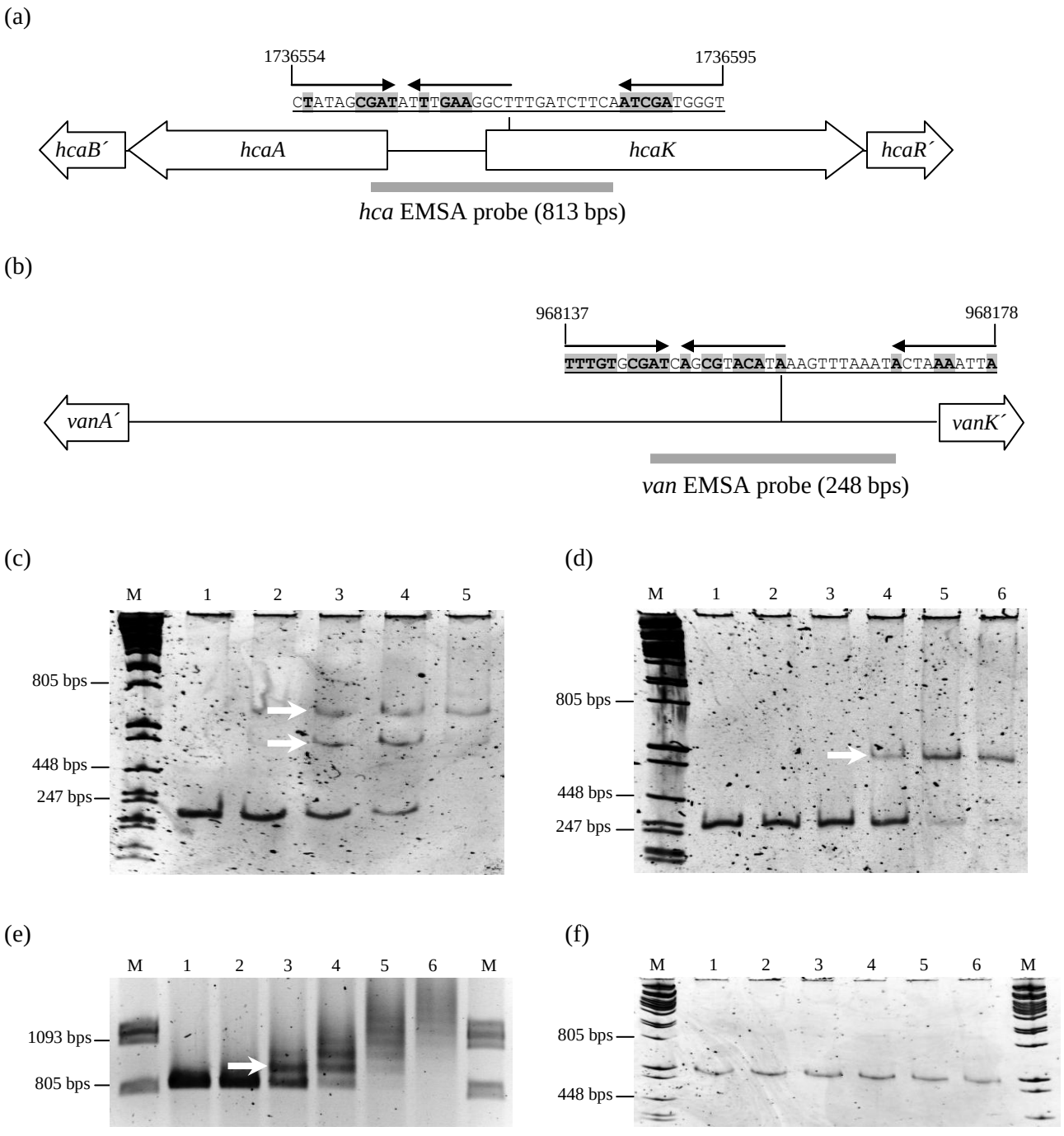

Figure 3.25. Electro mobility shift assays (EMSAs) to show interaction of PcaU with DNA fragments containing (putative) PcaU binding sites. The sequence of the putative new PcaU binding sites within the *hca* (a), and *van* (b) regions are shown, as well as their position in the chromosome. Conserved positions regarding the binding motif of the intergenic *pcaU-pcaI* region are highlighted. Probes used in EMSA experiments are indicated by a gray bar. Analysis of protein-DNA complexes using polyacrylamide or agarose gels are shown for the *pca* (positive control; (c)), *van* (d), *hca* (e), and *sucCD* regions (negative control; (f)). PcaU-6His was added in increasing concentrations (0, 93.4, 187, 374, 748, 1122 nM; lanes 1 to 5 or 1 to 6 in (c), (d), and (f); 0, 77.5, 155, 310, 620, 939 nM; lanes 1 to 6 in (e)). M: λ *Pst*I DNA ladder. Retarded protein-DNA complexes are marked by white arrows.

3.4.6 Exact determination of the PcaU binding site upstream of *vanK*

In order to determine the binding site of PcaU upstream of *vanK* experimentally, DNaseI footprinting assays were performed (Chapter 2.10.5). The *van* fragment used for this purpose was the same as in the EMSA experiments (248 bps; Chapter 3.4.5).

The template for the sequencing reaction (Chapter 2.10.5.2) was obtained by insertion of the amplified *van* fragment (Fig. 3.26 (a)) into the vector pDrive (QIAGEN; Chapter 2.8.5). The sequencing reaction was then performed using the T7 Sequencing Kit (USB Corporation; Chapter 2.10.5.2), 1.5 µg of plasmid DNA (pAC150; Table 2.2), primer vanK5_*Cla*I (Table 2.3; Fig. 3.26 (a)), and [α ^{32}P]-dATP. The T7 Sequencing Kit is based on the method described by Sanger and colleagues in 1997: four sequencing reactions are performed, containing ddATP, ddTTP, ddGTP, or ddCTP, repectively. The random incorporation of a dideoxynucleotide leads to premature termination of the strand synthesis, generating fragments of variable length. The radioactive [α ^{32}P]-dATP is incorporated instead of cold dATP. Using this method, a radiolabeled dideoxy sequencing ladder is obtained, which is run alongside the DNase I footprinting reaction of the same fragment.

For the footprinting reaction, the *van* fragment (Fig. 3.26 (a)) was radioactively end-labeled using T4 PNK (Fermentas; Chapter 2.8.3.3) and [γ ^{32}P]-ATP. To obtain only one radioactive labeled end, the fragment was treated with *Pvu*I. Binding of PcaU to this fragment was performed as explained in Chapter 2.10.5.1, using 15000 cpm of radiolabeled probe and PcaU in increasing concentrations (0 to 8976 nM). After DNase I digestion (Chapter 2.10.5.1) and DNA purification, DNA fragments were separated running a denaturing polyacrylamide gel electrophoresis (Chapter 2.9.3). Radioactivity was detected using a Bio Imager BAS (Fuji Photo Film Co., Ltd.).

The result of the footprinting experiment is shown in Fig 3.26 (b). However, the footprint did not turn out as expected, considering that the binding of a protein to a distinct sequence is commonly seen as an area where DNA fragments are absent, compared to the probe without protein. Nevertheless, some bands are decreasing in intensity and apparently disappearing at high PcaU concentrations (marked by arrows on the right border of the gel in Fig. 3.26 (b)). Those bands are all over the regions of R1 and R2 of the predicted PcaU binding site upstream of *vanK*. These findings may indicate DNA-PcaU interactions. However, results should be regarded as preliminary, and it will need some future work to confirm these findings.

(a)

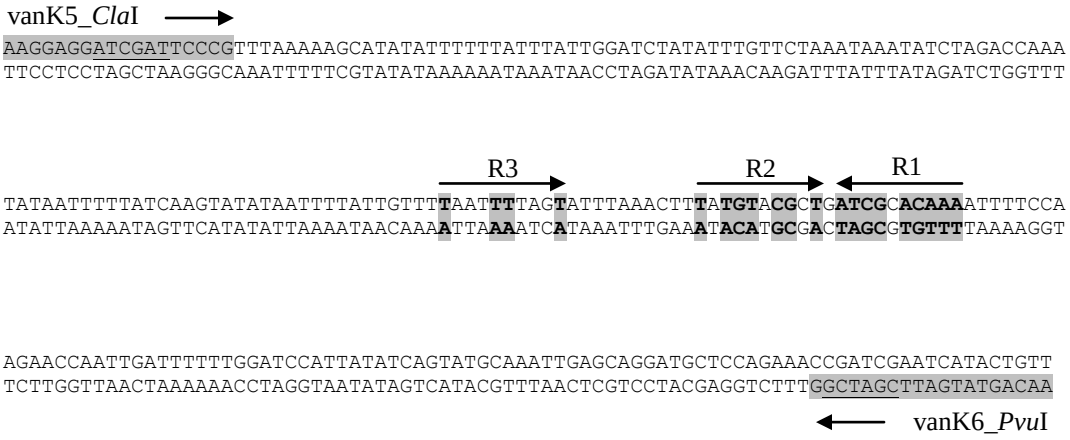

(b)

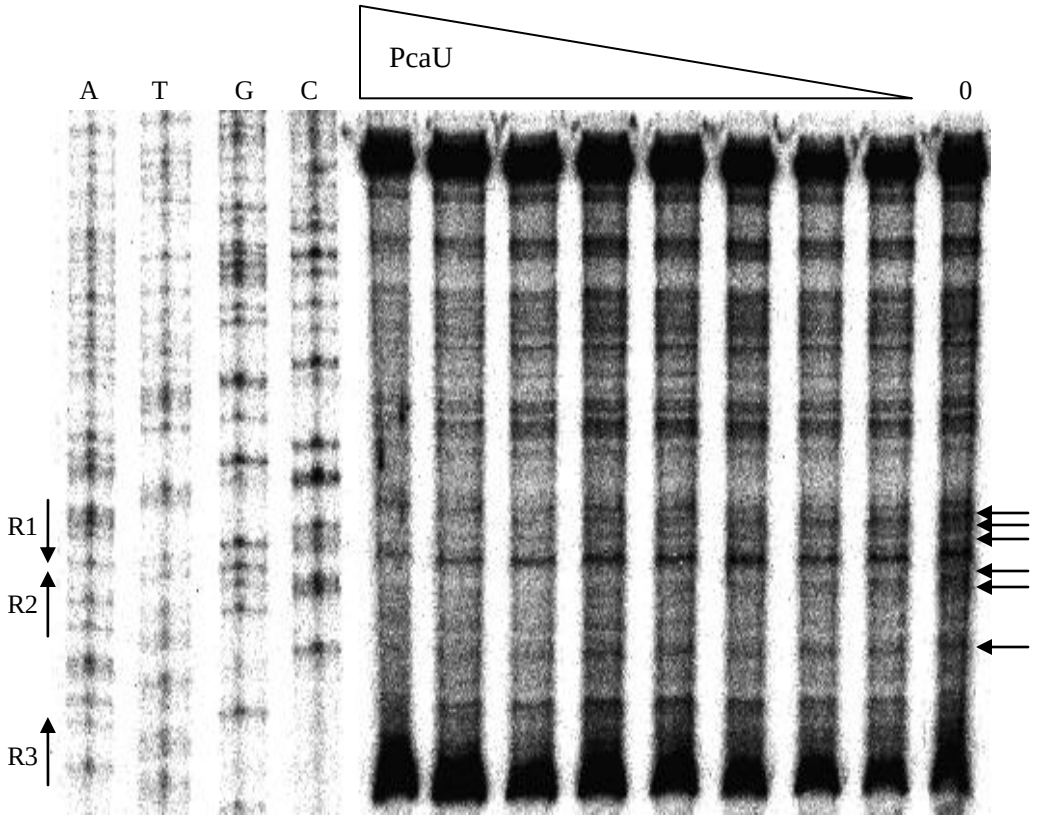

Figure 3.26. DNase I footprinting. (a) Sequence of the *van* fragment used in DNase I footprints; primer sites are indicated (vanK5_*Cla*I; vanK6_*Pvu*I); recognition sites of restriction endonucleases are underlined; the putative PcaU bindig site is indicated by arrows and the labels R1, R2, and R3. (b) DNase I footprinting with the *van* probe. The sequencing reaction of the fragment is shown on the left (A, T, G, C), and the digested fragment on the right. PcaU was added in decreasing concentrations (8976, 4488, 2244, 1122, 748, 374, 187, 93.4, 0 nM). Arrows on the left indicate the positions of the predicted PcaU binding site (R1, R2, and R3). Bands of decreasing intensity are marked by arrows on the right border.

3.5 Analysis of *vanK* expression

The *vanK* gene is encoding a transport protein, suggested to be involved in the transport of aromatic compounds, especially vanillate (Segura *et al.*, 1999, D'Argenio *et al.*, 1999). The *vanK* gene neighbors the *vanA,B* genes, essential for growth with vanillate. On the basis of its genetic location and its sequence similarity to other proteins associated with aromatic compound transport, it was designated *vanK* (Segura *et al.*, 1999). In *A. baylyi* strain ADP1, permeases associated with the β-ketoadipate pathway, are designated MucK (Williams & Shaw, 1997), BenK (Collier *et al.*, 1997), PcaK (Kowalchuk *et al.*, 1994), and VanK, responsible for the transportation of CCM, benzoate and benzaldehyde, PCA and POB , or vanillate, respectively. Those four transport proteins are all members of the major facilitator superfamily (MFS (Pao *et al.*, 1998)). Interestingly, studies described an overlapping specificity of VanK and PcaK, regarding substrate transport (D'Argenio *et al.*, 1999), explaining that earlier studies failed to identify a phenotype with *vanK* (Segura *et al.*, 1999). Authors showed that growth on PCA (and also quinate, as it is converted to PCA in the periplasm) as the sole carbon source, is impaired for strains containing a dysfunctional *vanK* and *pcaK*. In contrast, growth of these strains was not hindered in the presence of POB or vanillate. Thus, *vanK* is the first chromosomal locus that can specifically influence PCA catabolism and is not within the *dca-pca-qui-pob-hca* supraoperonic cluster (D'Argenio *et al.*, 1999). These results may provoke the hypothesis, that VanK has a broad substrate spectrum, of aromatic components transported.

3.5.1 Refining the substrate spectrum of VanK

3.5.1.1 Overlapping specificity of transport proteins

since earlier studies failed to identify a phenotype connected with *vanK* (Segura *et al.*, 1999), a strain harboring a non-functional *vanK* gene (ADPU112; Table 2.1; *vanK-luc* (Bleichrodt *et al.*, 2010)) was tested for its ability to grow on vanillate. Growth was performed overnight on solid minimal media containing vanillate (5 mM) as the sole carbon source at 30 °C, in comparison to the wild type strain ADP1. As expected, ADPU112 was able to grow on vanillate in the same manner as the wild type, indicating another transport system masking VanK. Further, additional carbon sources were tested, as POB, PCA, and quinate (5 mM each), with the same result, which was expected, since PcaK is considered to be responsible for their transportation. Since these experiments did not give any hint to a substrate transported by VanK, expression of the *vanK* gene in response to several aromatic compounds was analyzed.

3.5.1.2 Expression of *vanK* in response to several aromatic compounds

To identify substances that may be transported by VanK, the expression of the *vanK* gene was determined in response to different aromatic compounds which are degraded through the PCA branch of the β-ketoadipate pathway, as quinate, PCA, and POB, in comparison to the induced activity by vanillate (Bleichrodt *et al.*, 2010).

Therefore, luciferase assays (Chapter 2.11) were carried out with strain ADPU112 (*vanK-luc* transcriptional fusion (Bleichrodt *et al.*, 2010)). ADPU112 was grown on pyruvate (20 mM) as a non-repressing carbon source (Siehler *et al.*, 2007, Fischer *et al.*, 2008, Bleichrodt *et al.*, 2010), and induction of *vanK-luc* was determined upon growth in the presence of increasing concentrations (0.5 to 5.0 mM) of vanillate, quinate, PCA, and POB (Table 3.5). Results shown above (Chapter 3.7.1.1) ensure vanillate, quinate, PCA, and POB presence in the cell where they can act as inducers, since ADPU112 is able to grow on each aromatic compound as the sole carbon source.

Table 3.5 clearly shows that expression of *vanK* is activated by the addition of vanillate, quinate, POB, and PCA. These results may give first hints of VanK being able to transport each one of the tested aromatic compounds into the cell. However, all tested compounds are degraded to PCA in the β-ketoadipate pathway, and PCA may serve as the sole inducer releasing *vanK* expression. Interestingly, *vanK* expression did not increase with increasing quinate, POB, and PCA concentrations, as it did with increasing vanillate concentrations.

3.5.1.3 Expression of *vanK* in response to several aromatic compounds in strains blocked in PCA formation

To clearly identify aromatic compounds able to induce *vanK* expression, and to exclude the possibility of PCA being the sole inducer releasing *vanK* expression, a block in vanillate, quinate, or POB degradation was constructed. Those blocks were constructed based on ADPU112 (*vanK-luc*; Table 2.1 (Bleichrodt *et al.*, 2010)), by deleting *vanB*, *quiC*, and *pobA*, as described in methods (Chapter 2.1). As a consequence, strains ADPU153, ADPU154, and ADPU155 (Table 2.1) would not be able to degrade vanillate, POB, and quinate to PCA, respectively. Using those strains, *vanK* expression was determined in response to vanillate, POB, and quinate in increasing concentrations (0.5 to 5.0 mM; Table 3.6), as explained above for the parental strain ADPU112 (Chapter 3.7.1.2).

Results presented in Table 3.6 identify vanillate and POB as inducers for *vanK* expression, since *vanK* activity is increased 2.5 and 3.5-fold in the presence of vanillate and POB. Quinate failed to induce *vanK* activity. In contrast to results obtained for the parental strain ADPU112, *vanK* expression is not increasing

with increasing vanillate concentrations, and the activity is in each case as high as the activity measured for ADPU112 with the highest vanillate concentration. This may be due to the block in vanillate degradation, since vanillate is not degraded and present constantly. The same was observed for the activity measured in the presence of POB. However, the basal activity of strains ADPU153 to 155 is significant higher compared to ADPU112. The molecular mechanism forming the basis for this observation is not clear so far, and the analysis of this mechanism could be the subject of future investigations.

Nevertheless, results presented in Table 3.5 and 3.6 clearly show that *vanK* expression is specifically activated by at least vanillate and POB. Results further suggest a specific induction by PCA, but downstream metabolites cannot be excluded in mediating induction at this point.

Table 3.5. Expression of *vanK-luc* given as specific luciferase activity in response to increasing concentrations of vanillate, quinate, POB, and PCA.

		Luciferase activity[a]			
Basal activity	**Inductor**	**0.5 mM**	**1.0 mM**	**2.5 mM**	**5.0 mM**
478 ± 49	Vanillate	1981 ± 231	2098 ± 284	2748 ± 786	4730 ± 1828
	Quinate	1423 ± 128	1266 ± 227	1449 ± 243	1415 ± 256
	POB	1772 ± 303	1606 ± 163	1924 ± 255	1796 ± 188
	PCA	1618 ± 77	1573 ± 59	1544 ± 55	1270 ± 3

[a] Values are given as specific luciferase activity [RLU/OD_{600}], and are averages of at least three independent experiments, standard deviation is given.

Table 3.6. Expression of *vanK-luc* given as specific luciferase activity in strains carrying a block in PCA formation in response to increasing concentrations of vanillate, quinate, and POB

		Luciferase activity[a]				
Strain	**Inductor**	**0.5 mM**	**1.0 mM**	**2.5 mM**	**5.0 mM**	**Basal activity**
ADPU153	Vanillate	3995 ± 377	3422 ± 225	3785 ± 1028	4487 ± 1635	1778 ± 280
ADPU154	POB	3282 ± 695	3762 ± 54	3675 ± 153	3704 ± 281	1075 ± 82
ADPU155	Quinate	1038 ± 372	1122 ± 201	1078 ± 210	1180 ± 246	1034 ± 185

[a] Values are given as specific luciferase activity [RLU/OD_{600}], and are averages of at least three independent experiments, standard deviation is given.

4 Discussion

The ability to adapt gene expression is a powerful tool of an organism exposed to a continuously changing environment. For example, the mechanisms responsible for the adaptation of bacteria to the continuously changing presence of available carbon sources must be fast and unfailing. Only the best adapted organisms will have an advantage, regarding survival and reproduction. This advantage is dependent on energy conservation, since the carbon source which is easiest to degrade and which leads to maximal energy conservation has to be preferred over others. The mechanism leading to preferred carbon source degradation is commonly described as carbon catabolite repression (CCR). With respect to aromatic compound degradation through the β-ketoadipate pathway in *Acinetobacter baylyi*, CCR acts on different levels. These mechanisms are known as (i) CCR by succinate and acetate, (ii) cross-regulation by benzoate, and (iii) vertical regulation by protocatechuate (PCA). All three mechanisms share the ability to override the specific gene regulation, and are thus of elevated nature.

The analysis of these mechanisms is the central part of the current thesis, and mainly based on luciferase reporter gene strains, containing the *luc* gene (*Photinus pyralis*) as a transcriptional fusion in genes encoding enzymes involved in aromatic compound degradation. As described in the following chapters, regulatory proteins involved in CCR, cross-regulation and vertical regulation were identified *in vivo*. In addition, the compounds inducing the regulations were identified and hints about how the mechanisms could work were derived from in *in vivo*, *in vitro*, and *in silico* approaches.

4.1 The *salA* and *vanK* genes undergo CCR by organic acids

After the introduction of the luciferase reporter gene (Bonin *et al.*, 1994) as a transcriptional fusion into the *salA* and *vanK* gene, luciferase assays were performed in the presence of organic acids (Chapter 3.1). It was shown that both genes undergo a strong repression in the presence of succinate and acetate in addition to the aromatic inducers salicylate and vanillate. The repression was strongest when succinate and acetate were present simultaneously (down to 58 % and 12 %). The presence of either succinate or acetate also led to a repressed expression in the presence of the aromatic inducer, but to a lesser extent; down to 61 and 75 % for *salA*, and 19 and 15 % for *vanK*. The presence of pyruvate with aromatic inducer allowed high expression of both genes.

The repressing effect of the non aromatic compounds succinate and acetate on the enzymes of the β-ketoadipate pathway of *A. baylyi* (earlier known as *Moraxella calcoacetica*) is well known (Canovas & Stanier, 1967). Further studies showed, that the substrate combination succinate and acetate has a

repressing effect (down to 10 %) on the activity of the protocatechuate-3,4-dioxygenase, responsible for the breakdown of PCA to β-carboxy-*cis*, *cis*-muconate. The enzyme is encoded by the *pcaH,G* genes, which are part of the *pca-qui* operon. The expression of the operon was shown to be repressed by succinate and acetate, when added in addition to the aromatic compound, known to induce gene expression (Dal *et al.*, 2002). This repression, occurring at the transcriptional level, has also been shown for other operons involved in aromatic compound degradation in *A. baylyi*, such as *pob* (Dal *et al.*, 2002), *ant*, *are*, *ben*, *dca*, *hca* (Fischer *et al.*, 2008), *catA*, *catB,C,I,J,F,D*, and *vanA,B* (Bleichrodt *et al.*, 2010). Although some of these operons are clustered (*sal-are-ben-cat* and *dca-pca-qui-pob-hca*; exception: *ant* and *van*) and organized in catabolic islands on the *A. baylyi* chromosome (Fig 1.2), they all undergo a specific regulation by an individual transcriptional regulator in response to an aromatic inducer molecule. Keeping the distributed location on the chromosome and the specific regulation of the operons in mind, it can be concluded that CCR by succinate and acetate is a global regulatory effect.

Concerning the *sal* operon, there is a study describing CCR by succinate at the level of enzyme activity (Jones *et al.*, 2000). The *sal* region includes three genes: *salA*, encoding the salicylate monooxigenase; *salE*, encoding the salicylate esterase; and *salR*, encoding the transcriptional regulator. The activity of SalA and SalE was determined in the presence of the specific aromatic inducers salicylate and ethylsalicylate with or without the addition of succinate. It was shown that both enzymes showed a repressed activity in the presence of succinate. SalA was reduced down to 78 % in the presence of succinate in addition to salicylate, and down to 37 % when succinate was added with ethylsalicylate. The activity of SalE decreased to 20 % in the presence of succinate in addition to ethylsalicylate.

Concerning the *A. baylyi vanK* gene, this is the first data describing *vanK* expression in the presence of succinate and acetate. *vanK* is supposed to encode a transport protein (major facilitator superfamily) required for vanillate uptake, according to its sequence similarity to other transport proteins for aromatic compounds and to its genetic adjacency to the *van* region (Segura *et al.*, 1999, D'Argenio *et al.*, 1999). The finding that *vanK*, which is not directly involved in aromatic compound degradation through the β-ketoadipate pathway, is also undergoing repression by succinate and acetate may indicate that the principle of inducer exclusion is a part of CCR by succinate and acetate in addition to aromatic compounds. Since *vanK* expression is repressed by the organic acids, no protein may be build, and vanillate (as the inducer for *vanA,B* expression (Morawski *et al.*, 2000)) would be excluded from the cell, unable to induce activity of genes encoding enzymes required for vanillate degradation. The system of inducer exclusion was shown earlier for other Gram-negatives, such as *E. coli* (Hogema *et al.*, 1998). Here, the simultaneous presence of e. g. glucose-6-phosphate and lactose leads to CCR, since glucose-6-phosphate inhibits the uptake of lactose into the cell. Thus, lactose consumption is repressed. Among other

things, the mechanism realized in *E. coli* involves the phosphotransferase system (PTS) and especially enzyme IIA(Glc), which is blocking lactose uptake by binding the lactose carrier.

The results of this chapter were completely published in 2010 and are also discussed in the corresponding publication (see attachments).

4.2 CCR by succinate and acetate involves the catabolite repression control protein

The impact of the Crc (catabolite repression control) protein on CCR by succinate and acetate was analyzed by deleting the *crc* gene in strains, carrying the luciferase reporter gene (Bonin *et al.*, 1994) as a transcriptional fusion in the *antA*, *areA*, *salA*, and *vanK* genes. The activity of the operons was determined in the presence of succinate and/or acetate in addition to the aromatic inducer and compared to the activity shown by the respective *crc* positive strain (Chapter 3.1). In addition, the activity of the *ben*, *catA*, *catB,C,I,J,F,D*, *dca*, *hca*, and *vanA,B* operons was determined in a *crc* negative background in the presence of succinate or acetate, to complete earlier experiments using the substrate combination succinate and acetate (Bleichrodt, 2007). The experiments showed that CCR in the presence of the substrate combination succinate and acetate in addition to the aromatic inducer is dependent on a functional *crc* gene, since all operons (with the exception of *catA*) responded with a derepression of promoter activity in a *crc* negative background. This increase in expression ranged from 1.43-fold for the *ant* operon to 27.88-fold for the *ben* operon. The results obtained in the presence of either succinate or acetate in addition to the aromatic inducer, were comparable to those found for the substrate combination. However, there were some expectations, most remarkable the *ben* operon, which responded with a decrease of promoter activity in the presence of succinate (down to 13 %). The results for the *catA* operon were also outstanding, as no significant change in repression was observed in a *crc* negative background in the presence of succinate or acetate, and a decrease in expression was observed in the presence of the substrate combination succinate and acetate.

It can be concluded from the data described above, that (i) the Crc protein is a key player in CCR of aromatic compound degradation observed in the presence of the substrate combination succinate and acetate in addition to an aromatic compound, and (ii) that it acts at the transcriptional level regarding the operons studied here. As described for the mechanism CCR (Chapter 4.1), Crc has an impact on the expression of genes all undergoing a specific transcriptional regulation, and located mostly clustered but distributed on the *A. baylyi* chromosome (Fig. 1.2). It can be concluded herefrom, that Crc is a global regulator participating in the global mechanism of carbon catabolite repression in response to succinate and acetate governing the *A. baylyi* β-ketoadipate pathway.

Interestingly, *A. baylyi* Crc has also been shown to act postranscriptionally (Zimmermann *et al.*, 2009). In the corresponding study the effect of Crc was first analyzed at the level of enzyme activity. It was shown that the activity of the protocatechuate-3,4-dioxygenase (PcaH,G) is drastically increased in a strain lacking *crc*, after growth on the carbon source combination succinate and acetate in addition to the aromatic inducer. Surprisingly, a *lacZ* reporter gene fusion with *pcaIp*, directing expression of the *pca* genes, did not reveal a strong impact of Crc at the transcriptional level. But the half-life of the *pca-qui* transcript was shown to be drastically increased in the absence of *crc*. Thus, in this special case, Crc seems to act primary posttranscriptionaly.

The Crc protein was originally identified in *Pseudomonas aeruginosa* (MacGregor *et al.*, 1991, Wolff *et al.*, 1991). *Pseudomonas* Crc was shown to be involved in the repression of a number of genes, in several studies.

An example for the action of Crc is described for the *benA,B,C,D* genes from *P. putida* (Moreno & Rojo, 2008). The expression of the *benA,B,C,D* genes (encoding enzymes required for benzoate degradation) was shown to be strongly repressed when other preferred carbon sources are present. This repression is caused by Crc by binding the 5´end of the *benR* mRNA. Crc bound to the *benR* mRNA, acts by reducing the translation efficiency, thus reducing BenR levels below those required for the full *ben* gene expression. These findings were further supported by the observation of the sensitivity of a translational *benR-lacZ* fusion to Crc, what was not observed for the transcriptional fusion. Similar observations were made for the regulator of the alkane degradation pathway of *P. putida*, AlkS (Moreno *et al.*, 2007). The *bkd* operon of *P. putida* and *P. aeruginosa* is also subject to CCR and Crc (Hester *et al.*, 2000a, Hester *et al.*, 2000b). The *bkd* operon encodes enzymes required for the degradation of branched-chain keto acids. Crc has been shown to be involved in CCR of the *bkd* operon by regulating the amount of the BkdR regulator posttranscriptionaly.

If *A. baylyi* Crc is acting in a comparable manner as the *Pseudomonas* Crc, by influencing gene activity indirect by binding to the mRNA of specific transcriptional regulators is unclear so far, and has to be evaluated in the future.

The results of this chapter were completely published in 2010 and are also discussed in the corresponding publication (see attachments).

4.3 Expression pattern in the presence of lactate and gluconate

The expression pattern of the *ant*, *are*, *catA*, *catB,C,I,J,F,D*, *vanA,B*, *salA*, and *vanK* operons was analyzed in the presence of gluconate and lactate, in addition to the aromatic inducer, using the respective luciferase reporter gene strains. The activity of the operons under these conditions was compared to the activity on pyruvate plus aromatic inducer (Chapter 3.2). Luciferase reporter gene assays showed that the presence of lactate had a slight repressing effect on the *vanA,B* and *vanK* genes (down to 58 and 46 %), while no change in activity was seen for the *catB,C,I,J,F,D* and *salA* genes. The slight repressing effect of lactate in the presence of the aromatic inducer was previously seen for the *ant* and *are* operons (Fischer *et al.*, 2008). In the presence of gluconate and inducer, no change in expression was observed for the *salA* gene, a slight repressing effect on the *areA* gene (down to 63 %), and a moderate repressing effect on the *vanA,B*, *vanK*, *catB,C,I,J,F,D*, and *antA* genes (down to 48, 36, 35, and 16 %). The *catA* operon showed an ambivalent expression pattern, since expression increased on gluconate (2.4-fold), but was decreased down to 10 % on lactate.

Pyruvate is considered as a non repressing carbon source regarding expression of operons involved in aromatic compound degradation in *A. baylyi* (Dal *et al.*, 2002, Fischer *et al.*, 2008, Bleichrodt *et al.*, 2010). In contrast, the substrate combination succinate and acetate caused strong repression of all operons analyzed (Chapter 4.1). The comparison of the expression of operons on lactate and gluconate plus aromatic inducer, with the one on pyruvate or succinate and acetate plus aromatic inducer, allows the following conclusions:

Lactate is a non repressing carbon source for the *catB,C,I,J,F,D* and *salA* operons, since their expression is as strong as in the presence of pyruvate. Since only a slight repressing effect was observed for the *vanA,B*, *vanK*, *areA*, and *antA* genes, which is not at all comparable to the drastic repressing effect of the substrate combination succinate and acetate, lactate is considered to be a slightly repressing carbon source for *vanA,B*, *vanK*, *areA*, and *antA* gene expression. This is not conferrable to *catA*, as expression is significant repressed, although 10-fold higher than in the presence of the organic acids. However, a non repressing effect of lactate (as it is seen for pyruvate) would absolutely make sense, since lactate can easily be converted to pyruvate by the action of lactate/pyruvate dehydrogenase. The fact that lactate is only one step away from pyruvate, may implicate related effects. In *A. baylyi*, energy conservation occurs by the oxidation of succinyl-CoA and acetyl-CoA. The fact that lactate and pyruvate cause no or slight repression of the operons (with the exception of *catA*), may indicate that lactate and pyruvate are not such abundant carbon sources for *A. baylyi* in its natural habitat. Thus, no regulatory mechanism may have been evolved.

The results obtained for lactate are partially comparable to gluconate. Although, slight and moderate repressing effects are observed in the presence of gluconate for some operons, the repression by the organic acids was higher in each case (Fischer *et al.*, 2008, Bleichrodt *et al.*, 2010). The degradation of glucose (forming gluconate as an intermediate) by *A. baylyi* is complex and energy consuming (van Schie *et al.*, 1985), since it requires the involvement of a special enzyme (pyrrolquinoline quinone, PQQ (Goosen *et al.*, 1989)) and has to be taken into the cell by active transport. Gluconate then is activated to 6-phosphogluconate, which is another energy consuming step. The utilization of glucose or gluconate is an unusual trait among different *Acinetobacter* isolates. Thus, it seems to fit that there is no strong repression of operons associated with the β-ketoadipate pathway, by gluconate as observed for succinate and acetate.

The results of this chapter were completely published in 2010 and are also discussed in the corresponding publication (see attachments).

4.4 Crc is involved in the expression of operons on pyruvate and lactate, but not on gluconate

The dependence of the expression of the *ant*, *are*, *ben*, *catA*, *catB,C,I,J,F,D*, *dca*, *hca*, *sal*, *vanA,B*, and *vanK* on Crc in the presence of pyruvate, lactate and gluconate in addition to the aromatic inducer, was determined with the respective luciferase reporter gene strains, all containing an inactivated *crc* gene. The luciferase activity shown was compared to the activity of the respective *crc* positive strain (Chapter 3.2; Fig. 3.10). It was observed that five out of ten operons (*ben*, *catA*, *hca*, *vanA,B*, and *vanK*) responded with a drastically increased promoter activity in the presence of pyruvate ranging from 3.2-fold to 4.2-fold (*catA* only slightly increased; 1.6-fold), while only four out of ten did when lactate was present (*dca*, *salA*, *vanA,B*, *vanK*). The increase in the presence of lactate never reached values comparable to pyruvate; increase on lactate ranging from 1.4-fold to 2-fold. However, the activity of the *are* and *ant* operons decreased on pyruvate and lactate, and the expression of the *catB,C,I,J,F,D* operon remained unaffected under any condition. The expression pattern observed for the *ben* operon was outstanding, since an increase was observed on pyruvate, and a decrease on lactate. No change was detected for any operon in the presence of gluconate.

Results presented confirmed that there is an involvement of Crc on the expression of operons tested at the transcriptional level in the presence of at least pyruvate and lactate. However, a common effect is not observed, since some operons responded with an increase, some with a decrease, and some operons were not affected by the absence of *crc* at all, dependent of the carbon source present. It will be challenging to

identify the molecular mechanism forming the basis of this observation; however, this has to be evaluated in the future.

4.5 Cross-regulation

Cross-regulation was analyzed by the use of luciferase reporter gene strains, containing the *luc* gene as a transcriptional fusion in the *hcaA*, *dcaA*, and *vanB* genes. The expression of the genes was analyzed in *catA* negative strains (Chapter 3.3.1) in the presence of the aromatic inducer with or without the addition of benzoate. In contrast to the *catA* positive strains, it was seen that the *hca* and *vanA,B* operons did not show an repression by benzoate in the addition of the aromatic inducer, and activity was as high as in the absence of benzoate (Fig 3.11). This was not seen for the *dca* operon, since the activity was the same as in the *catA* positive strain. The expression of the *hcaA*, *vanA,B*, and *dca* operon was further analyzed after deleting the *benM* and/or *catM* gene in the respective luciferase reporter gene strains. The expression was then determined in the presence of the aromatic inducer with or without the addition of benzoate. Compared to the *benM* and/or *catM* positive strain, the *hca* operon showed higher activity in the absence of *benM* or *catM* in the presence of benzoate and aromatic inducer (Fig. 3.12 (a)). In the absence of both, *benM* and *catM*, the expression in the presence of benzoate was as strong as in the absence of benzoate. The same was seen for the *vanA,B* operon (Fig 3.12 (b)), with an exception in the absence of *catM*: in this case the activity of *vanA,B* in the presence of benzoate in addition to the aromatic inducer was still repressed as in a *benM* and *catM* positive background, and not elevated as seen for the *hca* operon. The activity of the *dca* operon did not change with the deletion of *benM* and/or *catM*.
The bioinformatical analysis of the *hca*, *van*, and *dca* regions (Chapter 3.3.3) revealed putative new binding sites for BenM and CatM in each case. Electro mobility shift assays (EMSAs) showed a binding of BenM and CatM to the *hca* and *van* region, but not to the *dca* region (Chapter 3.3.4). The determination of transcriptional start points showed, that the putative BenM and CatM binding sites are close to the suggested promoter regions of *hcaK* and *vanK*.

The analysis of cross-regulation in the current thesis shed some light on the molecular mechanism responsible for the repression by benzoate, in addition to the aromatic compound inducing gene expression, observed at the *hca* and *vanA,B* operons.
A synergistic effect of the two LysR-type transcriptional regulators in repression of *hca* and *vanA,B* can be concluded since cross-regulation is not completely lost until both, BenM and CatM, are absent (Fig. 3.12). This is not surprising, given the synergistic action of BenM and CatM in gene regulation shown in earlier studies: both regulators are able to respond to *cis*, *cis*-muconate (CCM) and to recognize the same binding sequences (Bundy *et al.*, 2002). It was also shown, that in some cases the loss of one regulator is

compensated by the remaining other regulator (e. g. activating the expression of *benP* or *catA* (Clark *et al.*, 2002, Romero-Arroyo *et al.*, 1995)). In addition, a synergistic effect of BenM and CatM in cross-regulation of the *pobA* gene was confirmed in earlier studies (Brzostowicz *et al.*, 2003): as shown here for the *hca* and *vanA,B* operons, the repression of *pobA* by benzoate in addition to the aromatic inducer *p*-hydroxybenzoate (POB) was not lost until both, BenM and CatM, were absent. The authors could also identify CCM as the mediator causing cross-regulation of *pobA*.
In the current thesis, evidence is presented that CCM is the mediator releasing repression of the *hca* and *vanA,B* operons, since strains blocked in CCM formation showed a loss of cross-regulation (Chapter 3.3.1, Fig. 3.11). Until now, it was not clear if repression of *hca* and *vanA,B* may be also mediated by benzoate, bound to BenM. However, benzoate was excluded as mediator, as it was present throughout each experiment. Nevertheless, downstream metabolites formed by the degradation of CCM cannot be excluded to be involved in cross-regulation at the *hca* and *vanA,B* operons. But the fact that (i) BenM and CatM were never shown to respond to another compound as benzoate and/or CCM, and (ii) CCM was clearly identified in mediating repression of the *pobA* gene, supports the hypothesis of CCM being the mediator releasing cross-regulation at *hca* and *vanA,B*.

The involvement of BenM and CatM in cross-regulation and the molecular mechanism was further enlightened by the identification of putative new binding sites of BenM and CatM within intergenic regions *hcaA-hcaK* and *vanA-vanK* (Chapter 3.3.3), using bioinformatic tools (Mrazek & Xie, 2006) and the well-known consensus sequence of the binding site as a query (Fig. 3.13 (Craven *et al.*, 2008)). Subsequent, BenM and CatM were shown to bind these regions (Chapter 3.3.4). The determination of transcriptional start sites of *hcaK* and *vanK* (Chapter 3.3.5) further suggests a regulatory involvement of BenM and CatM in the expression of *hcaK* and *vanK* (encoding transport proteins for hydroxycinnamates and vanillate), rather than influencing the structural genes encoding enzymes for the degradation of hydroxycinnamates or vanillate. This is because the predicted BenM and CatM binding site is directly sitting on the transcriptional start site of *hcaK* (Fig. 3.18 (b). This may suggest that bound BenM or CatM impede access of the RNA polymerase to this region, blocking *hcaK* expression. The putative binding site found upstream of *vanK* is separated by 106 bps from the transcriptional start site (Fig. 3.18 (c)). Although, this arrangement is uncommon for a repressing mechanism by a regulatory protein, it is more likely that BenM and CatM influence expression of *vanK* than of *vanA,B*, as their translational start point is separated by 533 bps from the putative binding site. However, this possibility cannot be excluded, since the transcriptional start point of *vanA,B* is still unknown.

The assumption of BenM and CatM blocking *hcaK* and *vanK* expression would lead to the hypothesis that repression of *hca* and *vanA,B* seen in the presence of benzoate in luciferase assays is indirect. Since *hcaK*

and *vanK* encode for transport proteins for hydroxycinnamates and vanillate, blocking their transcription would lead to exclusion of those compounds from the cell, where they could act as inducers releasing expression of the *hca* and *vanA,B* genes. Similar conclusions were drawn for the *pobA* gene (Brzostowicz *et al.*, 2003, Siehler *et al.*, 2007). The transport protein responsible for POB uptake (which serves as inducer of *pobA*), is encoded by *pcaK*. *pcaK* is part of the *pca* operon, which is activated by PcaU in response to protocatechuate (PCA). Here, a putative binding site of BenM and CatM was identified directly downstream of the transcriptional start site of *pcaU* (encoding the transcriptional regulator for the *pca* genes (Gerischer *et al.*, 1998)), rather than within *pobA* regulatory regions. Binding of BenM and CatM to this region was shown, and the presence of CCM enhanced this binding (which gives additional evidence of CCM being the effector releasing cross-regulation). Further, no binding was detected with regulatory regions of *pobA* (Brzostowicz *et al.*, 2003). Authors concluded that bound BenM and CatM impede *pcaU* expression, and as a consequence prohibit induction of the *pca* genes (including *pcaK*) by PcaU. Further studies in fact showed, that expression from promoters *pcaUp* and *pcaIp* is repressed in the presence of benzoate (Siehler *et al.*, 2007). Thus, *pobA* repression by benzoate seems to be indirect. However, it was not clear at this point if *vanK* expression is also repressed in the presence of benzoate, which is important as PcaK and VanK were shown to possess overlapping specificity regarding substrate transport (D'Argenio *et al.*, 1999). Here supporting evidence is presented, of BenM and CatM bound to CCM may simultaneously prevent *pcaK, hcaK* and *vanK* transcription in the presence of benzoate, leading to exclusion of POB, hydroxycinnamates, and vanillate from the cell, where they could act as inducers. Similar observations were made in studies with *P. putida*, as POB degradation is prevented in the presence of benzoate, leading to preferred consumption of the latter carbon source (Cowles *et al.*, 2000). The authors found, that *pcaK* expression is repressed in the presence of benzoate by BenR, a homologue of *A. baylyi* BenM. Whether *vanK* expression is truly repressed by benzoate has to be evaluated in the future.

Taken together, the results shown here for the *hca* and *vanA,B* operons indicates that the branches of the β-ketoadipate pathway are not regulated independently, and that benzoate consumption (degraded through the catechol branch) is favored over substrates of the PCA branch (e.g. vanillate and hydroxycinnamates).

The mechanism of repression observed for the *dca* genes at the transcriptional level in the presence of benzoate (Bleichrodt *et al.*, 2010), seems to be completely different. Here, the involvement of BenM and CatM was excluded, since repression was still visible in their absence (Chapter 3.3.2). In addition, CCM was shown not to be involved in *dca* repression (Chapter 3.3.1). Further, BenM and CatM did not bind to a fragment from the *dcaA-dcaE* intergenic region, although putative binding sites are present (Chapter 3.3.4). Thus, the mechanism leading to the repression of the *dca* genes remains unknown and has to be evaluated in the future.

4.6 Vertical regulation

Vertical regulation was analyzed with strains carrying the luciferase gene as a transcriptional fusion in the *hcaA* and *vanB* genes. After the deletion of the *pcaH* gene, the activity of the *hca* and *vanA,B* operons was determined in luciferase assays in the presence of the aromatic inducer with or without the addition of protocatechuate (PCA; Chapter 3.4.1). As observed for the *pcaH* positive strains, the activity of the *hca* and *vanA,B* operon was repressed in the presence of PCA, compared to the activity shown in the absence of PCA (Fig. 3.19). The expression of the *hca* and *vanA,B* operon was further analyzed in the absence of *pcaU* (Chapter 3.4.3), in the presence of the aromatic inducer, with or without the addition of PCA. Compared to the *pcaU* positive strains, the expression of both operons in a *pcaU* negative background was increased in the presence of PCA in addition to the aromatic inducer (Fig. 3.21 and 3.22). The expression of the operons was also determined in an *hcaR*/*vanR* negative background (Chapter 3.4.3). Both operons showed a strong increased basal activity (no aromatic compound) in the absence of *hcaR*/*vanR*. The activity measured in the presence of the aromatic inducer with or without the addition of PCA was as high as seen in an *hcaR*/*vanR* positive background (Fig. 3.21 and 3.22). The activity of the operons was further determined in the absence of *pcaU* and *hcaR*/*vanR*. The activity of the *vanA,B* operon was strongly induced under all conditions tested (no aromatic compound, aromatic compound, aromatic compound plus PCA; Fig. 3.21). This was also the case for the *hca* operon regarding low PCA concentrations (Fig. 3.22).
A bioinformatical analysis of the *hca* and *van* regions (Chapter 3.4.4) revealed putative new binding sites for PcaU in each case. Electro mobility shift assays (EMSAs) showed a specific binding of PcaU to the *hca* and *van* region (Chapter 3.4.5). The determination of transcriptional start points showed, that the putative PcaU binding site is close to the suggested promoter region of *vanK*. For *hca*, the predicted PcaU binding site is located at the very 5´end of the *hcaK* gene Fig. (3.23).

The *hca* and *vanA,B* operons encode enzymes required for the degradation of hydroxycinnamates and vanillate (Fig. 1.1). The operons are controlled by the transcriptional regulators HcaR (MarR-type) and VanR (GntR-type), repressing their transcription in the absence of hydroxycinnamoyl-CoA thioesters (Parke & Ornston, 2003) and vanillate (Morawski *et al.*, 2000), respectively. The *hca* and *vanA,B* genes were shown to be repressed in the presence of PCA in addition to their respective aromatic inducers (Bleichrodt *et al.*, 2010). This seems to be consequent in light of efficient use of available resources, as PCA is build upon the degradation of hydroxycinnamates and vanillate. Vertical regulation was previously observed for the *pobA* gene, since its expression is repressed in the presence of PCA in addition to POB, serving as the specific inducer of *pobA* bound to PobR (Brzostowicz *et al.*, 2003). However, studies failed to identify the regulatory protein causing repression, since PobR was excluded as mediator by sensing intracellular PCA (Siehler *et al.*, 2007).

To explore vertical regulation observed for the *hca* and *vanA,B* operons in the current thesis, PCA was first identified as effector causing vertical regulation by blocking its degradation, by the deletion of *pcaH*. Blocking PCA degradation did not lead to a loss of vertical regulation under any condition tested, and thus downstream metabolites formed by the degradation of PCA can be excluded as effectors (Chapter 3.4.1). The only known regulator able to bind PCA is PcaU (Gerischer *et al*., 1998). Its involvement in repressing *hca* and *vanA,B* expression in the presence of the aromatic inducer and PCA was confirmed, since the operons responded with increased expression in the absence of PcaU (Chapter 3.4.3). The *vanA,B* operon responded with a complete loss of vertical regulation in a *pcaU* negative background under any condition tested (Fig. 3.21). However, the *hca* operon still showed repression by PCA when added in high concentrations (Fig. 3.22). But it is worth to note that repression in a *pcaU* negative background never reached the strength seen in a *pcaU* positive background. In addition, vertical regulation of the *hca* operon was completely lost in a *pcaU* negative background in the presence of low PCA concentrations, which led to repression in a *pcaU* positive background (down to ~ 50 % of the induced activity). So far, it is not clear if additional factors are involved in repressing *hca* transcription in the presence of PCA, what has to be elucidated in the future.

The specific transcriptional regulators HcaR and VanR were excluded as mediators of vertical regulation, because the repression of the *hca* and *vanA,B* operons was still visible in their absence (Chapter 3.4.3). In addition, their nature of acting as repressors of gene expression in the absence of their inducers (Parke & Ornston, 2003, Morawski et al., 2000) was confirmed, since the *hca* and *vanA,B* operons responded with high level expression in the absence of any aromatic compound (which was comparable to the induced activity of the respective operon).

Interestingly, *vanA,B* expression was also induced by PCA when added in very low concentrations, while high concentrations did not (Fig. 3.11 (b)). This was not observed for *hca* (Fig. 3.11 (a)). The induction of *vanA,B* expression by vanillate or PCA was also shown in studies with *P. putida* (Venturi *et al.*, 1998). However, the reason therefore is currently not known. It may be speculated, that a mechanism exists which is able to distinguish between low and high PCA concentrations. Since low amounts of PCA are build upon vanillate degradation, this mechanism could ensure complete vanillate degradation when present in very low concentrations. In contrast, high amounts of PCA would lead to *vanA,B* repression, as PCA degradation is more beneficial in light of energy conservation.

The molecular mechanism leading to vertical regulation of *hca* and *vanA,B* by PcaU in response to PCA was further analyzed. The identification of putative new binding sites of PcaU within intergenic *hcaA-hcaK* and *vanA-vanK* regions was successfully employed using a bioinformatic tool (Münch *et al*., 2005)

and a consensus sequence representing the internal palindrome of the PcaU binding site, as query (Chapter 3.4.4; Fig. 3.23 (Gerischer *et al.*, 2008)). Subsequent PcaU was shown to bind these regions specifically (Chapter 3.4.5 and 3.4.6). Clues to the molecular mechanism can be drawn, as the predicted PcaU binding site within the *hca* region is located in *hcaK* (encoding the transport protein for hydroxycinnamates), 55 bps downstream of the gene start point (Fig. 3.23 (d)). Binding of PcaU to this region may result in a premature termination of the mRNA synthesis by the RNA polymerase. A different situation seems to be realized within the *vanA-vanK* intergenic region. Although the predicted PcaU binding site is located adjacent to the *vanK* gene (encoding the vanillate transport protein), it is arranged upstream of the transcriptional start site of *vanK*, neighboring a putative -35 region (Fig. 3.23 (c)). This arrangement is quite similar to the situation found at the native site, between *pcaU* and *pcaI* (Fig. 3.23 (b)). Since PcaU is known to be a dual function regulator and was shown to be able to activate and repress expression from promoter *pcaIp* (Dal *et al.*, 2005), it is likely that it is also repressing expression from *vanKp* in the presence of PCA, by hindering the RNA polymerase from initiating transcription. The genetic context of putative binding site to gene arrangement (for both, *vanK* and *hcaK*) indicates that repression of *vanA,B* and *hca* may again be indirect, accomplished by exclusion of aromatic inducer molecules from the cell. Since PcaK and VanK have been shown to have overlapping functions regarding substrate transport and are in some cases able to compensate the loss of the other (D'Argenio *et al.*, 1999), the validity of the theory sketched here needs to be evaluated in the future.

4.7 *vanK* expression is induced by vanillate, *p*-hydroxybenzaote, and protocatechuate

The *vanK* gene is part of the *van* region of *Acinetobacter baylyi*. The *vanA,B* genes, essential for growth of *Acinetobacter* with ferulate and vanillate were first characterized by Segura and colleagues in 1999. An adjacent open reading frame, which is transcribed divergently from *vanA,B* (ACIAD0982), was designated *vanK* due to its sequence similarity to other transporters associated with aromatic compounds, and its genetic location. However, authors failed to identify a phenotype with *vanK*. Further studies revealed an overlapping function of PcaK and VanK (D'Argenio *et al.*, 1999). Strains harboring both, a non-functional *pcaK* and *vanK* gene, were clearly impaired in growth using quinate or PCA as carbon source. In contrast, strains carrying either a non-functional *pcaK* or *vanK* gene were not. Interestingly, growth with vanillate or POB was not clearly impaired for strains in which both *vanK* and *pcaK* were dysfunctional. These findings shown by D´Argenio *et al.* (1999) suggest that PcaK and VanK have overlapping functions regarding PCA uptake, but also indicate that there must be another transport system responsible for POB and vanillate uptake. Anyway, these findings do not exclude the possibility of PcaK and VanK being able to transport POB and vanillate.

However, work presented by D´Argenio *et al.* (1999), first identified a phenotype with *vanK*. Results presented in the current study confirmed the finding that growth of *A. baylyi* in a *vanK* negative background is not impaired using vanillate, PCA, POB, or quinate as the sole carbon sources (Chapter 3.5.1.1). Furthermore, vanillate, POB, and PCA were identified to activate expression of the *vanK* gene, which may give first hints of VanK being able to transport these aromatic compounds into the cell (Chapter 3.5.1.2 and 3.5.1.3). Quinate failed to induce *vanK* expression, what was expected as quinate is converted to PCA in the periplasm, catalyzed by QuiA, QuiB, and QuiC (Elsemore & Ornston, 1994, Elsemore & Ornston, 1995). Thus, the induced activity by quinate of *vanK* observed in a strain not blocked in quinate degradation was indirect, since PCA is formed upon quinate breakdown acting as inducer (Table 3.5). Nevertheless, if VanK is able to transport PCA, POB, and vanillate has to be evaluated in the future, and it will be challenging to identify the transport systems which can act upon vanillate and POB, in addition to PcaK.

5 References

Barbe, V., D. Vallenet, N. Fonknechten, A. Kreimeyer, S. Oztas, L. Labarre, S. Cruveiller, C. Robert, S. Duprat, P. Wincker, L. N. Ornston, J. Weissenbach, P. Marliere, G. N. Cohen & C. Medigue, (2004) Unique features revealed by the genome sequence of *Acinetobacter* sp. ADP1, a versatile and naturally transformation competent bacterium. *Nucleic Acids Res* **32**: 5766-5779.

Birnboim, H. C. & J. Doly, (1979) A rapid alkaline extraction procedure for screening recombinant plasmid DNA. *Nucleic Acids Res* **7**: 1513-1523.

Bleichrodt, F. S., (2007) Charakterisierung der Transkriptionsregulation von am Aromatenabbau in *Acinetobacter baylyi* beteiligten Operons. *Diploma thesis*.

Bleichrodt, F. S., R. Fischer & U. C. Gerischer, (2010) The β-ketoadipate pathway of *Acinetobacter baylyi* undergoes carbon catabolite repression, cross-regulation and vertical regulation, and is affected by Crc. *Microbiology* **156**: 1313-1322.

Bonin, A. L., M. Gossen & H. Bujard, (1994) *Photinus pyralis* luciferase: vectors that contain a modified *luc* coding sequence allowing convenient transfer into other systems. *Gene* **141**: 75-77.

Bradford, M. M., (1976) A rapid and sensitive method for the quantitation of microgram quantities of protein utilizing the principle of protein-dye binding. *Anal Biochem* **72**: 248-254.

Brenowitz, M., D. F. Senear, M. A. Shea & G. K. Ackers, (1986) Quantitative DNase footprint titration: a method for studying protein-DNA interactions. *Methods Enzymol* **130**: 132-181.

Bruckner, R. & F. Titgemeyer, (2002) Carbon catabolite repression in bacteria: choice of the carbon source and autoregulatory limitation of sugar utilization. *FEMS Microbiol Lett* **209**: 141-148.

Brzostowicz, P. C., A. B. Reams, T. J. Clark & E. L. Neidle, (2003) Transcriptional cross-regulation of the catechol and protocatechuate branches of the β-ketoadipate pathway contributes to carbon source-dependent expression of the *Acinetobacter* sp. strain ADP1 *pobA* gene. *Appl Environ Microbiol* **69**: 1598-1606.

Bundy, B. M., A. L. Campbell & E. L. Neidle, (1998) Similarities between the *antABC*-encoded anthranilate dioxygenase and the *benABC*-encoded benzoate dioxygenase of *Acinetobacter* sp. strain ADP1. *J Bacteriol* **180**: 4466-4474.

Bundy, B. M., L. S. Collier, T. R. Hoover & E. L. Neidle, (2002) Synergistic transcriptional activation by one regulatory protein in response to two metabolites. *Proc Natl Acad Sci U S A* **99**: 7693-7698.

Canovas, J. L. & R. Y. Stanier, (1967) Regulation of the enzymes of the β-ketoadipate pathway in *Moraxella calcoacetica*. 1. General aspects. *Eur J Biochem* **1**: 289-300.

Clark, T. J., C. Momany & E. L. Neidle, (2002) The *benPK* operon, proposed to play a role in transport, is part of a regulon for benzoate catabolism in *Acinetobacter* sp. strain ADP1. *Microbiology* **148**: 1213-1223.

Collier, D. N., P. W. Hager & P. V. Phibbs, Jr., (1996) Catabolite repression control in the *Pseudomonads*. *Res Microbiol* **147**: 551-561.

Collier, L. S., N. N. Nichols & E. L. Neidle, (1997) *benK* encodes a hydrophobic permease-like protein involved in benzoate degradation by *Acinetobacter* sp. strain ADP1. *J Bacteriol* **179**: 5943-5946.

Cowles, C. E., N. N. Nichols & C. S. Harwood, (2000) BenR, a XylS homologue, regulates three different pathways of aromatic acid degradation in *Pseudomonas putida*. *J Bacteriol* **182**: 6339-6346.

Craven, S. H., O. C. Ezezika, S. Haddad, R. A. Hall, C. Momany & E. L. Neidle, (2009) Inducer responses of BenM, a LysR-type transcriptional regulator from *Acinetobacter baylyi* ADP1. *Mol Microbiol* **72**: 881-894.

Craven, S. H., Ezezika, O. C., Momany, C., Neidle, E. L., (2008) LysR homologs in *Acinetobacter*: insights into a diverse and prevalent family of transcriptional regulators. In: *Acinetobacter* molecular biology. U. C. Gerischer (ed). Norfolk, UK: Caister Academic Press, pp. 163-202.

D'Argenio, D. A., A. Segura, W. M. Coco, P. V. Bunz & L. N. Ornston, (1999) The physiological contribution of *Acinetobacter* PcaK, a transport system that acts upon protocatechuate, can be masked by the overlapping specificity of VanK. *J Bacteriol* **181**: 3505-3515.

Dal, S., I. Steiner & U. Gerischer, (2002) Multiple operons connected with catabolism of aromatic compounds in *Acinetobacter* sp. strain ADP1 are under carbon catabolite repression. *J Mol Microbiol Biotechnol* **4**: 389-404.

Dal, S., G. Trautwein & U. Gerischer, (2005) Transcriptional organization of genes for protocatechuate and quinate degradation from *Acinetobacter* sp. strain ADP1. *Appl Environ Microbiol* **71**: 1025-1034.

de Berardinis, V., D. Vallenet, V. Castelli, M. Besnard, A. Pinet, C. Cruaud, S. Samair, C. Lechaplais, G. Gyapay, C. Richez, M. Durot, A. Kreimeyer, F. Le Fevre, V. Schachter, V. Pezo, V. Doring, C. Scarpelli, C. Medigue, G. N. Cohen, P. Marliere, M. Salanoubat & J. Weissenbach, (2008) A complete collection of single-gene deletion mutants of *Acinetobacter baylyi* ADP1. *Mol Syst Biol* **4**: 174.

Elsemore, D. A. & L. N. Ornston, (1994) The *pca-pob* supraoperonic cluster of *Acinetobacter calcoaceticus* contains *quiA*, the structural gene for quinate-shikimate dehydrogenase. *J Bacteriol* **176**: 7659-7666.

Elsemore, D. A. & L. N. Ornston, (1995) Unusual ancestry of dehydratases associated with quinate catabolism in *Acinetobacter calcoaceticus*. *J Bacteriol* **177**: 5971-5978.

Ezezika, O. C., L. S. Collier-Hyams, H. A. Dale, A. C. Burk & E. L. Neidle, (2006) CatM regulation of the *benABCDE* operon: functional divergence of two LysR-type paralogs in *Acinetobacter baylyi* ADP1. *Appl Environ Microbiol* **72**: 1749-1758.

Fischer, R., F. S. Bleichrodt & U. C. Gerischer, (2008) Aromatic degradative pathways in *Acinetobacter baylyi* underlie carbon catabolite repression. *Microbiology* **154**: 3095-3103.

Gaines, G. L., 3rd, L. Smith & E. L. Neidle, (1996) Novel nuclear magnetic resonance spectroscopy methods demonstrate preferential carbon source utilization by *Acinetobacter calcoaceticus*. *J Bacteriol* **178**: 6833-6841.

Gerischer, U. & L. N. Ornston, (1995) Spontaneous mutations in *pcaH* and -*G*, structural genes for protocatechuate 3,4-dioxygenase in *Acinetobacter calcoaceticus*. *J Bacteriol* **177**: 1336-1347.

Gerischer, U., A. Segura & L. N. Ornston, (1998) PcaU, a transcriptional activator of genes for protocatechuate utilization in *Acinetobacter*. *J Bacteriol* **180**: 1512-1524.

Gerischer, U. C., Jerg, B., Fischer, R., (2008) Spotlight on the *Acinetobacter* β-ketoadipate pathway: multiple levels of regulation. In: *Acinetobacter* molecular biology. U. C. Gerischer (ed). Norfolk, UK: Caister Academic Press, pp. 203-230.

Goosen, N., H. P. Horsman, R. G. Huinen & P. van de Putte, (1989) *Acinetobacter calcoaceticus* genes involved in biosynthesis of the coenzyme pyrrolo-quinoline-quinone: nucleotide sequence and expression in *Escherichia coli* K-12. *J Bacteriol* **171**: 447-455.

Harwood, C. S. & R. E. Parales, (1996) The β-ketoadipate pathway and the biology of self-identity. *Annu Rev Microbiol* **50**: 553-590.

Hester, K. L., J. Lehman, F. Najar, L. Song, B. A. Roe, C. H. MacGregor, P. W. Hager, P. V. Phibbs, Jr. & J. R. Sokatch, (2000a) Crc is involved in catabolite repression control of the *bkd* operons of *Pseudomonas putida* and *Pseudomonas aeruginosa*. *J Bacteriol* **182**: 1144-1149.

Hester, K. L., K. T. Madhusudhan & J. R. Sokatch, (2000b) Catabolite repression control by *crc* in 2xYT medium is mediated by posttranscriptional regulation of *bkdR* expression in *Pseudomonas putida*. *J Bacteriol* **182**: 1150-1153.

Hogema, B. M., J. C. Arents, R. Bader, K. Eijkemans, T. Inada, H. Aiba & P. W. Postma, (1998) Inducer exclusion by glucose 6-phosphate in *Escherichia coli*. *Mol Microbiol* **28**: 755-765.

Inoue, H., H. Nojima & H. Okayama, (1990) High efficiency transformation of *Escherichia coli* with plasmids. *Gene* **96**: 23-28.

Jerg, B. & U. Gerischer, (2008) Relevance of nucleotides of the PcaU binding site from *Acinetobacter baylyi*. *Microbiology* **154**: 756-766.

Jones, R. M., V. Pagmantidis & P. A. Williams, (2000) *sal* genes determining the catabolism of salicylate esters are part of a supraoperonic cluster of catabolic genes in *Acinetobacter* sp. strain ADP1. *J Bacteriol* **182**: 2018-2025.

Juni, E., (1972) Interspecies transformation of *Acinetobacter*: genetic evidence for a ubiquitous genus. *J Bacteriol* **112**: 917-931.

Juni, E. & A. Janik, (1969) Transformation of *Acinetobacter calco-aceticus* (*Bacterium anitratum*). *J Bacteriol* **98**: 281-288.

Kowalchuk, G. A., G. B. Hartnett, A. Benson, J. E. Houghton, K. L. Ngai & L. N. Ornston, (1994) Contrasting patterns of evolutionary divergence within the *Acinetobacter calcoaceticus pca* operon. *Gene* **146**: 23-30.

Lessie, T. G. & P. V. Phibbs, Jr., (1984) Alternative pathways of carbohydrate utilization in *Pseudomonads*. *Annu Rev Microbiol* **38**: 359-388.

MacGregor, C. H., J. A. Wolff, S. K. Arora & P. V. Phibbs, Jr., (1991) Cloning of a catabolite repression control (*crc*) gene from *Pseudomonas aeruginosa*, expression of the gene in *Escherichia coli*, and identification of the gene product in *Pseudomonas aeruginosa*. *J Bacteriol* **173**: 7204-7212.

Morales, G., J. F. Linares, A. Beloso, J. P. Albar, J. L. Martinez & F. Rojo, (2004) The *Pseudomonas putida* Crc global regulator controls the expression of genes from several chromosomal catabolic pathways for aromatic compounds. *J Bacteriol* **186**: 1337-1344.

Morawski, B., A. Segura & L. N. Ornston, (2000) Repression of *Acinetobacter* vanillate demethylase synthesis by VanR, a member of the GntR family of transcriptional regulators. *FEMS Microbiol Lett* **187**: 65-68.

Moreno, R. & F. Rojo, (2008) The target for the *Pseudomonas putida* Crc global regulator in the benzoate degradation pathway is the BenR transcriptional regulator. *J Bacteriol* **190**: 1539-1545.

Moreno, R., A. Ruiz-Manzano, L. Yuste & F. Rojo, (2007) The *Pseudomonas putida* Crc global regulator is an RNA binding protein that inhibits translation of the AlkS transcriptional regulator. *Mol Microbiol* **64**: 665-675.

Mrazek, J. & S. Xie, (2006) Pattern locator: a new tool for finding local sequence patterns in genomic DNA sequences. *Bioinformatics* **22**: 3099-3100.

Münch, R., K. Hiller, A. Grote, M. Scheer, J. Klein, M. Schobert & D. Jahn, (2005) Virtual Footprint and PRODORIC: an integrative framework for regulon prediction in prokaryotes. *Bioinformatics* **21**: 4187-4189.

Neidle, E. L. & L. N. Ornston, (1987) Benzoate and muconate, structurally dissimilar metabolites, induce expression of *catA* in *Acinetobacter calcoaceticus*. *J Bacteriol* **169**: 414-415.

Nichols, N. N. & C. S. Harwood, (1995) Repression of 4-hydroxybenzoate transport and degradation by benzoate: a new layer of regulatory control in the *Pseudomonas putida* β-ketoadipate pathway. *J Bacteriol* **177**: 7033-7040.

Pao, S. S., I. T. Paulsen & M. H. Saier, Jr., (1998) Major facilitator superfamily. *Microbiol Mol Biol Rev* **62**: 1-34.

Parke, D., M. A. Garcia & L. N. Ornston, (2001) Cloning and genetic *characterization* of *dca* genes required for β-oxidation of straight-chain dicarboxylic acids in *Acinetobacter* sp. strain ADP1. *Appl Environ Microbiol* **67**: 4817-4827.

Parke, D. & L. N. Ornston, (2003) Hydroxycinnamate (*hca*) catabolic genes from *Acinetobacter* sp. strain ADP1 are repressed by HcaR and are induced by hydroxycinnamoyl-coenzyme A thioesters. *Appl Environ Microbiol* **69**: 5398-5409.

Popp, R., T. Kohl, P. Patz, G. Trautwein & U. Gerischer, (2002) Differential DNA binding of transcriptional regulator PcaU from *Acinetobacter* sp. strain ADP1. *J Bacteriol* **184**: 1988-1997.

Romero-Arroyo, C. E., M. A. Schell, G. L. Gaines, 3rd & E. L. Neidle, (1995) *catM* encodes a LysR-type transcriptional activator regulating catechol degradation in *Acinetobacter calcoaceticus*. *J Bacteriol* **177**: 5891-5898.

Saier, M. H., Jr., (1998) Multiple mechanisms controlling carbon metabolism in bacteria. *Biotechnol Bioeng* **58**: 170-174.

Sanger, F., S. Nicklen & A. R. Coulson, (1977) DNA sequencing with chain-terminating inhibitors. *Proc Natl Acad Sci U S A* **74**: 5463-5467.

Segura, A., P. V. Bunz, D. A. D'Argenio & L. N. Ornston, (1999) Genetic analysis of a chromosomal region containing *vanA* and *vanB*, genes required for conversion of either ferulate or vanillate to protocatechuate in *Acinetobacter*. *J Bacteriol* **181**: 3494-3504.

Siehler, S. Y., S. Dal, R. Fischer, P. Patz & U. Gerischer, (2007) Multiple-level regulation of genes for protocatechuate degradation in *Acinetobacter baylyi* includes cross-regulation. *Appl Environ Microbiol* **73**: 232-242.

Studier, F. W., (2005) Protein production by auto-induction in high density shaking cultures. *Protein Expr Purif* **41**: 207-234.

Taylor, W. H. & E. Juni, (1961) Pathways for biosynthesis of a bacterial capsular polysaccharide. I. Carbohydrate metabolism and terminal oxidation mechanisms of a capsuleproducing coccus. *J Bacteriol* **81**: 694-703.

Titgemeyer, F. & W. Hillen, (2002) Global control of sugar metabolism: a Gram-positive solution. *Antonie Van Leeuwenhoek* **82**: 59-71.

Trautwein, G. & U. Gerischer, (2001) Effects exerted by transcriptional regulator PcaU from *Acinetobacter* sp. strain ADP1. *J Bacteriol* **183**: 873-881.

Tresguerres, M. E., G. de Torrontegui, W. M. Ingledew & J. L. Canovas, (1970) Regulation of the enzymes of the β-ketoadipate pathway in *Moraxella*. Control of quinate oxidation by protocatechuate. *Eur J Biochem* **14**: 445-450.

Tropel, D. & J. R. van der Meer, (2004) Bacterial transcriptional regulators for degradation pathways of aromatic compounds. *Microbiol Mol Biol Rev* **68**: 474-500.

van Schie, B. J., K. J. Hellingwerf, J. P. van Dijken, M. G. Elferink, J. M. van Dijl, J. G. Kuenen & W. N. Konings, (1985) Energy transduction by electron transfer via a pyrrolo-quinoline quinone-dependent glucose dehydrogenase in *Escherichia coli*, *Pseudomonas aeruginosa*, and *Acinetobacter calcoaceticus* (var. *lwoffi*). *J Bacteriol* **163**: 493-499.

Vaneechoutte, M., D. M. Young, L. N. Ornston, T. De Baere, A. Nemec, T. Van Der Reijden, E. Carr, I. Tjernberg & L. Dijkshoorn, (2006) Naturally transformable *Acinetobacter* sp. strain ADP1 belongs to the newly described species *Acinetobacter baylyi*. *Appl Environ Microbiol* **72**: 932-936.

Venturi, V., F. Zennaro, G. Degrassi, B. C. Okeke & C. V. Bruschi, (1998) Genetics of ferulic acid bioconversion to protocatechuic acid in plant-growth-promoting *Pseudomonas putida* WCS358. *Microbiology* **144 (Pt 4)**: 965-973.

Williams, P. A., Kay, C. A., (2008) The catabolism of aromatic compounds by *Acinetobacter*. In: *Acinetobacter* molecular biology. U. C. Gerischer (ed). Norfolk, UK: Caister Academyc Press, pp. 99-117.

Williams, P. A. & L. E. Shaw, (1997) *mucK*, a gene in *Acinetobacter calcoaceticus* ADP1 (BD413), encodes the ability to grow on exogenous *cis,cis*-muconate as the sole carbon source. *J Bacteriol* **179**: 5935-5942.

Wolff, J. A., C. H. MacGregor, R. C. Eisenberg & P. V. Phibbs, Jr., (1991) Isolation and characterization of catabolite repression control mutants of *Pseudomonas aeruginosa* PAO. *J Bacteriol* **173**: 4700-4706.

Young, D. M., D. Parke & L. N. Ornston, (2005) Opportunities for genetic investigation afforded by *Acinetobacter baylyi*, a nutritionally versatile bacterial species that is highly competent for natural transformation. *Annu Rev Microbiol* **59**: 519-551.

Zimmermann, T., T. Sorg, S. Y. Siehler & U. Gerischer, (2009) Role of *Acinetobacter baylyi* Crc in catabolite repression of enzymes for aromatic compound catabolism. *J Bacteriol* **191**: 2834-2842.

6 Summary

The topic of the current thesis, was to analyze certain regulatory mechanisms governing aromatic compound degradation through the β-ketoadipate pathway of *Acinetobacter baylyi*. Multiple levels of regulation were addressed all of which had in common to be of an elevated nature, such as carbon catabolite repression (CCR), cross-regulation, and vertical regulation. Elevated nature is meant in terms of overriding the specific gene regulation which responds to the specific inducers and in many cases governs the expression of only one operon. The involvement of the Crc protein in CCR was determined for several operons in the presence of acetate and/or succinate, pyruvate, lactate, or gluconate. Furthermore, the expression of the *vanK* gene in response to several aromatic compounds was analyzed.

- Cross-regulation was in depth analyzed for the *hca*, *dca*, and *vanA,B* operons. The regulatory proteins responsible for cross-regulation at *hca* and *vanA,B* were identified as BenM and CatM. The effector mediating cross-regulation at *hca* and *vanA,B* is *cis*, *cis*-muconate (CCM). Repression observed at the *dca* operon in the presence of benzoate turned out to be independent of BenM, CatM, and CCM. *In silico* analysis revealed putative binding sites within the intergenic regions between *hcaA-hcaK*, *dcaA-dcaE*, and *vanA-vanK*. BenM and CatM were shown to bind to fragments containing binding sites upstream of *hcaK* and *vanK in vitro*. No binding was observed using the *dca* probe.

- Vertical regulation of the *vanA,B* and *hca* operons was identified to rely on PcaU in response to protocatechuate (PCA). The specific transcriptional regulators VanR and HcaR, were excluded to be involved in vertical regulation, but were confirmed to act as repressors of *vanA,B* and *hca* gene expression. *In silico* analysis of the *van* and *hca* regions revealed putative new binding sites for PcaU upstream of *vanK* (directly adjacent to a suggested promoter region) and in the beginning of the *hcaK* gene. PcaU was shown to bind to fragments specifically containing these sites.

- An *A. baylyi* strain lacking a functional *vanK* gene (encoding for the vanillate transporter) was shown to be able to grow on quniate, *p*-hydroxybenzoate, protocatechuate, and vanillate. The *vanK* gene was shown to be induced in response to *p*-hydroxybenzoate, protocatechuate, and vanillate, but not quinate.

- To analyze carbon catabolite repression, *Acinetobacter baylyi* strains were constructed, containing transcriptional reporter gene fusions in genes encoding enzymes required for salicylate degradation (*salA*) and vanillate transport (*vanK*) with the luciferase gene of *Photinus pyralis*. The activity of the

salA and *vanK* gene was detected in luciferase assays upon growth, in the presence of the aromatic inducer and different carbon sources, as acetate, succinate, pyruvate, lactate, gluconate, and the substrate combination succinate and acetate. Results showed that:

- Both genes undergo strong carbon catabolite repression at the transcriptional level.
- Carbon catabolite repression of *salA* and *vanK* is strongest in the presence of the substrate combination succinate and acetate. The presence of acetate or succinate also led to carbon catabolite repression, but to a lesser extent.
- The *salA* gene showed strong induction in the presence of pyruvate, lactate and gluconate.
- The *vanK* gene showed strong expression in the presence of pyruvate, but was repressed down to 46 and 36 % in the presence of lactate and gluconate.

- The expression of the *catA*, *catB,C,I,J,F,D*, *salA*, *vanA,B*, and *vanK* genes, coding for enzymes required for the degradation of catechol, *cis*, *cis*-muconate, salicylate, vanillate, and vanillate transport, was analyzed in the presence of gluconate and lactate in the addition to the specific aromatic inducer using the respective luciferase reporter gene strains. The activity of the operons was compared to the activity shown on pyruvate:
  - The presence of lactate led to a decreased activity of the *catA*, *vanA,B*, and *vanK* operon (down to 10 % for *catA*), while no effect was detected for the *catB,C,I,J,F,D* operon.
  - The presence of gluconate, led to a decreased activity of the *catB,C,I,J,F,D*, *vanA,B*, and *vanK* operon (down to 35 % for *catB,C,I,J,F,D*), and an increase in activity for the *catA* operon (up to 2.4-fold).
  - The activity of the *salA* operon in the presence of lactate and gluconate was comparable to the activity shown on pyruvate.
- The expression of the *ant* and *are* operons, encoding enzymes for the degradation of anthranilate and benzyl esters, was analyzed in the presence of gluconate in the addition to the specific aromatic inducer using the respective luciferase reporter gene strains. The activity of the operons was compared to the activity shown on pyruvate plus aromatic inducer:
  - The activity of both operons was decreased in the presence of gluconate; down to 16 % for the *ant* operon and down to 63 % for the *are* operon.

- The involvement of the Crc protein in on the expression was characterized by deleting the *crc* gene in strains containing transcriptional reporter gene fusions in genes encoding enzymes required for the degradation of anthranilate (*antA*), benzyl esters (*areA*), benzoate (*ben*), catechol (*catA*), *cis*, *cis*-muconate (*catB,C,I,J,F,D*), dicarboxylates (*dca*), hydroxycinnamates (*hca*), salicylate (*salA*), vanillate (*vanA,B*), and vanillate transport (*vanK*) with the luciferase gene of *Photinus pyralis*.

- The activity of the *antA*, *areA*, *salA* and *vanK* gene was detected in luciferase assays upon growth, in the presence of the aromatic inducer and the substrates succinate and/or acetate. By comparing the activity of the genes in a *crc* positive with the *crc* negative background it was shown that:
    - The activity of all genes increased in the absence of *crc* in the presence of the substrate combination succinate and acetate (from 1.4-fold for the *antA* gene, to 9.1-fold for the *areA* gene).
    - The activity of all genes increased in the absence of *crc* in the presence of succinate (from 2.7-fold for the *antA* gene, to 7.2-fold for the *areA* gene).
    - The *areA* gene activity decreased in the presence of acetate in a *crc* negative background (down 24 %).
    - The *antA* gene activity was not affected in the presence of acetate in a *crc* negative background.
    - The *salA* and *vanK* gene activity increased in a crc negative background in the presence of acetate; 1.6 and 4.3-fold.
- The activity of the *ben*, *catA*, *catB,C,I,J,F,D*, *hca*, *dca* and *vanA,B* genes in the presence of the aromatic inducer and the substrates succinate or acetate was detected in luciferase assays upon growth, and compared to the activity of the respective *crc* positive strain:
    - The activity of *dca* and *vanA,B* operons was increased in a *crc* negative background in the presence of succinate or acetate (up to 7.5-fold for the *dca* operon on succinate), and no change was observed for the *catA* and the *catB,C,I,J,F,D* operon.
    - The *hca* operon showed a slight increase in activity in the presence of succinate and a slight decrease in the presence of acetate.
    - The *ben* operon was not affected by the absence of *crc* in the presence of acetate, but activity decreased dramatically in the presence of succinate (down to 13 %)
- The activity of the *ant*, *are*, *ben*, *catA*, *catB,C,I,J,F,D*, *dca*, *hca*, *salA*, *vanA,B*, and *vanK* operons in the presence of the aromatic inducer and the substrates pyruvate, lactate and gluconate was detected in luciferase assays upon growth, and compared to the activity of the respective *crc* positive strain:
    - The activity of the *ben*, *catA*, *hca*, *vanA,B*, and *vanK* operons increased in a *crc* negative background on pyruvate (up to 4.1-fold for *vanA,B*), while the activity of *are* and *ant* was decreased (3.5-fold for *are*). No change was observed for the *catB,C,I,J,F,D*, *dca*, and *sal* operons.
    - The presence of lactate led to an increase in activity of the *dca*, *sal*, *vanA,B*, and *vanK* operons (up to 2-fold for *vanK*), and a decrease in activity for the *ant*, *are*, and *ben* operons (down to 1.8-fold for *ben*). No change was observe for the *catB,C,I,J,F,D*, *catA*, and *hca* operon.

- The absence of *crc* did not affect activity of any operon in the presence of gluconate, but strains containing luciferase fusion in the *are*, *sal*, and *vanA,B* operons did not show any growth on gluconate.

7 Zusammenfassung

Die Analyse von verschiedenen regulatorischen Mechanismen, welche den Abbau von Aromaten durch den β-Ketoadipatweg von *Acinetobacter baylyi* regeln, war das Thema der vorliegenden Arbeit. Die analysierten Regulationsmechanismen, C-Katabolitrepression, Kreuzregulation und vertikale Regulation, überlagern die spezifische Kontrolle der Operons durch ihre spezifischen Transkriptionsregulatoren, und agieren somit alle auf einer höheren Ebene. Des Weiteren wurde die Beteiligung des Crc Proteins am Mechanismus der C-Katabolitrepression an verschiedenen Operons untersucht, und das auf verschiedenen C-Quellen: auf Succinat, Pyruvat, Acetat, Glukonat, Laktat, und auf der Substratkombination Succinat und Acetat. Außerdem wurde Expression des *vanK* Gens als Antwort auf das Vorhandensein von verschiedenen Aromaten analysiert.

- Der Mechanismus der Kreuzregulation wurde an den *hca*, *dca* und *vanA,B* Operons genau untersucht. Es zeigte sich, dass die regulatorischen Proteine BenM und CatM für die Kreuzregulation an *hca* und *vanA,B* verantwortlich sind, und das der Effektor *cis*, *cis*-Mukonat (CCM) ist. Die Kreuzregulation am *dca* Operon zeigte sich unabhängig von BenM, CatM und CCM. *In silico* Analysen enthüllten putativ neue Bindestellen für CatM und BenM an allen untersuchten Operons. Die Funktionalität der Bindestellen an *hca* und *vanA,B,* aber nicht an *dca*, konnte bewiesen werden.

- Die vertikale Regulation wurde für das *hca* und *vanA,B* Operon untersucht, und es zeigte sich, dass PcaU mit dem Effektor Protocatechuat (PCA) für diesen Mechanismus verantwortlich ist. Die spezifischen Regulatoren HcaR und VanR sind nicht an der vertikalen Regulation beteiligt. Es konnte aber bewiesen werden, dass sie als Repressoren agieren. Es wurden putativ neue Bindestellen für PcaU stromaufwärts von *vanK* und im *hcaK* Gen entdeckt. Eine Bindung von PcaU an diese Stellen konnte gezeigt werden.

- Es konnte gezeigt werden, dass ein in *vanK* (codiert für den Vanillat-Transporter) inaktivierter *A. baylyi* Stamm in der Lage ist auf Chinasäure, *p*-Hydroxybenzoat, Protocatechuat und Vanillat zu wachsen. Das *vanK* Gen konnte außerdem durch *p*-Hydroxybenzoat, Protocatechuat und Vanillat, aber nicht durch Chinasäure, induziert werden.

- Die C-Katabolitrepression wurde am Beispiel des *salA* und des *vanK* Gens analysiert. Diese Gene codieren für am Salicylsäureabbau und an der Aufnahme von Vanillat beteiligte Enzyme. Nachdem eine Fusion mit dem *luc*-Reportergen aus *Photinus pyralis* mit den Genen etabliert wurde, wurde die

Aktivität von *salA* und *vanK* in der Anwesenheit ihrer aromatischen Induktoren in Luciferaseassays gemessen. Als Substrate dienten Acetat, Succinat, Pyruvat, Laktat, Glukonat und die Substratkombination aus Succinat und Acetat. Es zeigte sich, dass:

- Beide Gene einer starken transkriptionellen C-Katabolitrepression unterliegen.
- Diese C-Katabolitrepression ist am stärksten in der Anwesenheit der Substratkombination aus Succinat und Acetate. Die Anwesenheit nur einer organischen Säure reichte aber auch schon um die C-Katabolitrepression auszulösen.
- In der Anwesenheit von Pyruvat, Laktat und Glukonat wurde das *salA* Gen stark induziert.
- Das *vanK* Gen zeigte starke Expression in der Anwesenheit von Pyruvat, wurde aber in der Anwesenheit von Laktat und Glukonat reprimiert (46 bzw. 36 % Restaktivität).

- Die Expression des *catA*, *catB,C,I,J,F,D*, *salA*, *vanA,B*, und *vanK* Gens, die für Enzyme codieren welche am Abbau von Brenzcatechin, Cis, cis-mukonat, Salicylat, Vanillat und am Vanillat-Transport beteiligt sind, wurde in Anwesenheit von Glukonat und Laktat zusätzlich zum aromatischen Induktor gemessen. Dazu wurden die entsprechenden Luciferasereportergen-Stämme verwendet. Die gemessene Aktivität wurde mit der Aktivität auf Pyruvat verglichen:
  - Die Anwesenheit von Laktat führte zu einer erniedrigten Aktivität des *catA*, *vanA,B* und *vanK* Operons (bis zu 10 % Restaktivität für *catA*), während kein Effekt für das *catB,C,I,J,F,D* Operon festgestellt werden konnte.
  - Die Anwesenheit von Glukonat, führte zu einer erniedrigten Aktivität des *catB,C,I,J,F,D*, *vanA,B* und *vanK* Operons (bis zu 35 % Restaktivität für *catB,C,I,J,F,D*), und einer verstärkten Aktivität für das *catA* Operon (2,4-fach).
  - Die Aktivität des *salA* Operons in Anwesenheit von Laktat und Glukonat war vergleichbar zu der auf Pyruvat.
- Die Expression der *ant* und *are* Operons, welche für am Anthranilat- und Benzylester-Abbau beteiligte Proteine codieren, wurde in Anwesenheit von Glukonat und aromatischen Induktor analysiert. Dazu wurden wieder die entsprechenden Luciferasereportergen-Stämme verwendet. Die gemessene Aktivität wurde mit der Aktivität auf Pyruvat verglichen:
  - Die Aktivität beider Operons zeigte sich erniedrigt in Anwesenheit von Glukonat. Bis zu 16 % für das *ant* Operon und bis zu 63 % für das *are* Operon.

- Die Beteiligung des Crc Proteins auf die Expression wurde charakterisiert, indem das *crc* Gen in Stämmen deletiert wurde, welche eine transkriptionelle Luciferasereportergen-Fusion in Genen tragen, welche für den Abbau von Anthranilat (*ant*), Benzylestern (*are*), Benzoat (*ben*), Brenzkatechin

(*catA*), *cis*, *cis*-Mukonat (*catB,C,I,J,F,D*), Dicarboxylsäuren (*dca*), Hydroxyzimtsäuren (*hca*), Salicylsäure (*salA*), Vanillat (*vanA,B*) und den Vanillat-Transport (*vanK*) codieren.

- Die Aktivität des *antA*, *areA*, *salA* und *vanK* Gens wurde in Luciferaseassays in der Anwesenheit des aromatischen Induktors und den Substraten Succinat und Acetat, allein oder in Kombination, aufgezeichnet. Beim Vergleich der Aktivität des *crc* negativen Stammes zu der des *crc* positiven Stammes zeigte sich, dass:
    - Die Aktivität aller Gene in der Abwesenheit von *crc* in Anwesenheit der Substratkombination Succinat und Acetat verstärkt wurde (von 1,4-fach für das *antA* Gen, bis 9,1-fach für das *areA* Gen).
    - In der Anwesenheit von Succinat verstärkte sich die Expression aller Gene vor einem *crc*-negativen Hintergrund (von 2,7-fach für das *antA* Gen, bis 7,2-fach für das *areA* Gen).
    - Die Aktivität des *areA* Gens war vermindert in Anwesenheit von Acetat vor einem *crc*-negativen Hintergrund (bis zu 24 % Restaktivität).
    - Die Aktivität des *antA* Gens sich in Anwesenheit von Acetat nicht mit der Deletion von *crc* änderte.
    - Die Aktivität des *salA* und *vanK* Gens verstärkte sich vor einem *crc*-negativen Hintergrund in Anwesenheit von Acetat (1,6 und 4,3-fach).
- Die Aktivität der *ben*, *catA*, *catB,C,I,J,F,D*, *hca*, *dca* und *vanA,B* Gene in Anwesenheit des aromatischen Induktors und der Substrate Succinat oder Acetat wurde in Luciferaseassays gemessen, und mit der Aktivität des *crc*-positiven Stammes verglichen:
    - Die Aktivität des *dca* und *vanA,B* Gens verstärkte sich mit der Deletion von *crc* in der Anwesenheit von Succinat oder Acetat (bis zu 7,5-fach für das dca Operon auf Succinat). Keine Änderung zeigte sich für das *catA* und das *catB,C,I,J,F,D* Operon.
    - Das *hca* Operon zeigte eine leichte Erhöhung der Aktivität in Anwesenheit von Succinat und eine leichte Erniedrigung in Anwesenheit von Acetat.
    - Die Aktivität des *ben* Operons zeigte sich unverändert in der Abwesenheit von *crc* auf Acetat, verminderte sich allerdings dramatisch in der Anwesenheit von Succinat (runter auf 13 %).
- Die Aktivität der *ant*, *are*, *ben*, *catA*, *catB,C,I,J,F,D*, *dca*, *hca*, *salA*, *vanA,B*, und *vanK* Operons wurden in einem *crc*-negativen auf den Substraten Pyruvat, Laktat und Glukonat in Anwesenheit des aromatischen Induktors bestimmt. Verglichen mit der Aktivität des *crc*-positiven Stammes zeigte sich, dass:
    - Sich die Aktivität des *ben*, *catA*, *hca*, *vanA,B* und *vanK* Operons in Anwesenheit von Pyruvat vor einem *crc*-negativen Hintergrund verstärkte (bis zu 4,1-fach für das *vanA,B* Operon), während sich die Aktivität des *are* und *ant* Operons verminderte (bis zu 3,5-fach für *are*). Keine Änderung der Aktivität wurde für das *catB,C,I,J,F,D*, *dca* und *sal* Operon beobachtet.

- Die Anwesenheit von Laktat zu einer Steigerung der Aktivität des *dca*, *sal*, *vanA,B* und *vanK* Operons (bis zu 2-fach für *vanK*), und einer Abnahme der Aktivität des *ant*, *are* und *ben* Operons (bis zu 1,8-fach für *ben*) führte. Keine Änderung der Aktivität wurde für das *catB,C,I,J,F,D*, *catA* und *hca* detektiert.
- Die Deletion von *crc* keinen Effekt auf die Aktivität aller Operons in der Anwesenheit von Glukonat hatte. Allerdings waren die Stämme mit Luciferasereportergen-Fusionen in den Genen *areA*, *salA* und *vanB*, nicht mehr in der Lage auf Glukonat zu wachsen, wenn *crc* deletiert wurde.

8 Curriculum vitae

1. Personal Data

Name:	Fenja Sabine Bleichrodt
Family Status	Single
Nationality	German
Date of Birth	10-12-1981
City of Birth	Berlin
Country of Birth	Germany
Address	Weinsteige 1
	89075 Ulm
	Germany
Phone:	+49731 / 9630076
	+49179 / 9227500
Email:	FenjaSB@gmail.com
Command of Language	German, English, French

2. Education

09-1988 – 05-1989	Lietzensee Elementary School Berlin / Charlottenburg
05-1989 – 06-1992	Elementary School Neustadtgödens / Friesland
09-1992 – 06-1994	Two-Grade Middle School Sande
09-1994 – 06-1998	Secondary School, Mariengymnasium Jever
09-1998 – 06-2001	Secondary School, Hans und Sophie Scholl Gymnasium Ulm
10-2002 – 04-2003	University of Konstanz; Field of Study: Biosciences
05-2003 – 10-2007	University of Ulm; Field of Study: Biosciences
10-2002 – 11-2004	Grundstudium (Basic Study Period)
11-2004 – 10-2007	Hauptstudium (Advanced Study Period)
01-2007 – 10-2007	Diploma Thesis
	Institute of Microbiology and Biotechnology, University of Ulm
Since 12-2007	Doctoral Thesis
	Institute of Microbiology and Biotechnology, University of Ulm

9 Publications

Fischer, R., F. S. Bleichrodt & U. C. Gerischer, (2008) Aromatic degradative pathways in *Acinetobacter baylyi* underlie carbon catabolite repression. *Microbiology* **154**: 3095-3103.

Bleichrodt, F. S., R. Fischer & U. C. Gerischer, (2010) The β-ketoadipate pathway of *Acinetobacter baylyi* undergoes carbon catabolite repression, cross-regulation and vertical regulation, and is affected by Crc. *Microbiology* **156**: 1313-1322.

Waidmann, M. S., F. S. Bleichrodt, T. Laslo & C. U. Riedel (2011) Bacterial luciferase reporters. The swiss army knife of molecular biology. *Bioengineered Bugs* 2: 1-9.

10 Poster presentations

Bleichrodt F. S., R. Fischer and U. C. Gerischer (2008) All catabolic funneling pathways for aromatic compounds in *Acinetobacter baylyi* are subject to carbon catabolite repression. Annual meeting of the VAAM 2008, Frankfurt.

Bleichrodt F. S. & U. C. Gerischer (2009) Vertical regulation, a new layer of transcriptional regulation acts upon protocatechuate degradation in *Acinetobacter baylyi*. Annual meeting of the VAAM 2009, Bochum.

Bleichrodt F. S., E. L. Neidle & U. C. Gerischer (2010) Cross-regulation in the β-ketoadipate pathway of *Acinetobacter baylyi* is mediated by two LysR-type transcriptional regulators, BenM and CatM. Annual meeting of the VAAM 2010, Hannover.

Bleichrodt F. S., E. L. Neidle & U. C. Gerischer (2010) Cross-regulation in the β-ketoadipate pathway of *Acinetobacter baylyi* is mediated by two LysR-type transcriptional regulators, BenM and CatM in response to *cis*, *cis*-muconate. 8th International Symposium on the Biology of *Acinetobacter*, 2010, Rome.

The β-ketoadipate pathway of *Acinetobacter baylyi* undergoes carbon catabolite repression, cross-regulation and vertical regulation, and is affected by Crc

Fenja S. Bleichrodt, Rita Fischer and Ulrike C. Gerischert

Institute of Microbiology and Biotechnology, University of Ulm, 89069 Ulm, Germany

Correspondence
Ulrike C. Gerischer
ulrike.gerischer@mpibpc.mpg.de

Received 20 December 2009
Revised 24 January 2010
Accepted 26 January 2010

The degradation of many structurally diverse aromatic compounds in *Acinetobacter baylyi* is accomplished by the β-ketoadipate pathway. In addition to specific induction of expression by certain aromatic compounds, this pathway is regulated by complex mechanisms at multiple levels, which are the topic of this study. Multiple operons feeding into the β-ketoadipate pathway are controlled by carbon catabolite repression (CCR) caused by succinate plus acetate. The pathways under study enable the catabolism of benzoate (*ben*), catechol (*catA*), *cis*,*cis*-muconate (*catB*,*C*,*I*,*J*,*F*,*D*), vanillate (*van*), hydroxycinnamates (*hca*), dicarboxylates (*dca*), salicylate (*sal*), anthranilate (*ant*) and benzyl esters (*are*). For analysis of CCR at the transcriptional level a luciferase reporter gene cassette was introduced into the operons. The Crc (catabolite repression control) protein is involved in repression of all operons (except for *catA*), as demonstrated by the analysis of respective *crc* strains. In addition, cross-regulation was demonstrated for the *vanA*,*B*, *hca* and *dca* operons. The presence of protocatechuate caused transcriptional repression of the *vanA*,*B*- and *hca*-encoded funnelling pathways (vertical regulation). Thus the results presented extend the understanding both of CCR and of the effects of Crc for all aromatic degradative pathways of *A. baylyi* and increase the number of operons known to be controlled by two additional mechanisms, cross-regulation and vertical regulation.

INTRODUCTION

The bacterium *Acinetobacter baylyi* is a soil organism known to be able to use aromatic substances through the β-ketoadipate pathway (Harwood & Parales, 1996). Numerous more complex aromatic compounds can be converted into the two central starting compounds of the β-ketoadipate pathway, protocatechuate (PCA) and catechol, by additional short metabolic pathways (funnelling pathways). The expression of all the respective operons is thoroughly controlled by specific inducers. Furthermore, to cope with an array of environmental changes, the β-ketoadipate pathway and its funnelling pathways are controlled by a regulatory network the complexity of which is only beginning to be elucidated (Vaneechoutte *et al.* 2006; Gerischer, 2008; Williams & Kay, 2008). One part of this network is carbon catabolite repression (CCR) (Cánovas & Stanier, 1967; Tresguerres *et al.*, 1970; Dal *et al.*, 2005; Fischer *et al.*, 2008). The molecular mechanisms of CCR are well understood in *Escherichia coli* and Gram-positive bacteria such as *Bacillus subtilis*, but not in bacteria belonging to the genera *Pseudomonas* and *Acinetobacter*. In these bacteria, organic acids such as succinate and acetate, as well as the protein Crc (catabolite repression control), play an important role in CCR (Wolff *et al.*, 1991; Zimmermann *et al.*, 2009). *A. baylyi* Crc has been shown to be involved in the degradation of the *pca-qui* transcript, which encodes enzymes dealing with quinate and PCA degradation (Zimmermann *et al.*, 2009). In *Pseudomonas putida*, Crc affects the expression of genes involved in aromatic compound degradation (*ben*, *cat*, *pca* and *pobA*) (Morales *et al.*, 2004). Direct binding of Crc to the RNA region directing translation of the regulators BenR and AlkS was demonstrated, indicating translational repression (Moreno *et al.*, 2007; Moreno & Rojo, 2008).

In addition to CCR, cross-regulation becomes effective when mixtures of substrates feeding into both branches of the pathway are presented to an organism. In *A. baylyi*, cross-regulation results in a dominance of the catechol branch over the PCA branch (Brzostowicz *et al.*, 2003; Siehler *et al.*, 2007). There is evidence that transcriptional

†Present address: Max Planck Institute for Biophysical Chemistry, Theoretical and Computational Biophysics Department, D-37077 Göttingen, Germany.

Abbreviations: CCR, carbon catabolite repression; PCA, protocatechuate; POB, *p*-hydroxybenzoate.

regulators BenM and CatM, which can bind regulatory regions upstream of *pcaU* (Gerischer *et al.*, 1998), are involved in this cross-regulation. Finally, vertical regulation has also been observed in the presence of PCA. For example, the degradation of *p*-hydroxybenzoate (POB) is repressed by its own reaction product, PCA (Brzostowicz *et al.*, 2003; Siehler *et al.*, 2007).

In this investigation we analysed more operons with respect to CCR, cross-regulation and vertical regulation. Given the indicated global nature of the mechanism it is relevant to know whether multiple operons are affected, and in the future to examine whether the same mechanism is the cause. We used chromosomal luciferase reporter gene fusions in operons encoding enzymes for the degradation of benzoate, benzyl esters, anthranilate, hydroxycinnamates, dicarboxylic acids, vanillate, salicylate and catechol to gain a more comprehensive understanding of gene expression within the aromatic degradative pathways of *A. baylyi*. We addressed the involvement of Crc by investigating *crc* strains in parallel. We showed that all the operons analysed are affected by CCR; the withdrawal of Crc derepresses gene expression in most cases. Cross-regulation and/or vertical regulation was observed in all operons investigated (cross-regulation in *hca*, *van* and *dca*; vertical regulation in *hca* and *van*).

METHODS

Bacterial strains and growth conditions. Strains of *A. baylyi* were grown on minimal medium at 30 °C as described earlier (Trautwein & Gerischer, 2001). Carbon sources were used at the following concentrations unless indicated otherwise: pyruvate, 20 mM; lactate, 20 mM; gluconate, 20 mM; acetate, 15 mM; succinate, 30 mM; succinate and acetate, 15 mM each. The following concentrations were used for induction: benzoate, 0.5 mM; *p*-coumarate, 1 μM; adipate, 1 mM; vanillate, 0.5 mM; salicylate, 0.5 mM; anthranilate, 1 mM; benzyl alcohol, 2 mM. Benzyl alcohol, *p*-coumarate, vanillate and adipate were dissolved in DMSO. Antibiotics for *A. baylyi* strains were used at the following concentrations: 100 μg spectinomycin ml^{-1}; 20 μg streptomycin ml^{-1}.

Strains of *E. coli* were grown in LB medium at 37 °C. Antibiotics were used in the following concentrations: 100 μg ampicillin ml^{-1}; 100 μg spectinomycin ml^{-1}; 20 μg streptomycin ml^{-1}.

For growth experiments, *A. baylyi* strains (Table 1) with luciferase transcriptional gene fusions were precultured on minimal medium complemented with the carbon source that would later be used in the experiment (except for the aromatic compound).

Plasmid and strain construction. To integrate the luciferase reporter gene into specific genes, PCRs were performed with primers listed in Table 2, using chromosomal DNA from *A. baylyi* as a template. The fragments were cleaved with restriction enzymes and cloned (Table 1). After integration of the *luc* cassette, the fusion constructs were cleaved with the indicated enzymes and used for transformation of *A. baylyi*. The *aad9*-mediated spectinomycin resistance was used for selection. The restriction sites used for the plasmid and strain construction were native sites in all cases. Standard methods were used for plasmid isolation, DNA purification, restriction endonuclease cleavage, ligation and transformation. Transformation of *A. baylyi* was done as described by Fischer *et al.* (2008).

To verify that luciferase fusions were integrated into the genome of *A. baylyi* strain ADP1 at the correct position, PCR analysis was employed, using a gene-specific primer (catA5, catB1, vanB2, vanK1 and salA1) and the luc primer (Table 2), specific for the *luc-aad9* cassette. The gene-specific primer targeted a sequence outside the DNA that was used for transformation.

Plasmid pAC57 was used to disrupt the *crc* gene in all strains containing the chromosomal luciferase reporter gene fusion (Zimmermann *et al.*, 2009). pAC57 carries a *crc* gene that was rendered non-functional by the insertion of an Ω cassette, which carries a spectinomycin and streptomycin resistance gene. This construct was cleaved from the vector backbone by the restriction endonucleases *Xba*I and *Pst*I and used for transformation of strains containing a luciferase reporter gene fusion to create the respective *crc* strain (Table 1). Growth in the presence of spectinomycin and streptomycin was used to identify candidates with the desired modification. PCR analysis with primers crc3 and crc4 (Table 2) was employed to confirm the correct integration of the construct into the corresponding region on the chromosome. Again, primers targeted loci outside the DNA that had been used for transformation.

PCR. Cells of an overnight culture were suspended in water, boiled for 10 min, cooled on ice and centrifuged. The supernatant contained the chromosomal DNA and was used as template. The conditions using *Taq* DNA polymerase were 95 °C for 3 min, followed by 30 cycles of denaturation for 1 min at 95 °C, annealing for 1 min at 53 to 68 °C (depending on the primers) and elongation at 72 °C for a variable period (depending on the length of the amplified fragment).

Determination of luciferase activity. At different time points during growth, samples of *A. baylyi* cells were taken and mixed with D-luciferin. The luciferase activity was detected as described earlier (Siehler *et al.*, 2007). The measured relative light units (RLU) were divided by the respective OD_{600} to normalize the results. A value from the mid-exponential growth phase was read as characteristic for the strain and condition. Each growth experiment was carried out at least three times independently. The luciferase activity on different carbon sources was normalized to the corresponding activity on pyruvate (set to 100 %), or with the corresponding activity of the parental strain (crc^+) on succinate and/or acetate (set to 100 %) for the *crc* strains. Error bars indicate standard deviation.

RESULTS

CCR of operons encoding funnelling pathways for aromatic compound degradation in *A. baylyi*

To investigate CCR, growth experiments were performed with the strains carrying *catA-luc*, *catB,C,I-luc*, *vanA,B-luc*, *salA-luc* and *vanK-luc* transcriptional fusions (Fig. 1). Prior to this study, nothing was known about CCR of these operons by succinate and/or acetate. In all approaches, strains were grown on succinate and/or acetate with the specific aromatic inducer added (*catA-luc*, *catB,C,I-luc*, 0.5 mM benzoate; *vanA,B*, *vanK-luc*, 0.5 mM vanillate; *salA-luc*, 0.5 mM salicylate). We evaluated the effect of the carbon sources alone or in combination since it is known for the *pca-qui* operon that they have a much stronger effect in combination (Dal *et al.*, 2002). The resulting luciferase activities were compared with the activity after growth on the non-repressing carbon source pyruvate with the specific aromatic inducer (Table 3). The presence of

Table 1. Bacterial strains and plasmids used in this study

Strain or plasmid	Relevant characteristics	Source or reference
A. baylyi		
ADP1	Wild-type (strain BD413, ATCC 33305)	Juni & Janik (1969)
ADPU92	*benA-luc* fusion, inserted into *benA*	Fischer *et al.* (2008)
ADPU93	*hcaA-luc* fusion, inserted into *hcaA*	Fischer *et al.* (2008)
ADPU94	*dcaA-luc* fusion, inserted into *dcaA*	Fischer *et al.* (2008)
ADPU95	*areA-luc* fusion, inserted into *areA*	Fischer *et al.* (2008)
ADPU96	*antA-luc* fusion, inserted into *antA*	Fischer *et al.* (2008)
ADPU97	*benA-luc* fusion, inserted into *benA*, Δ*crc*Ω, 50 bp *Bsg*I fragment	This work
ADPU98	*hcaA-luc* fusion, inserted into *hcaA*, Δ*crc*Ω, 50 bp *Bsg*I fragment	This work
ADPU99	*dcaA-luc* fusion, inserted into *dcaA*, Δ*crc*Ω, 50 bp *Bsg*I fragment	This work
ADPU100	*catA-luc* fusion, inserted into *catA*	This work
ADPU101	*catB,C,I-luc* fusion, inserted into *catI*	This work
ADPU102	*vanA,B-luc* fusion, inserted into *vanB*	This work
ADPU104	*catA-luc* fusion, inserted into *catA*, Δ*crc*Ω, 50 bp *Bsg*I fragment	This work
ADPU105	*catB,C,I-luc* fusion, inserted into *catI*, Δ*crc*Ω, 50 bp *Bsg*I fragment	This work
ADPU106	*vanA,B-luc* fusion, inserted into *vanB*, Δ*crc*Ω, 50 bp *Bsg*I fragment	This work
ADPU110	*salA-luc* fusion, inserted into *salA*	This work
ADPU111	*salA-luc* fusion, inserted into *salA*, Δ*crc*Ω, 50 bp *Bsg*I fragment	This work
ADPU112	*vanK-luc* fusion, inserted into *vanK*	This work
ADPU113	*vanK-luc* fusion, inserted into *vanK*, Δ*crc*Ω, 50 bp *Bsg*I fragment	This work
ADPU120	*areA-luc* fusion, inserted into *areA*, Δ*crc*Ω, 50 bp *Bsg*I fragment	This work
ADPU121	*antA-luc* fusion, inserted into *antA*, Δ*crc*Ω, 50 bp *Bsg*I fragment	This work
E. coli		
DH5α	F^- ϕ80d*lacZ*ΔM15 Δ(*lacZYA-argF*)U169 *deoR recA1 endA1 hsdR17*($r_k^- m_k^+$) *phoA supE44* λ^- *thi-1 gyrA96 relA1*	Hanahan (1983)
Plasmids		
pBluescript II SK(+)	Ap^r, *lacZ*	Stratagene; Alting-Mees & Short (1989)
pUC18	Ap^r, *lacZ*	Yanisch-Perron *et al.* (1985)
pFW11_luc	Contains the *Photinus pyralis* luciferase gene, *luc-aad9*	Podbielski *et al.* (1999)
pAC57	Δ*crc*Ω insertion, 50 bp deletion between two *Bsg*I restriction sites and insertion of the $\Omega Sm^r Spc^r$ cassette	Zimmermann *et al.* (2009)
pAC126	pUC18 with a 3371 bp *Hin*cII–*Xba*I fragment, containing *catA*	This work
pAC127	pBSKII with a 3709 bp *Eco*RI–*Sac*II fragment, containing the *catB,C,I,J,F* region	This work
pAC128	pBSKII with a 2267 bp *Psh*AI–*Xba*I fragment, containing the *vanA,B* region	This work
pAC129	pBSKII with a 2810 bp *Eco*RV/*Xba*I fragment, containing *vanK*	This work
pAC130	*luc*Spc^r *Xmn*I–*Bss*HII fragment from pFW11_luc ligated into pAC126 *Swa*I/*Bss*HII (*catA-luc* fusion; cleaved from the vector backbone with *Nco*I and *Pml*I)	This work
pAC131	*luc*Spc^r *Xmn*I–*Sma*I fragment from pFW11_luc ligated into pAC127 *Eco*47III (*catB,C,I-luc* fusion; cleaved from the vector backbone with *Pml*I and *Kas*I)	This work
pAC132	*luc*Spc^r *Xmn*I–*Nco*I fragment from pFW11_luc ligated into pAC128 *Swa*I/*Nco*I (*vanA,B-luc* fusion; cleaved from the vector backbone with *Xba*I and *Bsg*I)	This work
pAC133	pBSKII with a 4107 bp *Bgl*II–*Eco*RV fragment, containing *salA*	This work
pAC135	*luc*Spc^r *Xmn*I–*Kas*I fragment from pFWII_luc ligated into pAC133 *Eco*72I (*salA-luc* fusion; cleaved from the vector backbone with *Pvu*II)	This work
pAC139	*luc*Spc^r *Xmn*I–*Sma*I fragment from pFWII_luc ligated into pAC129 *Msc*I (*vanK-luc* fusion; cleaved from the vector backbone with *Xba*I and *Eco*RV)	This work

Table 2. Primers used in this study

Primer	Sequence	Plasmid construction or application
catA5	CAAGGCTGAGGCAAACCAAG	Amplification of *catA* with catA6, to generate pAC126
catA6	GCAATACGCTACGCCAGAC	
catB1	GACGCTTGTGCAGTATGAGTC	Amplification of the *catB,C,I,J,F* region with catB2, to generate pAC127
catB2	TTTGCGCTGTGGAATCGTG	
vanB2	TCCCAATCTGGACAGGAGATAC	Amplification of the *vanA,B* region with vanB3, to generate pAC128
vanB3	AAGCCATGTTCGAGCAAGG	
vanK1	TCATGCGTTGTTCGTCAAG	Amplification of *vanK* with vanK2, to generate pAC129
vanK2	CGGGAATACGATATCCCAACTC	
salA1	CTGAGTGCAGGTGTTGTTTG	Amplification of *salA* with catA2, to generate pAC133
salA2	GCCAGAACGTTATGGAATCG	
luc	AAACCGGGAGGTAGATGAGATG	Confirmation of the insertion of the *luc-aad9* cassette in the chromosome at the right position; used with catA5, catB1, vanB2, vanK1 or salA1
crc3	ATGATACCAAAGGATAGC	Confirmation of the insertion of the Ω cassette in the chromosome at the right position
crc4	TTGTGTAAGAAATTGGCG	Used with crc3

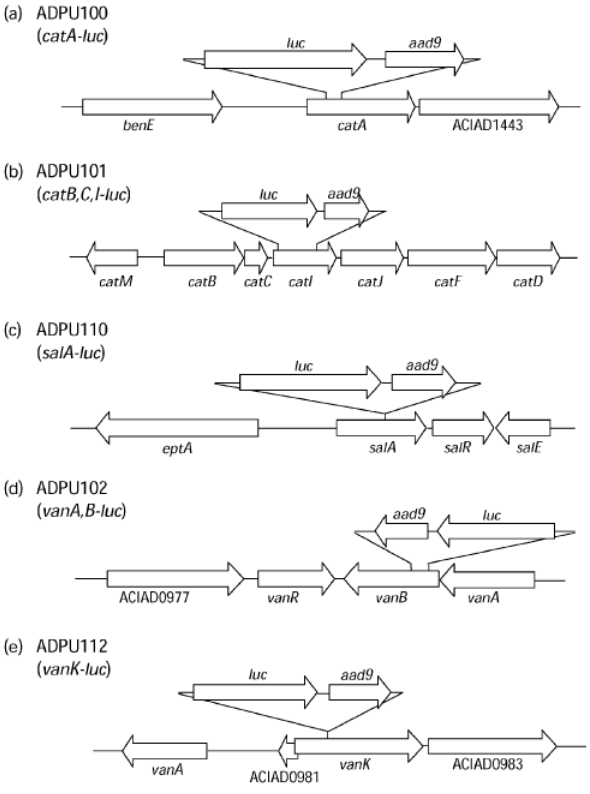

Fig. 1. Transcriptional fusions between *A. baylyi* genes and a luciferase reporter cassette (*luc-aad9*) made and used in this study. Arrangement and nomenclature of open reading frames is from the published and annotated genome sequence (http://www.genoscope.fr).

pyruvate in addition to the aromatic substrate is known to have no effect on the *pca-qui* expression level compared to growth solely on the aromatic substrate (Dal *et al.*, 2002). While the presence of succinate and acetate in combination caused strong repression of all operons analysed, succinate alone was able to repress the *catA*, *catB,C,I,J,F,D* and *sal* operons to a similar degree, while acetate failed to repress the *catB,C,I,J,F,D* and *sal* operons to that extent. However, the *vanA,B* and *vanK* operons showed only a slight increase on either succinate or acetate compared to both acids in combination. The strongest repression of promoter activity (up to 98 %) was observed for the *catA* operon. The activity under CCR conditions was comparable with the uninduced activity of this operon (data not shown). The *catB,C,I,J,F,D*, the *vanA,B* and the *vanK* operons showed slightly lower repression, while the *sal* operon showed only a moderate repression of promoter activity (up to 42 %).

Expression pattern in the presence of lactate and gluconate

Prior to this study, pyruvate (in addition to an inducing carbon source) was shown to be a non-repressing carbon source for the *ben*, *hca*, *dca*, *are* and *ant* operons of the *β*-ketoadipate pathway with regard to CCR (Fischer *et al.*, 2008). Lactate forms the precursor of pyruvate in the reaction catalysed by lactate/pyruvate dehydrogenase, suggesting that these two carbon sources might have related effects. Glucose is a repressing carbon source in *E. coli* and other bacteria and it was thus interesting to investigate its effect in *A. baylyi* CCR. While *A. baylyi* is able to use glucose, it first converts it to gluconate in the periplasm (Young *et al.*, 2005). Gluconate is a much better growth substrate than glucose and was thus chosen instead. Therefore, the effects of lactate and gluconate on the expression control of the operons named above were tested. Growth experiments were performed using three

Table 3. CCR of *A. baylyi* operons involved in aromatic compound degradation by succinate and acetate

Strain	Transcriptional fusion	Specific inducer (0.5 mM)	Luciferase activity after growth on specific inducer plus secondary carbon source(s)*		
			Succinate + acetate	Succinate	Acetate
ADPU100	*catA-luc*	Benzoate	1.68 ± 0.43	1.98 ± 0.58	1.71 ± 0.17
ADPU101	*catB,C,I-luc*	Benzoate	13.96 ± 1.0	14.16 ± 3.98	33.56 ± 6.87
ADPU102	*vanA,B-luc*	Vanillate	10.01 ± 1.25	18.73 ± 6.13	19.42 ± 2.60
ADPU111	*salA-luc*	Salicylate	57.60 ± 5.01	60.70 ± 1.93	75.30 ± 0.32
ADPU112	*vanK-luc*	Vanillate	11.68 ± 0.32	19.39 ± 1.93	15.06 ± 5.01

*Expressed as a percentage of the activity on pyruvate plus the aromatic inducer (set to 100 %). Values are means ± SD of at least three independent experiments.

different carbon sources (pyruvate, lactate and gluconate) to characterize the expression of the *catA*, *catB,C,I,J,F,D*, *vanA,B*, *vanK* and *sal* operons (Table 4). Furthermore, expression levels of the *are* and *ant* operons were also analysed in the presence of gluconate as carbon source with addition of the aromatic inducer (*areA-luc*, 2.0 mM benzyl alcohol; *antA-luc*, 1.0 mM anthranilate). To summarize the observations: while the carbon source lactate turned out to be non-repressing for the expression of the *catB,C,I,J,F,D* and *sal* operons, a slight repressing effect on *vanA,B* and *vanK* expression was observed, as previously shown for the *ant* and *are* operons (Fischer *et al.*, 2008). Gluconate is non-repressing for the expression of the *sal* genes, but has a slight repressing effect on the *are* operon. Furthermore, gluconate has a moderate repressing effect on the expression of the *vanA,B*, *vanK*, *catB,C,I,J,F,D* and *ant* operons. The most remarkable result was obtained for the *catA* operon. Here, lactate is a repressing carbon source whereas the presence of gluconate causes an increased expression (more than twofold higher than in the presence of pyruvate). This is not an effect of Crc since the same expression pattern was seen in the *crc* strain (data not shown). It should be noted in particular that neither compound significantly repressed the *sal* operon.

Connection between CCR and Crc

A. baylyi Crc has been shown to strongly affect the stability of the *pca-qui* transcript but there is also a transcriptional effect (significantly increased expression under all conditions in the absence of Crc: Zimmermann *et al.*, 2009). To determine whether the Crc protein is involved in CCR of additional operons involved in aromatic compound degradation at the transcriptional level, *crc* was disrupted in strains carrying a luciferase reporter gene fusion (Table 1). Growth experiments were performed with *crc* strains containing a *benA-luc*, *hcaA-luc*, *dcaA-luc*, *catA-luc*, *catB,C,I-luc*, *salA-luc*, *vanA,B-luc*, *vanK-luc*, *areA-luc* or *antA-luc* transcriptional fusion and luciferase activity was determined (Table 5). Inducers were added as follows: benzoate, 0.5 mM (*benA-luc*, *catA-luc*, *catB,C,I-luc*); *p*-coumarate, 1 μM (*hcaA-luc*); adipate, 1.0 mM (*dcaA-luc*); salicylate, 0.5 mM (*salA-luc*); vanillate, 0.5 mM (*vanA,B-luc*, *vanK-luc*); benzyl alcohol, 2.0 mM (*areA-luc*); anthranilate, 1.0 mM (*antA-luc*). Almost all the operons (with the exception of *catA*) responded with a derepression of promoter activity on succinate plus acetate to various degrees (from 3-fold for the *sal* operon, up to 28-fold for the *ben* operon) in comparison with the crc^+ strain. On

Table 4. Effect of lactate or gluconate on the expression of the indicated operons

Strain	Transcriptional fusion	Specific inducer	Concn	Luciferase activity after growth on specific inducer plus secondary carbon source*	
				Lactate	Gluconate
ADPU95	*areA-luc*	Benzyl alcohol	2.0 mM	66 ± 12†	63 ± 6
ADPU96	*antA-luc*	Anthranilate	1.0 mM	45 ± 2†	16 ± 2
ADPU100	*catA-luc*	Benzoate	0.5 mM	10 ± 2	243 ± 16
ADPU101	*catB,C,I-luc*	Benzoate	0.5 mM	90 ± 12	35 ± 2
ADPU102	*vanA,B-luc*	Vanillate	0.5 mM	58 ± 5	48 ± 4
ADPU110	*salA-luc*	Salicylate	0.5 mM	90 ± 23	96 ± 11
ADPU112	*vanK-luc*	Vanillate	0.5 mM	46 ± 12	36 ± 4

*Expressed as a percentage of the activity on pyruvate plus the aromatic inducer (set to 100 %). Values are means ± SD of at least three independent experiments.
†Data from Fischer et al. (2008).

Table 5. Effect of *crc* deletion on the expression of the indicated operons under CCR conditions

Strain	Relevant characteristics	Specific inducer	Concn	Luciferase activity after growth on specific inducer plus secondary carbon source(s)*		
				Succinate + acetate	Succinate	Acetate
ADPU97	*benA-luc*, Δ*crc*	Benzoate	0.5 mM	2788 ± 917	13 ± 2	74 ± 45
ADPU98	*hcaA-luc*, Δ*crc*	*p*-Coumarate	1.0 μM	307 ± 146	139 ± 28	66 ± 21
ADPU99	*dcaA-luc*, Δ*crc*	Adipate	1.0 mM	1222 ± 195	757 ± 134	432 ± 38
ADPU104	*catA-luc*, Δ*crc*	Benzoate	0.5 mM	51 ± 10	109 ± 18	134 ± 27
ADPU105	*catB,C,I-luc*, Δ*crc*	Benzoate	0.5 mM	288 ± 26	121 ± 35	89 ± 18
ADPU106	*vanA,B-luc*, Δ*crc*	Vanillate	0.5 mM	822 ± 352	575 ± 198	720 ± 213
ADPU111	*salA-luc*, Δ*crc*	Salicylate	0.5 mM	185 ± 67	282 ± 106	160 ± 71
ADPU113	*vanK-luc*, Δ*crc*	Vanillate	0.5 mM	288 ± 31	432 ± 46	437 ± 141
ADPU120	*areA-luc*, Δ*crc*	Benzyl alcohol	2.0 mM	914 ± 18	721 ± 411	24 ± 6
ADPU121	*antA-luc*, Δ*crc*	Anthranilate	1.0 mM	143 ± 18	269 ± 51	92 ± 22

*Expressed as a percentage of the activity in the parental strain (*crc*$^+$) grown under the same conditions. Values are means ± SD of at least three independent experiments.

succinate or acetate alone, the results were comparable to those on succinate and acetate except for a few cases, the most notable of which being the *ben* operon. Here, the absence of *crc* caused a repression on succinate but no significant effect on acetate. Obviously, Crc negatively affects transcription at most promoters tested. The observation of the derepression in the absence of Crc first made for the *pca-qui* operon can now be extended to almost all additional operons investigated here.

Cross-regulation

It was shown earlier that *pobA*, which encodes the enzyme for the degradation of POB to PCA, is strongly repressed when benzoate is present in addition to POB, although POB is the specific inducer for *pobA* expression (Brzostowicz *et al.*, 2003). This interaction between the two branches of the β-ketoadipate pathway was named cross-regulation. Here, the effect of different benzoate concentrations (0.1–5.0 mM) on the transcriptional activity of the *hca*, *vanA,B* and *dca* operons was determined (Fig. 2a). Probably due to the toxicity of benzoate, strains grown in the presence of higher amounts of benzoate (3.0 and 5.0 mM) showed a decrease in the growth rate, but reached the same final optical density as the culture grown without benzoate in the medium (data not shown). Since the effects were observed at much lower benzoate concentrations, the growth inhibition at higher benzoate concentration is not disturbing. For the *hca* and *vanA,B* operons, a strong decrease in transcriptional activity was observed with increasing benzoate concentrations. This repression is even stronger than CCR by succinate and acetate in combination (90 % for *vanA,B*; Table 3) and 93 % for *hca* (Fischer *et al.*, 2008)). For the *dca* operon, a slightly different behaviour was observed: benzoate concentrations lower than 1.0 mM led to increased promoter activity, while higher concentrations caused repression which was not as strong as in the case of *van* and *hca*.

Vertical regulation

It was shown earlier that PCA inhibits *pobA* expression in the presence of the specific inducer POB (Brzostowicz *et al.*, 2003). Here, we investigated the effect of PCA (0.1–5.0 mM) on promoter activity of the *hca* and *vanA,B* operons in the presence of the specific aromatic inducer. In contrast to cultures grown in the presence of higher concentrations of benzoate, no decrease in growth rate was observed for cultures grown in the presence of higher amounts of PCA. Both operons are affected by vertical regulation as well (shown in Fig. 2b). At higher concentrations of PCA, the expression of both operons decreased, as observed for the *pobA* gene. We refer to this type of regulation as vertical regulation, since a downstream metabolite (with respect to the catabolic pathway, PCA) affects the expression of an operon encoding a pathway for its generation from various precursors.

DISCUSSION

Strong repression of all investigated operons

Earlier studies analysing the *ben*, *dca*, *hca*, *are* and *ant* operons (Fischer *et al.*, 2008) and the *pca-qui* operon (Dal *et al.*, 2005; Siehler *et al.*, 2007) revealed a strong repression of promoter activity when the organic acids succinate and acetate were present in addition to the specific aromatic inducer of the respective pathway. Here, we extended these observations by analysing additional operons all connected to the degradation of aromatic compounds (*catA*, *catB,C,I,J,F,D*, *vanA,B*, *sal*, *vanK*, repression between 42 and 98 %; Tables 3 and 5). Furthermore, the investigation included the additional carbon sources lactate and gluconate. While pyruvate generally can be regarded as neutral for gene expression (Dal *et al.*, 2002), the presence of lactate or gluconate has different effects on the expression of the operons analysed, ranging from no effect

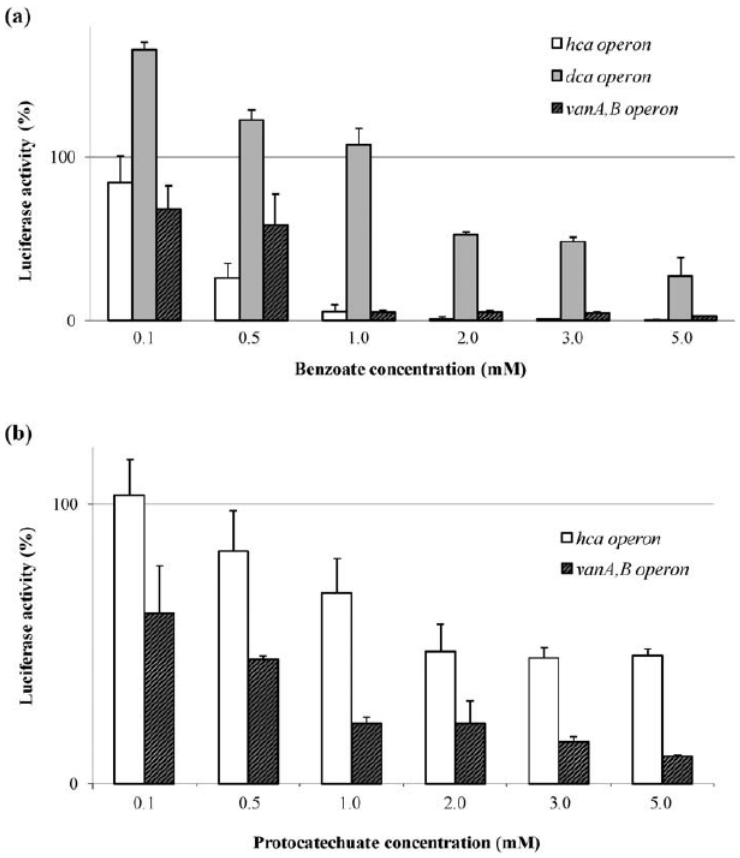

Fig. 2. Repression of operons in the presence of benzoate (cross-regulation) or PCA (vertical regulation). Luciferase activity of *A. baylyi* strains containing the indicated transcriptional *luc* fusions in the presence of the specific inducer and increasing concentrations of (a) benzoate or (b) PCA. The activity of each operon in the absence of benzoate or PCA was set to 100 %. Each growth experiment was carried out at least three times independently. Error bars indicate standard deviation.

to a slight repression in most cases (Table 4). A surprising result is the induction of *catA* by gluconate whereas all other tested carbon sources caused strong repression at this operon. Thus in this single case, gluconate has an even smaller negative effect on induction than pyruvate. In contrast, pyruvate has a small repressing effect, which is negligible when looking at the strong repression in all other cases. The repression of the operons encoding the funnelling reactions by elevated concentrations of succinate and acetate is meaningful in the context of energy preservation. The β-ketoadipate pathway and all the funnelling reactions do not lead to energy conservation. It thus seems advantageous to express these funnelling pathways only to the least necessary extent (an argument which also applies to the other regulatory phenomena, cross-regulation and vertical regulation, discussed below). Energy conservation occurs subsequently by oxidation of succinyl-CoA and acetyl-CoA. Lactate and pyruvate cause no or only a moderate repression of the operons (with the exception of lactate on *catA*). These two substrates may not be such abundant carbon sources for *A. baylyi* in its natural habitat and thus no regulatory mechanism may have evolved. The degradation of gluconate by *A. baylyi* is energy consuming, because gluconate has to be taken into the cell by active transport and then be converted to 6-phosphogluconate, which is also an energy-requiring step. Gluconate degradation then is accomplished by a modified Entner–Doudoroff pathway (Barbe *et al.*, 2004; Young *et al.*, 2005). Furthermore, the utilization of gluconate or glucose is unusual among species of *Acinetobacter*; thus it seems to fit that there is no strong repression of aromatic degradative pathways by gluconate as observed for succinate and acetate.

Crc is involved in the transcriptional expression control of numerous aromatic degradative pathways

The absence of Crc had a significant effect on the expression of the operons *are*, *sal*, *ben*, *catB,C,I,J,F,D*, *dca*, *hca*, *vanA,B*, *vanK* and *sal*, as shown here and earlier for *pca-qui* and *pobA* (Dal *et al.*, 2002; Zimmermann *et al.*, 2009). The inactivation of *crc* resulted in a significant transcriptional derepression of most operons analysed. Only *catA*, forming a separate regulatory unit in *A. baylyi*, did not show a significant dependence on Crc. While the results presented here focus on the transcriptional level, *A. baylyi* Crc also acts post-transcriptionally by (directly or indirectly) dramatically changing the mRNA half-life of the *pca-qui* transcript (Zimmermann *et al.*, 2009). In *P. putida*

it has been shown that Crc directly affects translation of the regulator AlkS (Yuste & Rojo, 2001). Similar observations have been made for *P. putida* BenR mRNA. In these bacteria, Crc blocks translation by binding the translation initiation site (Moreno & Rojo, 2008). In summary, Crc turns out to have complex effects at both the transcriptional and the post-transcriptional level. Furthermore, Crc affects all operons investigated so far, an observation supported by investigations of *P. putida* Crc, which is known to be a truly global regulator (Moreno *et al.*, 2009).

Cross-regulation

Cross-regulation takes place between the two branches of the β-ketoadipate pathway, indicating that these branches are not regulated independently (Fig. 3). Our results suggest that the consumption of benzoate (degraded via the catechol branch) is favoured over substrates of the PCA branch (e.g. vanillate or other hydroxycinnamates), as shown by the transcriptional repression of the respective operons in the presence of benzoate. Furthermore, the presence of increased benzoate concentrations led to a repression of the *dca* genes. The repression of the *vanA,B* and *hca* operons caused by benzoate is even stronger than the repression caused by the organic acids succinate and acetate in combination. It is important to note that all strains used for the analysis of cross-regulation are able to degrade benzoate to *cis,cis*-muconate via the catechol branch. Thus, *cis,cis*-muconate is available as an effector for BenM and CatM. These transcriptional regulators are in fact responsible for the regulated expression of the *ben* and *cat* genes in response to benzoate and *cis,cis*-muconate (Craven *et al.*, 2008). However, while no interaction of the two regulators with the *pobA* promoter could be detected, both BenM and CatM are able to bind to a fragment upstream of *pcaU*, an interaction that is promoted by *cis,cis*-muconate (Brzostowicz *et al.*, 2003). Subsequently, it was shown that *pca-qui* expression also undergoes cross-regulation by benzoate (Siehler *et al.*, 2007). It is still unclear how these observations connect with the cross-regulation of *pobA*. It may be that POB transport is limited when the *pca-qui* operon (including *pcaK*) is repressed, but the involvement of the second POB transporter, VanK, needs to be characterized. Studies on VanK suggest an

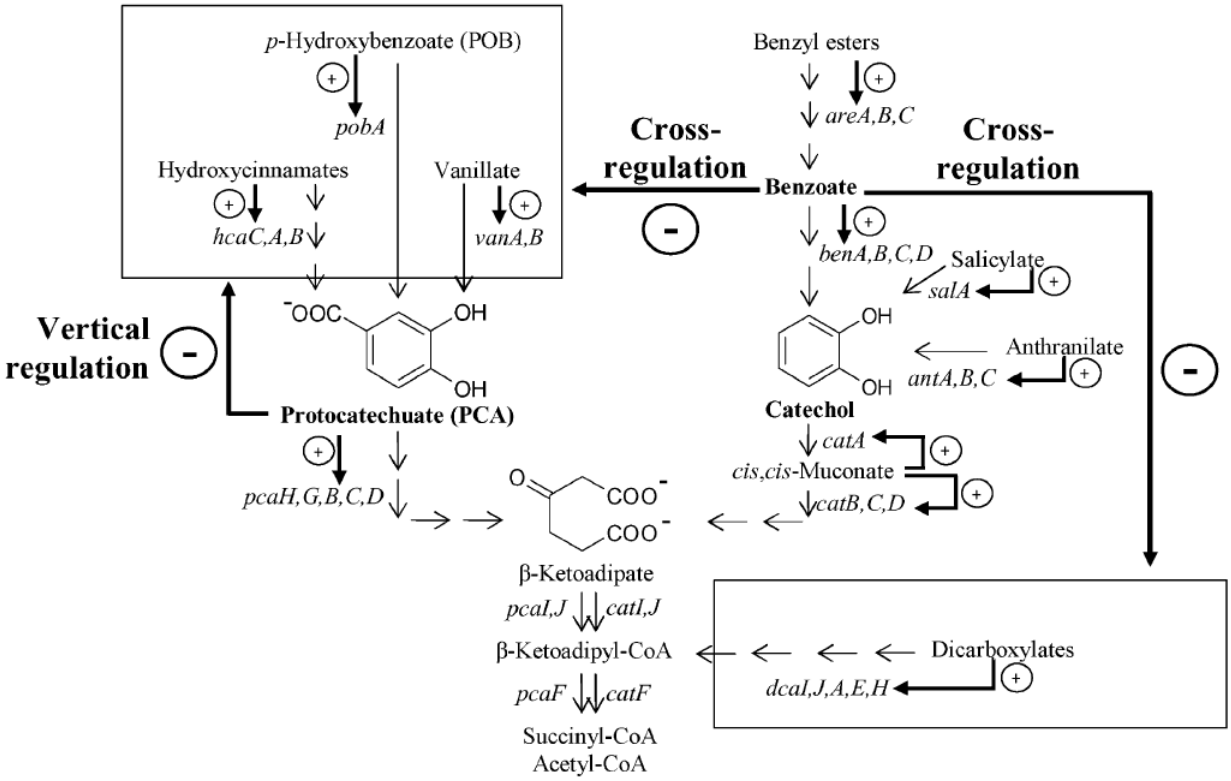

Fig. 3. Summary of the regulatory levels within the aromatic catabolic pathways of *A. baylyi*. All operons are affected negatively in expression by CCR triggered by succinate and acetate (not included in the scheme). Thin arrows indicate the direction of the metabolic pathway; thick arrows indicate transcriptional regulation effects. Repression (−) or activation (+) is symbolized by plus or minus signs next to the arrows.

involvement in PCA uptake, since a double knockout of *vanK* and *pcaK* prevents growth on PCA, while a knockout of *pcaK* alone does not (D'Argenio *et al.*, 1999). However, it has to be determined whether there is involvement of VanK in POB uptake. For all other operons under study, the presence of binding sites for BenM or CatM needs to be evaluated to determine if these proteins are centrally involved in the mechanism of cross-regulation.

Vertical regulation

We showed here that the addition of PCA to the medium containing the specific inducers (vanillate, *p*-coumarate) triggers a mechanism that represses the *vanA,B* and *hca* operons encoding funnelling reactions to PCA. This regulatory mechanism was termed vertical regulation (Fig. 3). An analogous observation was made earlier for *pobA*. PobR had been excluded as a mediator of this effect (Siehler *et al.*, 2007). Furthermore, PcaU, the transcriptional regulator of the *pca* genes, is naturally able to bind PCA but is not able to bind the *pobA* promoter (Siehler *et al.*, 2007). The molecular basis of vertical regulation observed for the *pobA* promoter thus remains unknown, but the phenomenon seems to be common, as shown for the *vanA,B* and *hca* operons. The biological relevance appears to be that increased internal PCA concentrations prevent the expensive expression of any funnelling pathway leading to more PCA production. Only when the internal PCA level falls under a certain level, will this mechanism cease to be active and more PCA can be produced from the respective precursor. Furthermore, external PCA in concentrations high enough to promote growth will also lead to the repression of funnelling pathways producing it, which also supports the organism in saving resources.

Conclusion

The first mechanisms of regulation found within the pathways for aromatic compound degradation in *A. baylyi* included induction brought about by specific regulators and their respective effectors. In the current study, additional levels of regulation were characterized more comprehensively, namely carbon catabolite repression, cross-regulation and vertical regulation. All of these consist of repressing effects. Besides efficient induction in response to the presence of the substrates, three different mechanisms decreasing expression under several conditions override specific induction. This indicates that the expression of genes for the degradation of aromatic compounds only occurs under well-defined conditions and in a well-defined order to best fit the needs of the bacterium.

ACKNOWLEDGEMENTS

We would like to thank Michael Vogl for his contributions. This work was supported by personal grants (LGFG) to F. S. B. and R. F. by the state of Baden-Württemberg, Germany.

REFERENCES

Alting-Mees, M. A. & Short, J. M. (1989). pBluescript II: gene mapping vectors. *Nucleic Acids Res* **17**, 9494.

Barbe, V., Vallenet, D., Fonknechten, N., Kreimeyer, A., Oztas, S., Labarre, L., Cruveiller, S., Robert, C., Duprat, S. & other authors (2004). Unique features revealed by the genome sequence of *Acinetobacter* sp. ADP1, a versatile and naturally transformation competent bacterium. *Nucleic Acids Res* **32**, 5766–5779.

Brzostowicz, P. C., Reams, A. B., Clark, T. J. & Neidle, E. L. (2003). Transcriptional cross-regulation of the catechol and protocatechuate branches of the β-ketoadipate pathway contributes to carbon source-dependent expression of the *Acinetobacter* sp. strain ADP1 *pobA* gene. *Appl Environ Microbiol* **69**, 1598–1606.

Cánovas, J. L. & Stanier, R. Y. (1967). Regulation of the enzymes of the β-ketoadipate pathway in *Moraxella calcoacetica*. *Eur J Biochem* **1**, 289–300.

Craven, S. H., Ezezika, O. C., Momany, C. & Neidle, E. L. (2008). LysR homologs in *Acinetobacter*: insights into a diverse and prevalent family of transcriptional regulators. In *Acinetobacter Molecular Biology*, 1st edn, pp. 163–202. Edited by U. C. Gerischer. Norwich, UK: Caister Academic Press.

D'Argenio, D. A., Segura, A., Coco, W. M., Bunz, P. V. & Ornston, L. N. (1999). The physiological contribution of *Acinetobacter* PcaK, a transport system that acts upon protocatechuate, can be masked by the overlapping specificity of VanK. *J Bacteriol* **181**, 3505–3515.

Dal, S., Steiner, I. & Gerischer, U. (2002). Multiple operons connected with catabolism of aromatic compounds in *Acinetobacter* sp. strain ADP1 are under carbon catabolite repression. *J Mol Microbiol Biotechnol* **4**, 389–404.

Dal, S., Trautwein, G. & Gerischer, U. (2005). Transcriptional organization of genes for protocatechuate and quinate degradation from *Acinetobacter* sp. strain ADP1. *Appl Environ Microbiol* **71**, 1025–1034.

Fischer, R., Bleichrodt, F. S. & Gerischer, U. C. (2008). Aromatic degradative pathways in *Acinetobacter baylyi* underlie carbon catabolite repression. *Microbiology* **154**, 3095–3103.

Gerischer, U. C. (2008). *Acinetobacter Molecular Biology*, 1st edn. Norwich, UK: Caister Academic Press.

Gerischer, U., Segura, A. & Ornston, L. N. (1998). PcaU, a transcriptional activator of genes for protocatechuate utilization in *Acinetobacter*. *J Bacteriol* **180**, 1512–1524.

Hanahan, D. (1983). Studies on transformation of *Escherichia coli* with plasmids. *J Mol Biol* **166**, 557–580.

Harwood, C. S. & Parales, R. E. (1996). The β-ketoadipate pathway and the biology of self-identity. *Annu Rev Microbiol* **50**, 553–590.

Juni, E. & Janik, A. (1969). Transformation of *Acinetobacter calcoaceticus* (*Bacterium anitratum*). *J Bacteriol* **98**, 281–288.

Morales, G., Linares, J. F., Beloso, A., Albar, J. P., Martinez, J. L. & Rojo, F. (2004). The *Pseudomonas putida crc* global regulator controls the expression of genes from several chromosomal catabolic pathways for aromatic compounds. *J Bacteriol* **186**, 1337–1344.

Moreno, R. & Rojo, F. (2008). The target for the *Pseudomonas putida crc* global regulator in the benzoate degradation pathway is the BenR transcriptional regulator. *J Bacteriol* **190**, 1539–1545.

Moreno, R., Ruiz-Manzano, A., Yuste, L. & Rojo, F. (2007). The *Pseudomonas putida crc* global regulator is an RNA binding protein that inhibits translation of the AlkS transcriptional regulator. *Mol Microbiol* **64**, 665–675.

Moreno, R., Martínez-Gomariz, M., Yuste, L., Gil, C. & Rojo, F. (2009). The *Pseudomonas putida crc* global regulator controls the hierarchical

assimilation of amino acids in a complete medium: evidence from proteomic and genomic analyses. *Proteomics* 9, 2910–2928.

Podbielski, A., Woischnik, M., Leonard, B. A. & Schmidt, K. H. (1999). Characterization of *nra*, a global negative regulator gene in group A streptococci. *Mol Microbiol* 31, 1051–1064.

Siehler, S. Y., Dal, S., Fischer, R., Patz, P. & Gerischer, U. (2007). Multiple-level regulation of genes for protocatechuate degradation in *Acinetobacter baylyi* includes cross-regulation. *Appl Environ Microbiol* 73, 232–242.

Trautwein, G. & Gerischer, U. (2001). Effects exerted by transcriptional regulator PcaU from *Acinetobacter* sp. strain ADP1. *J Bacteriol* 183, 873–881.

Tresguerres, M. E. F., DeTorrontequi, G., Ingledew, W. M. & Cánovas, J. L. (1970). Regulation of the enzymes of the β-ketoadipate pathway in *Moraxella*. Control of quinate oxidation by protcatechuate. *Eur J Biochem* 14, 445–450.

Vaneechoutte, M., Young, D. M., Ornston, L. N., De Baere, T., Nemec, A., Van Der Reijden, T., Carr, E., Tjernberg, I. & Dijkshoorn, L. (2006). Naturally transformable *Acinetobacter* sp. strain ADP1 belongs to the newly described species *Acinetobacter baylyi*. *Appl Environ Microbiol* 72, 932–936.

Williams, P. A. & Kay, C. M. (2008). The catabolism of aromatic compounds by *Acinetobacter*. In *Acinetobacter Molecular Biology*, 1st edn, pp. 99–118. Edited by U. C. Gerischer. Norwich, UK: Caister Academic Press.

Wolff, J. A., MacGregor, C. H., Eisenberg, R. C. & Phibbs, P. V., Jr (1991). Isolation and characterization of catabolite repression control mutants of *Pseudomonas aeruginosa* PAO. *J Bacteriol* 173, 4700–4706.

Yanisch-Perron, C., Vieira, J. & Messing, J. (1985). Improved M13 phage cloning vectors and host strains: nucleotide sequences of the M13mp18 and pUC19 vectors. *Gene* 33, 103–119.

Young, D. M., Parke, D. & Ornston, L. N. (2005). Opportunities for genetic investigation afforded by *Acinetobacter baylyi*, a nutritionally versatile bacterial species that is highly competent for natural transformation. *Annu Rev Microbiol* 59, 519–551.

Yuste, L. & Rojo, F. (2001). Role of the *crc* gene in catabolic repression of the *Pseudomonas putida* GPo1 alkane degradation pathway. *J Bacteriol* 183, 6197–6206.

Zimmermann, T., Sorg, T., Siehler, S. Y. & Gerischer, U. (2009). Role of *Acinetobacter baylyi crc* in catabolite repression of enzymes for aromatic compound catabolism. *J Bacteriol* 191, 2834–2842.

Edited by: H. L. Drake

11 Attachments

11.1 Supplementary data to Chapter 3.2

Table 10.1. Activity of the *ant* operon in the presence of pyruvate, lactate, or gluconate (20 mM each) in the presence or absence of the inducer anthranilate (+ I; 1 mM), in a *crc*-positive and *crc*-negative background.

		Luciferase activity[a]					
Strain	**Characteristic**	**Pyruvate**	**Lactate**	**Gluconate**	**Pyruvate + I**	**Lactate + I**	**Gluconate + I**
ADPU96	*antA-luc*	2171 ± 169[b]	809 ± 158[b]	900 ± 81	103731 ± 1668[b]	46948 ± 2420[b]	16621 ± 1588[c]
ADPU121	*antA-luc*, Δ*crc*Ω	996 ± 238	665 ± 50	803 ± 100	67065 ± 20003	29368 ± 5829	14154 ± 3806

[a] Values are given as specific luciferase activity [RLU/OD_{600}], and are averages of at least three independent experiments. Standard deviation is given. [b] Fischer *et al*, 2008. [c] Bleichrodt *et al.*, 2010.

Table 10.2. Activity of the *are* operon in the presence of pyruvate, lactate, or gluconate (20 mM each) in the presence or absence or the inducer benzyl alcohol (+ I; 2 mM), in a *crc*-positive and *crc*-negative background.

		Luciferase activity[a]					
Strain	**Characteristic**	**Pyruvate**	**Lactate**	**Gluconate**	**Pyruvate + I**	**Lactate + I**	**Gluconate + I**
ADPU95	*areA-luc*	261 ± 12[b]	239 ± 82[b]	214 ± 25	7245 ± 3116[b]	4780 ± 893[b]	4596 ± 438[c]
ADPU120	*areA-luc*, Δ*crc*Ω	1998 ± 175	1474 ± 106	n. g.	2069 ± 543	3186 ± 628	n. g.

[a] Values are given as specific luciferase activity [RLU/OD_{600}], and are averages of at least three independent experiments. Standard deviation is given. [b] Fischer *et al*, 2008. [c] Bleichrodt *et al.*, 2010.

Table 10.3. Activity of the *ben* operon in the presence of pyruvate, lactate, or gluconate (20 mM each) in the presence or absence of the inducer benzoate (+ I; 0.5 mM), in a *crc*-positive and *crc*-negative background.

		Luciferase activity[a]					
Strain	**Characteristic**	**Pyruvate**	**Lactate**	**Gluconate**	**Pyruvate + I**	**Lactate + I**	**Gluconate + I**
ADPU92	*benA-luc*	17 ± 9[b]	21 ± 5[b]	29 ± 18	1306 ± 586[b]	2014 ± 600[b]	907 ± 241
ADPU97	*benA-luc*, Δ*crc*Ω	56 ± 27	29 ± 10	27 ± 7	4620 ± 760	1090 ± 120	658 ± 109

[a] Values are given as specific luciferase activity [RLU/OD_{600}], and are averages of at least three independent experiments. Standard deviation is given. [b] Fischer *et al*, 2008.

Table 10.4. Activity of the *catA* operon in the presence of pyruvate, lactate, or gluconate (20 mM each) in the presence or absence of the inducer benzoate (+ I; 0.5 mM), in a *crc*-positive and *crc*-negative background.

		Luciferase activity[a]					
Strain	**Characteristic**	**Pyruvate**	**Lactate**	**Gluconate**	**Pyruvate + I**	**Lactate + I**	**Gluconate + I**
ADPU100	*catA-luc*	1171 ± 369	1838 ± 370	805 ± 25	24105 ± 8267[b]	2308 ± 459[b]	58657 ± 3851[b]
ADPU104	*catA-luc*, Δ*crc*Ω	1203 ± 168	1309 ± 201	1134 ± 101	38585 ± 2705	1746 ± 245	50688 ± 12186

[a] Values are given as specific luciferase activity [RLU/OD_{600}], and are averages of at least three independent experiments. Standard deviation is given. [b] Bleichrodt *et al.*, 2010.

Table 10.5. Activity of the *catB,C,I,J,F,D* operon in the presence of pyruvate, lactate, or gluconate (20 mM each) in the presence or absence of the inducer benzoate (+ I; 0.5 mM), in a *crc*-positive and *crc*-negative background.

		Luciferase activity[a]					
Strain	**Characteristic**	**Pyruvate**	**Lactate**	**Gluconate**	**Pyruvate + I**	**Lactate + I**	**Gluconate + I**
ADPU101	*catB,C,I-luc*	267 ± 90	368 ± 80	183 ± 35	6334 ± 647[b]	5725 ± 756[b]	2245 ± 134[b]
ADPU105	*catB,C,I-luc*, Δ*crc*Ω	306 ± 39	250 ± 15	200 ± 52	6365 ± 1721	4448 ± 699	1537 ± 234

[a] Values are given as specific luciferase activity [RLU/OD_{600}], and are averages of at least three independent experiments. Standard deviation is given. [b] Bleichrodt *et al.*, 2010.

Table 10.6. Activity of the *dca* operon in the presence of pyruvate, lactate, or gluconate (20 mM each) in the presence or absence of the inducer adipate (+ I; 1 mM), in a *crc*-positive and *crc*-negative background.

		Luciferase activity[a]					
Strain	**Characteristic**	**Pyruvate**	**Lactate**	**Gluconate**	**Pyruvate + I**	**Lactate + I**	**Gluconate + I**
ADPU94	*dcaA-luc*	155 ± 51[b]	399 ± 317[b]	278 ± 146	11698 ± 859[b]	9605 ± 2230[b]	17007 ± 5412
ADPU99	*dcaA-luc*, Δ*crc*Ω	138 ± 81	71 ± 14	63 ± 8	17267 ± 3167	17441 ± 3718	13088 ± 2028

[a] Values are given as specific luciferase activity [RLU/OD_{600}], and are averages of at least three independent experiments. Standard deviation is given. [b] Fischer *et al*, 2008.

Table 10.7. Activity of the *hca* operon in the presence of pyruvate, lactate, or gluconate (20 mM each) in the presence or absence of the inducer *p*-coumarate (+ I; 1 µM), in a *crc*-positive and *crc*-negative background.

		Luciferase activity[a]					
Strain	**Characteristic**	**Pyruvate**	**Lactate**	**Gluconate**	**Pyruvate + I**	**Lactate + I**	**Gluconate + I**
ADPU93	*hcaA-luc*	1768 ± 789[b]	20761 ± 12593[b]	16292 ± 8027	63060 ± 10533[b]	83418 ± 9047[b]	43642 ± 17264
ADPU98	*hcaA-luc*, Δ*crc*Ω	739 ± 93	177 ± 34	2512 ± 358	204252 ± 61496	69587 ± 10274	42640 ± 9757

[a] Values are given as specific luciferase activity [RLU/OD_{600}], and are averages of at least three independent experiments. Standard deviation is given. [b] Fischer *et al*, 2008.

Table 10.8. Activity of the *sal* operon in the presence of pyruvate, lactate, or gluconate (20 mM each) in the presence or absence of the inducer salicylate (+ I; 0.5 mM), in a *crc*-positive and *crc*-negative background.

		Luciferase activity[a]					
Strain	**Characteristic**	**Pyruvate**	**Lactate**	**Gluconate**	**Pyruvate + I**	**Lactate + I**	**Gluconate + I**
ADPU110	*salA-luc*	1679 ± 939	275 ± 202	411 ± 220	4987 ± 1167[b]	4468 ± 1151[b]	4803 ± 573[b]
ADPU111	*salA-luc*, Δ*crc*Ω	639 ± 182	446 ± 168	n. g.	5307 ± 1822	8516 ± 2798	n. g.

[a] Values are given as specific luciferase activity [RLU/OD_{600}], and are averages of at least three independent experiments. Standard deviation is given. [b] Bleichrodt *et al.*, 2010.

Table 10.9. Activity of the *vanA,B* operon in the presence of pyruvate, lactate, or gluconate (20 mM each) in the presence or absence of the inducer vanillate (+ I; 0.5 mM), in a *crc*-positive and *crc*-negative background.

		Luciferase activity[a]					
Strain	**Characteristic**	**Pyruvate**	**Lactate**	**Gluconate**	**Pyruvate + I**	**Lactate + I**	**Gluconate + I**
ADPU102	*vanA,B-luc*	1670 ± 340	1609 ± 105	1225 ± 73	50241 ± 4932[b]	29303 ± 2343[b]	24287 ± 2033[b]
ADPU106	*vanA,B-luc*, Δ*crc*Ω	3214 ± 656	1283 ± 130	n. g.	208379 ± 51227	40933 ± 6650	n. g.

[a] Values are given as specific luciferase activity [RLU/OD_{600}], and are averages of at least three independent experiments. Standard deviation is given. [b] Bleichrodt *et al.*, 2010.

Table 10.10. Activity of the *vanK* operon in the presence of pyruvate, lactate, or gluconate (20 mM each) in the presence or absence of the inducer vanillate (+ I; 0.5 mM), in a *crc*-positive and *crc*-negative background.

		Luciferase activity[a]					
Strain	**Characteristic**	**Pyruvate**	**Lactate**	**Gluconate**	**Pyruvate + I**	**Lactate + I**	**Gluconate + I**
ADPU112	*vanK-luc*	1222 ± 103	1007 ± 329	725 ± 80	2098 ± 284[b]	2527 ± 669[b]	24287 ± 2033[b]
ADPU113	*vanK-luc*, Δ*crc*Ω	1626 ± 166	1409 ± 279	n. g.	7050 ± 1060	5156 ± 1089	2201 ± 200

[a] Values are given as specific luciferase activity [RLU/OD_{600}], and are averages of at least three independent experiments. Standard deviation is given. [b] Bleichrodt *et al.*, 2010.

11.2 Supplementary data to Chapter 3.3.2

Table 10.11. Effect of BenM and CatM on cross-regulation of the *hca* operon. Luciferase activity was measured in the presence of pyruvate (20 mM) in the absence (Basal) or presence of the inducer *p*-coumarate (Induced; 1 µM), with increasing concentrations of benzoate (Ben; 0.5 to 5.0 mM).

		Luciferase activity[a]						
Strain	**Char.**	**Basal**	**Induced**	**Ben 0.5 mM**	**Ben 1 mM**	**Ben 2 mM**	**Ben 3 mM**	**Ben 5 mM**
ADPU93	*hcaA-luc*	1768 ± 789[b]	63060 ± 10533[b]	16090 ± 280[c]5	3282 ± 945[c]	491 ± 293[c]	381 ± 27[c]	201 ± 46[c]
ADPU135	*hcaA-luc*, Δ*benM*	55257 ± 7105	28661 ± 3798	33454 ± 5817	31319 ± 6179	26153 ± 3631	20664 ± 1853	14664 ± 908
ADPU124	*hcaA-luc*, *catM*Ω	119 ± 59	42326 ± 13687	42024 ± 17509	38455 ± 13269	34114 ± 20395	19280 ± 4967	11170 ± 3688
ADPU140	*hcaA-luc*, Δ*benM*, *catM*Ω	15049 ± 3977	14489 ± 3422	12552 ± 2123	11983 ± 2207	14012 ± 517	17454 ± 2782	17249 ± 991

[a] Values are given as specific luciferase activity [RLU/OD_{600}], and are averages of at least three independent experiments. Standard deviation is given. [b] Fischer *et al.*, 2008. [c] Bleichrodt *et al.*, 2010.

Table 10.12. Effect of BenM and CatM on cross-regulation of the *vanA,B* operon. Luciferase activity was measured in the presence of pyruvate (20 mM) in the absence (Basal) or presence of the inducer vanillate (Induced; 0.5 mM), with increasing concentrations of benzoate (Ben; 0.5 to 5.0 mM).

		Luciferase activity[a]						
Strain	**Char.**	**Basal**	**Induced**	**Ben 0.5 mM**	**Ben 1 mM**	**Ben 2 mM**	**Ben 3 mM**	**Ben 5 mM**
ADPU102	*vanA,B-luc*	1670 ± 340	50241 ± 4932[b]	32200 ± 10230[b]	2689 ± 584[b]	2646 ± 454[b]	2469 ± 214[b]	1485 ± 72[b]
ADPU137	*vanA,B-luc*, Δ*benM*	47090 ± 17896	60856 ± 4056	76634 ± 23461	59121 ± 17618	44119 ± 6168	35612 ± 4049	12642 ± 1542
ADPU126	*vanA,B-luc*, *catM*Ω	3854 ± 43	58763 ± 19594	4954 ± 1518	4123 ± 959	2873 ± 170	3665 ± 1950	3429 ± 872
ADPU142	*vanA,B-luc*, Δ*benM*, *catM*Ω	14185 ± 329	15070 ± 852	16322 ± 499	15411 ± 1558	14109 ± 3118	15567 ± 844	13537 ± 1504

[a] Values are given as specific luciferase activity [RLU/OD_{600}], and are averages of at least three independent experiments. Standard deviation is given. [b] Bleichrodt *et al.*, 2010.

Table 10.13. Effect of BenM and CatM on cross-regulation of the *dca* operon. Luciferase activity was measured in the presence of pyruvate (20 mM) in the absence (Basal) or presence of the inducer adipate (Induced; 1 mM), with increasing concentrations of benzoate (Ben; 0.5 to 5.0 mM).

		Luciferase activity[a]						
Strain	**Char.**	**Basal**	**Induced**	**Ben 0.5 mM**	**Ben 1 mM**	**Ben 2 mM**	**Ben 3 mM**	**Ben 5 mM**
ADPU94	*dcaA-luc*	155 ± 51[b]	11698 ± 859[b]	14368 ± 721[c]	12547 ± 1201[c]	6134 ± 226[c]	5645 ± 319[c]	3183 ± 1294[c]
ADPU136	*dcaA-luc*, Δ*benM*	1940 ± 228	8929 ± 3279	11364 ± 2377	6233 ± 2826	3574 ± 1404	3422 ± 1754	2853 ± 696
ADPU125	*dcaA-luc*, *catM*Ω	155 ± 102	29538 ± 13099	19651 ± 6753	19567 ± 10311	13045 ± 1241	n. g.	n. g.
ADPU141	*dcaA-luc*, Δ*benM*, *catM*Ω	566 ± 276	12351 ± 1863	10700 ± 2573	7522 ± 2250	4195 ± 716	3465 ± 1419	2453 ± 47

[a] Values are given as specific luciferase activity [RLU/OD_{600}], and are averages of at least three independent experiments. Standard deviation is given. [b] Fischer *et al.*, 2008. [c] Bleichrodt *et al.*, 2010.

11.3 Supplementary data to Chapter 3.3.4

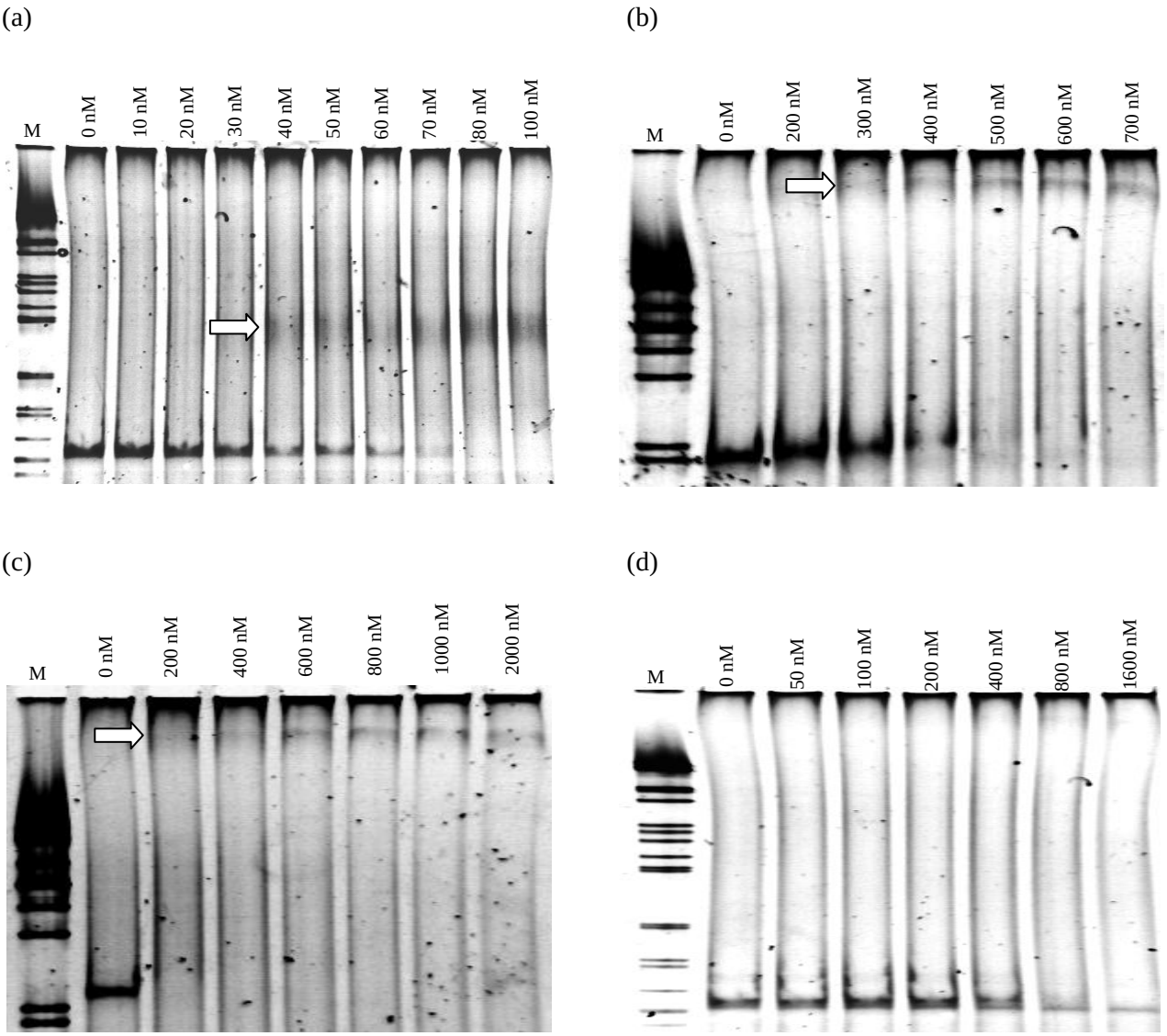

Figure 10.1. Electro mobility shifts assays (EMSAs) to show interaction of BenM with DNA fragments containing (putative) BenM binding sites. (a) *benM-benA* region (positive control), (b) *hcaA-hcaK* region, (c) *vanA-vanK* region, (d) *dcaA-dcaE* region. BenM-6His was added in increasing concentrations, as indicated. M: λ BglI DNA ladder. DNA fragments were used at a final concentration of 2.3 nM or 1.5 nM for (a) and (d), or (b) and (c), respectively. Retarded protein-DNA complexes are marked by white arrows.

11.4 Supplementary data to Chapter 3.4.2

Table 10.14. Effect of blocking PCA degradation on vertical regulation of the *hca* operon. Luciferase activity was measured in the presence of pyruvate (20 mM) in the absence (Basal) or presence of the inducer *p*-coumarate (Induced; 1 µM), with increasing concentrations of PCA (0.5 to 5.0 mM).

		Luciferase activity[a]						
Strain	**Char.**	**Basal**	**Induced**	**PCA 0.5 mM**	**PCA 1 mM**	**PCA 2 mM**	**PCA 3 mM**	**PCA 5 mM**
ADPU93	*hcaA-luc*	1768 ± 789[b]	63060 ± 10533[b]	52390 ± 9094[c]	43003 ± 7740[c]	29795 ± 6274[c]	28354 ± 2440[c]	28955 ± 1410[c]
ADPU162	*hcaA-luc*, Δ*pcaH*	39604 ± 13424	197634 ± 18785	215274 ± 47767	148362 ± 9280	101666 ± 5496	86401 ± 4296	74282 ± 9267

[a] Values are given as specific luciferase activity [RLU/OD_{600}], and are averages of at least three independent experiments. Standard deviation is given. [b] Fischer *et al.*, 2008. [c] Bleichrodt *et al.*, 2010.

Table 10.15. Effect of blocking PCA degradation on vertical regulation of the *vanA,B* operon. Luciferase activity was measured in the presence of pyruvate (20 mM) in the absence (Basal) or presence of the inducer vanillate (Induced; 0.5 mM), with increasing concentrations of PCA (0.5 to 5.0 mM).

		Luciferase activity[a]						
Strain	**Char.**	**Basal**	**Induced**	**PCA 0.5 mM**	**PCA 1 mM**	**PCA 2 mM**	**PCA 3 mM**	**PCA 5 mM**
ADPU102	*vanA,B-luc*	1670 ± 340	50241 ± 4932[b]	24332 ± 773[b]	11806 ± 1197[b]	11812 ± 4473[b]	8191 ± 1041[b]	5427 ± 158[b]
ADPU164	*vanA,B-luc*, Δ*pcaH*	76694 ± 13448	71220 ± 12052	55427 ± 12846	37767 ± 7994	28626 ± 8345	28143 ± 10759	14275 ± 2341

[a] Values are given as specific luciferase activity [RLU/OD_{600}], and are averages of at least three independent experiments. Standard deviation is given. [b] Bleichrodt *et al.*, 2010.

Table 10.16. *hca* and *vanA,B* expression in the presence of PCA. Luciferase activity was measured in the presence of pyruvate (20 mM) with increasing concentrations of PCA (0.5 to 5.0 mM).

		Luciferase activity[a]					
Strain	**Char.**	**Basal**	**PCA 0.5 mM**	**PCA 1 mM**	**PCA 2 mM**	**PCA 3 mM**	**PCA 5 mM**
ADPU93	*hcaA-luc*	1768 ± 789[b]	2150 ± 2724	1215 ± 1341	1213 ± 1163	1005 ± 948	1182 ± 1136
ADPU102	*vanA,B-luc*	1670 ± 340	30714 ± 7367	8592 ± 4918	687 ± 261	457 ± 85	424 ± 135

[a] Values are given as specific luciferase activity [RLU/OD_{600}], and are averages of at least three independent experiments. Standard deviation is given. [b] Fischer *et al*, 2008.

11.5 Supplementary data to Chapter 3.4.3

Table 10.17. Effect of PcaU and VanR on the expression of *vanA,B-luc*. Luciferase activity was measured in the presence of pyruvate (20 mM) in the absence (Basal) or presence of the inducer vanillate (Induced; 0.5 mM), with increasing concentrations of PCA (0.5 to 5.0 mM).

		Luciferase activity[a]						
Strain	**Char.**	**Basal**	**Induced**	**PCA 0.5 mM**	**PCA 1 mM**	**PCA 2 mM**	**PCA 3 mM**	**PCA 5 mM**
ADPU102	*vanA,B-luc*	1670 ± 340	50241 ± 4932[b]	24332 ± 773[b]	11806 ± 1200[b]	11812 ± 4473[b]	8191 ± 1041[b]	5427 ± 158[b]
ADPU123	*vanA,B-luc*, Δ*pcaU*Ω	118 ± 3	42021 ± 8144	47032 ± 10558	42848 ± 9961	51568 ± 20851	35634 ± 12557	40564 ± 9067
ADPU127	*vanA,B-luc*, *vanR*-Kn[r]	40214 ± 1292	41322 ± 5798	22514 ± 3372	12201 ± 3935	15580 ± 592	11941 ± 50	8581 ± 992
ADPU128	*vanA,B-luc*, Δ*pcaU*Ω, *vanR*-Kn[r]	47399 ± 8129	55933 ± 3077	59307 ± 4070	51563 ± 3938	51261 ± 136	50491 ±7251	51754 ± 7429

[a] Values are given as specific luciferase activity [RLU/OD_{600}], and are averages of at least three independent experiments. Standard deviation is given. [b] Bleichrodt *et al.*, 2010.

Table 10.18. Effect of PcaU and HcaR on the expression of *hcaA-luc*. Luciferase activity was measured in the presence of pyruvate (20 mM) in the absence (Basal) or presence of the inducer *p*-coumarate (Induced; 1 µM), with increasing concentrations of PCA (0.5 to 5.0 mM).

		Luciferase activity[a]						
Strain	**Char.**	**Basal**	**Induced**	**PCA 0.5 mM**	**PCA 1 mM**	**PCA 2 mM**	**PCA 3 mM**	**PCA 5 mM**
ADPU93	*hcaA-luc*	1768 ± 789[b]	63060 ± 10533[b]	52390 ± 9094[c]	43003 ± 7740[c]	29795 ± 6274[c]	28354 ± 2440[c]	28955 ± 1410[c]
ADPU122	*hcaA-luc*, Δ*pcaU*Ω	417 ± 16	47992 ± 7970	49317 ± 1939	42137 ± 11169	43776 ± 4047	35919 ± 2091	32514 ± 4430
ADPU138	*hcaA-luc*, *hcaR*-Kn^r	79796 ± 14704	52179 ± 16146	19890 ± 876	25290 ± 2149	25394 ± 4422	21315 ± 2515	23088 ± 5582
ADPU139	*hcaA-luc*, Δ*pcaU*Ω, *hcaR*-Kn^r	111820 ± 18059	75284 ± 21935	(23080 ± 1737)	(26810 ± 8309)	(25251 ± 3847)	(16248 ± 4462)	(17995 ± 6130)

[a] Values are given as specific luciferase activity [RLU/OD_{600}], and are averages of at least three independent experiments. Standard deviation is given. [b] Fischer *et al.*, 2008. [c] Bleichrodt *et al.*, 2010. Bracketed values: preliminary results.

12 Acknowledgments

I would like to thank apl. Prof. Dr. Ulrike Gerischer, for offering the opportunity to prepare my work in her lab, for her supervision and her guidance during the study.

I want to thank Prof. Dr. Peter Dürre for the possibility to prepare my work in his department, for instructive discussions, and his support. Thank you for reviewing this thesis.

I would like to thank Prof. Dr. Bernhard Eikmanns for his professional support.

The work was supported by a fellowship (Graduiertenstipendium) of Baden-Württemberg. I greatly appreciate this grant.

This work was in parts prepared at the University of Georgia, Athens, GA, USA, in the lab of Dr. Ellen L. Neidel. She gave me the amazing opportunity to spend six month in her workgroup, and supported everything with great enthusiasm. The time was unforgettable for me not only because all my hard work paid off, but also because I met brilliant people and researchers, made new friends and gained insights into a (at that time) foreign culture. The exchange was supported by the DAAD ("Deutscher Akademischer Austausch Dienst"), what I appreciate.

My special thanks goes to Esther Heupel, Mark Waidmann, and José Montoya for their critical proof-reading and their personally support. I further thank Iris Steiner for her brilliant assistance and her words of encouragement during the whole time in the lab. Thanks for the technical support from Brigitte Ehrler, Brigitte Zickner, and Petra Dangel.

I want to thank everyone working in the department for the collaboration.

Special thanks to my family.

13 Statement

I confirm that the thesis is my own work, and that all published or other sources of material consulted have been acknowledged in notes to the text or the bibliography.

Ulm, 2011-03

Fenja S. Bleichrodt